MUSCULOSKELETAL BIOMECHANICAL COMPUTATIONAL ANALYSIS OF SITTING POSTURE AND SEAT DESIGN

HUANG MENGJIE

NATIONAL UNIVERSITY OF SINGAPORE

2013

MUSCULOSKELETAL BIOMECHANICAL COMPUTATIONAL ANALYSIS OF SITTING POSTURE AND SEAT DESIGN

HUANG MENGJIE

(B.Eng., SICHUAN UNIVERSITY)

A THESIS SUBMITTED FOR THE DEGREE OF DOCTOR OF PHILOSOPHY

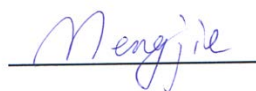## DEPARTMENT OF MECHANICAL ENGINEERING

NATIONAL UNIVERSITY OF SINGAPORE

2013

Declaration

I hereby declare that this thesis is my original work and it has been written by me in its entirety. I have duly acknowledged all the sources of information which have been used in the thesis.

This thesis has also not been submitted for any degree in any university previously.

Huang Mengjie

15 August 2013

ACKNOWLEDGEMENTS

TABLE OF CONTENTS

SUMMARY

Nowadays, low back pain has become one of the most common healthcare problems. Poor sitting posture is regarded as the main contributing factor in the development of back problems. The sitting situation is worse for the people with scoliosis, who suffer from the unbalanced sitting when compared to the healthy people. Seat design is also a very important topic in the study of sitting. Therefore, the aim of this research is to investigate the biomechanics and ergonomics of sitting posture and seat design through the approach of musculoskeletal computational analysis.

In the study of sitting posture of healthy people, the motion data obtained through the motion capture experiments of subjects, were used to drive the musculoskeletal human body models for the analysis. The musculoskeletal models of subjects were developed according to the individual anthropometric data using LifeMOD software. The analysis is based on the inverse and forward dynamic simulations. The results indicate that the compressive loading condition of spine is highly dependent on the human body posture. Some commonly adopted postures in daily life including slumped sitting, cross-legged sitting, flexion sitting and extension sitting, can introduce higher compressive loads on spinal joints, which are likely to be harmful to the intervertebral discs and cause low back pain. The influence of varied seat design parameters on spinal loadings has also evaluated and presented. The parameters studied include backrest inclination, seat pan inclination, seat pan height, seat pan depth and backrest height. The sitting stability of people with scoliosis has also been investigated. It is found that the sitting stability of people with scoliosis can be improved by the reduction of Cobb angle, the application of backrest and the better function of lumbar muscle groups.

This research contributes to a deeper insight of the biomechanics of healthy spine and scoliosis spine in different sitting postures and seat designs. It can also help advocate better sitting postures to people with different requirements, and provide guidelines for the optimized seat design.

LIST OF TABLES

LIST OF FIGURES

LIST OF SYMBOLS

Ci	The ith vertebra in the cervical spine region
Ti	The ith vertebra in the thoracic spine region
Li	The ith vertebra in the lumbar spine region
Si	The ith vertebra in the sacrum region
ROM	Range of motion
LBP	Low back pain
FEM	Finite element model
IAP	Intra-abdominal pressure
LifeMOD	LifeMOD Biomechanics Modeller
3D	Three dimensional
pCSA	Physiological cross sectional area
LOG	Line of gravity
NUH	National University Hospital
CPSS	Computerised Patient Support System
COM	Center of mass
Pi	Patient i

CHAPTER 1

INTRODUCTION

The human spine is one of the most important parts in human body. With the strong and flexible structure, it provides support to the human body and enables the body movements. However it is also a vulnerable structure and a number of problems can happen to it. Two types of spinal problems are introduced in this thesis: the low back pain (LBP) and the scoliosis.

Nowadays, LBP has become one of the most common healthcare problems and is strongly associated with the degeneration of intervertebral disc (Luoma et al., 2000). It usually happens to people with sedentary jobs who spend hours sitting in a chair with the lower back being forced away from its natural lordotic curvature. It was found that 80% of people in the United States had LBP during their lifetime (Vällfors, 1984). LBP is still a mystery and has not been fully understood due to its complexity. The factors which can lead to LBP include but not limited to: muscular dysfunction, joint irritation, breakdown of vertebral bodies, postural distortions and spinal deformities. Sitting, especially prolonged sitting, is generally accepted as a risk factor in the development of LBP (Andersson, 1981, Frymoyer et al., 1980, Kelsey and White III, 1980, Kelsey, 1975). It has been reported in one study that prolonged sitting for a period of 4 hours or more can cause LBP in the lumbar region of spine (Magora, 1972). However poor sitting postures, which are very common in daily life, are suggested to lead to LBP and other complications in people (Kirkaldy et al., 1999, Kottke, 1961, McKenzie and May, 1981, Vergara and Page, 2002).

Compared to LBP, spinal deformity is a less common but more complicated problem. The scoliosis is one type of spinal deformity and it is a medical condition in which the spine is curved from side to side in the frontal plane, affecting between 1.5% and 3% of the population. The spine of people with scoliosis looks more like an "S" or "C" than a straight line from the X-ray image. The three-dimensional deformity of spine in the frontal plane can affect the functions of internal organs and impede the

motion of the trunk. It has been demonstrated that the center of weight of patients with scoliosis are not in the midline of upper body in sitting posture (Smith and Emans, 1992, Larsson et al., 2002). Thus the sitting posture should be carefully considered in the selection of the wheelchair seating system for patients with scoliosis, because they may suffer from the unbalanced sitting due to the asymmetrical weight distribution.

Hence, the research studies about spinal biomechanics of sitting posture and seat design for healthy people and patients with scoliosis are very important and significant at present. Many biomechanical models have been developed to gain a better understanding of spinal biomechanics.

1.1 Biomechanical Modeling of Spine

Generally there are four types of biomechanical models of human spine: physical model, *in-vitro* model, *in-vivo* model and computer model. Among these models, the computer model has been extensively applied in the past decades due to its associated advantage. Compared with other types of models, computer model is able to provide the researchers with the information which cannot be easily or quickly obtained through other models. Two types of computer models have been commonly used for the insight of spinal biomechanics these years: multi-body model (MBM) and finite element model (FEM).

FEM is definitely very powerful for the local analysis of stress and deformation of body segments. It can be basically divided into two categories: the static model and the dynamic model. The static model usually provides a more detailed geometric structure of the vertebra and is able to predict the stress, strain and other properties under loading conditions; while the dynamic model including ligaments and intervertebral discs is able to predict the dynamic response of a part of spine. However, FEM only includes one or two motion segments (Belytschko et al., 1974, Bozic et al., 1994, Greaves et al., 2008, Kumaresan et al., 1999, Shirazi-Adl et al., 1986, Teo and Ng, 2001, Yoganandan et al., 1996), or a series of vertebrae of spine (Goel et al., 1994, Schmidt et al., 2008, Seidel et al., 2001, Rohlmann et al., 2007, Maurel et al., 1997, Pankoke et al., 1998, Zander et al., 2002, Zhang et al.,

2005), without considering the biomechanics of the whole spine and the effects of other body segments.

Compared with FEM, MBM is a more useful tool for the global study of the kinematic dynamics of the whole spine when considering the effects of segments, connecting joints and soft tissues in the human body. In the MBM, the rigid bodies representing the bone segments are connected with each other by bushing elements, and the soft tissues including the intervertebral discs, ligaments and muscles are represented by massless spring-damper elements. Based on this detailed musculoskeletal human body computation model, the kinematics and kinetics of the whole spine can be simulated and analyzed. This type of model has been applied in many research areas, such as car collision and whole body vibration. However until now, most of the MBMs only include a partially discretized spine, with the location usually at the cervical region (de Jongh et al., 2007, Kim et al., 2007) or the lumbar region (DeZee et al., 2007, Christophy et al., 2011).

1.2 Research Objectives

A validated musculoskeletal model with a fully discretized whole spine has been first proposed by the author's research group (Huynh et al., 2013) using the software LifeMOD. This model has already been applied in the investigation of the effects of sitting postures on the human body (Huang et al., 2012) and the development of scoliotic spine models (Gibson and Liu, 2013, Hajizadeh et al., 2012b). In this thesis, the musculoskeletal model of human body with the fully discretized spine model (Figure 1.1), established according to the anthropometric data and referring to the procedures in the paper by Huynh et al. (Huynh et al., 2013), was used in the inverse and forward dynamic simulations for the analysis of loading conditions of spinal joints in sitting posture and seat design.

The main aim of this thesis is to investigate the effects of sitting posture and seat design on spinal biomechanics for both healthy people and patients with scoliosis using the musculoskeletal modeling. The main research methodology is based on the multi-body musculoskeletal modeling using LifeMOD. For the study about sitting posture, the motion data of the experimental subjects were captured and integrated to drive the computational simulations.
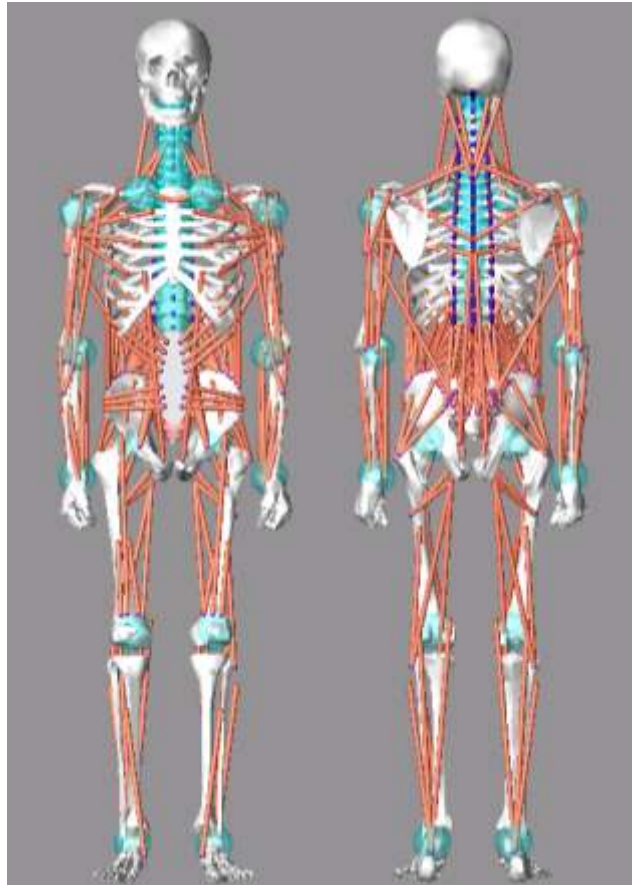
Figure 1.1 The musculoskeletal human body with the enhanced spine model

Since the mechanical load distribution of spine is a crucial factor in the ergonomics and physiotherapy areas (Bakker et al., 2009, Hoogendoorn et al., 1999, Marras et al., 1995), the loading condition of intervertebral joints is the main focus of this thesis. The term "intervertebral joint" used here includes not only the intervertebral disc, but also the facet joints between two adjacent vertebrae. The specific objectives of this research are:

- To propose an procedure to study the loading conditions of intervertebral joints in standing and sitting postures through motion capture experiments and musculoskeletal modeling of healthy subjects;

- To investigate the influence of varying seat design parameters on compressive loads of intervertebral joint;

- To study the sitting stability of people with scoliosis and the corresponding improvement strategies.

1.3 Outline of Thesis

This thesis includes six chapters which can be summarized as follows: Chapter 1 introduces the overall background of the research topic, the objectives, and the outline of this thesis. Chapter 2 presents a detailed literature review of this thesis with four main topics: human spine, sitting posture, seat design and spine modeling. The research work is introduced and discussed in detail in the following three chapters. The spine angles and compressive forces of intervertebral joints in standing and sitting postures of healthy people are provided in Chapter 3. The influence of different seat design parameters, including backrest inclination, seat pan inclination, seat pan height, seat pan depth and backrest height, on the spinal joint forces is shown in Chapter 4. The study of sitting stability of people with scoliosis is presented in Chapter 5. Finally, the conclusions and some suggestions for the future studies are documented in Chapter 6.

CHAPTER 2

LITERATURE REVIEW

In this chapter, an overview of human spine is first introduced. Next, a review of studies about sitting posture in the past decades is presented, followed by a history of seat design. The review highlights the development of the spine modeling method applied in this thesis. A short summary is provided in the end.

2.1 Human Spine

The spine is a crucial and complex structure in the human body. It offers main upright support for the human body and protection to the spinal cord and the nerve roots. Meanwhile, it allows the body to perform different motions, such as bending and rotating. In order to understand the spinal biomechanics and find the solutions to engineering related problems, the basic knowledge of human spine is necessary.

2.1.1 Spinal anatomy

The human spine consists of 33 vertebrae, which are stacked on top of each other to form the spinal column. These hard elements can be divided into five regions as shown in Figure 2.1: seven cervical vertebrae (C1-C7), twelve thoracic vertebrae (T1-T12), five lumbar vertebrae (L1-L5), five sacral vertebrae (S1-S5) and fused four coccygeal vertebrae. The size of vertebra increases slightly and gradually from T1 to L5, which helps to support larger muscles in the lower back area.

Although different in sizes, the components of vertebrae are almost the same (Figure 2.2). The largest part of vertebra is called the vertebral body, which appears cylindrical and is on the anterior side of the spinal column. Facet joints are paired joints which are found on the posterior side of the spinal column. Each vertebra has two facet joints connecting the upper and lower vertebrae. The surfaces of facet joints

are covered by cartilage which smoothens the glide between two vertebrae. There is one pedicle on each side of the vertebra on the posterior side of spinal column, which helps form a ring to protect the spinal cord.
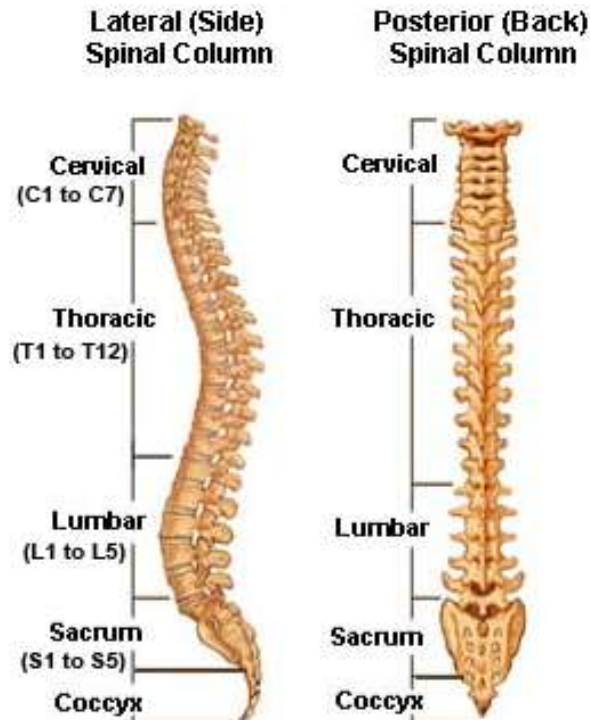
Figure 2.1 Spinal column (Bridwell, 2013)
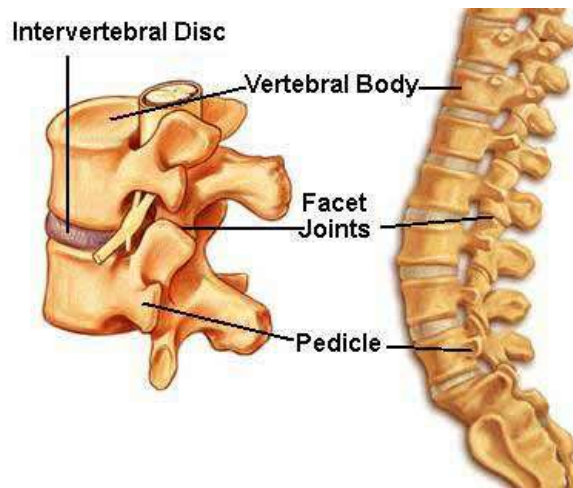
Figure 2.2 Components of vertebrae (Garfin, 2012)

The soft tissue structures located between two vertebrae from C1 to L5 are intervertebral discs (Figure 2.2). They separate the spine into individual segments, enabling the angular motion in the sagittal and frontal planes. The intervertebral disc is composed of two elements: the inner nucleus pulposus and the outer surrounding

annulus fibrosus (Figure 2.3). The annulus fibrosus mainly supports the axial loading on the intervertebral disc. The nucleus pulposus, containing a semi-fluid substance - proteoglycans, helps prevent the buckling of the annulus. When the disc is under compression, the fluid of the nucleus pulposus generates pressure at the inner surface of the annulus to prevent the inward buckling of the lamellae of collagen fibers which make up the outer annulus fibrosus. The inner nucleus pulposus also functions as a shock absorber for the spine to prevent any related injury due to a sudden impact.
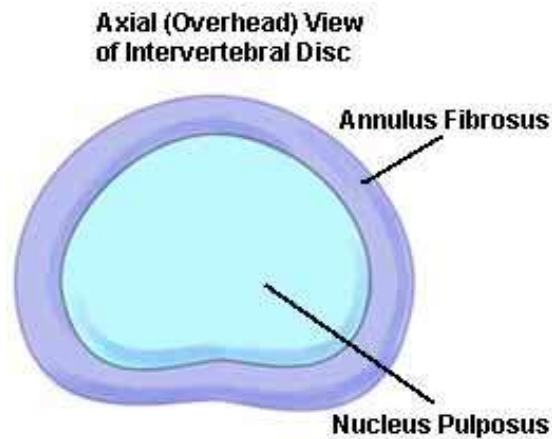
Figure 2.3 Two elements of intervertebral disc (Bridwell, 2010)
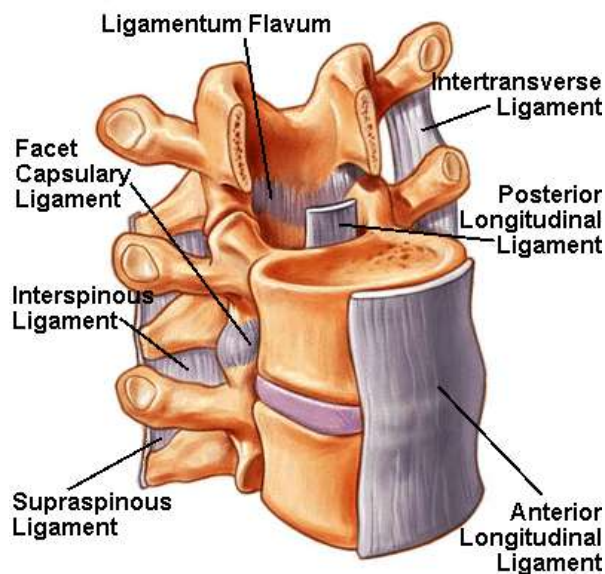
Figure 2.4 Spinal ligaments (Eidelson, 2012)

Ligaments and muscles are both very important and necessary for the good functioning of spine. Seven types of spinal ligaments are shown in Figure 2.4: anterior longitudinal ligament, posterior longitudinal ligament, intertransverse ligament, ligamentum flavum, facet capsulary ligament, interspinous ligament and supraspinous ligament, with the most important being the anterior longitudinal ligament and the

posterior longitudinal ligament from the skull all the way down to the sacrum. The main functions of ligaments are to separate bones of joints and prevent severe movements of vertebrae by limiting the mobility of joints. Various muscles are also attached to the spine. The main functions of muscles are to maintain the posture of spine, control the movement of trunk and protect the spine against external forces. Generally, the large muscles are responsible for producing larger trunk movements and providing stiffness, and the small muscles control the precise movements (Panjabi and White, 1990). Basically the cervical muscles aim to maintain the position of head accurately against gravity. The thoracic muscles are responsible for the stabilization of neck and the movement of scapula. The lumbar muscles serve to control the movement of truck and maintain trunk stability (Levangie and Norkin, 2001). Muscles and ligaments work together and play crucial roles in supporting the spine, providing stability and controlling the spinal movements.

2.1.2 Spinal motion

A healthy spine provides the main support for human body to allow movements in three planes. In general, there are some differences among the motions of spinal regions. For example, the cervical spine, which supports the human head, is more flexible to enable wide range of motion: rotation to left and right and flexion from up to down. The mid-back region, also termed as thoracic spine, is relatively immobile with attached ribs. Meantime, the lumbar spine, carrying the most weight of upper body, is quite flexible to allow movements of trunk. Compared to the other three regions, the sacrum and coccyx are much more fixed with little movements.

Forward bending   Backward Bending   Lateral bending   Rotation,
(flection)   (extension)   right and left   right and left
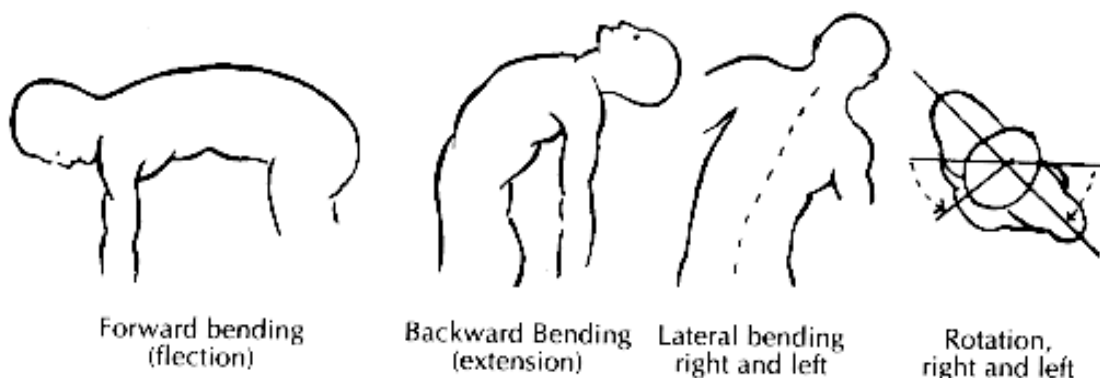
Figure 2.5 Motion of spine (WKC, 2006)

Motion of spine is usually measured in degrees of range of motion (ROM). The measured four movements are flexion, lateral flexion, extension and rotation

(Figure 2.5). The S-shape curve of a normal spine is able to absorb shock and maintain balance as a coiled spring to ensure of the full ROM. However, an abnormal curve of spine, such as lordosis, kyphosis and scoliosis, can lead to lots of restrictions in the spinal motion.

2.1.3 Spinal deformity

As one type of spinal deformity, scoliosis shows a curved spine for patient instead of a straight spine for healthy people in the frontal plane (Figure 2.6). It can be classified into three types according to the causes for the deformation: congenital, idiopathic and neuromuscular scoliosis. Among these, adolescent idiopathic scoliosis is the most common type in daily life. The exact reasons for idiopathic scoliosis have not been fully understood yet. However it is suggested that it is related to several factors, such as heredity, genetics, neuromotor mechanisms, muscular disorders, connective tissue problems and hormonal system dysfunction (Kurtz and Edidin, 2006). Usually, spinal instrumentation and fusion are applied for severe cases of scoliosis to stabilize and straighten the spinal curvature. The recommended treatments for the non-serious scoliosis include trunk support, braces, jackets, internal structures, etc.
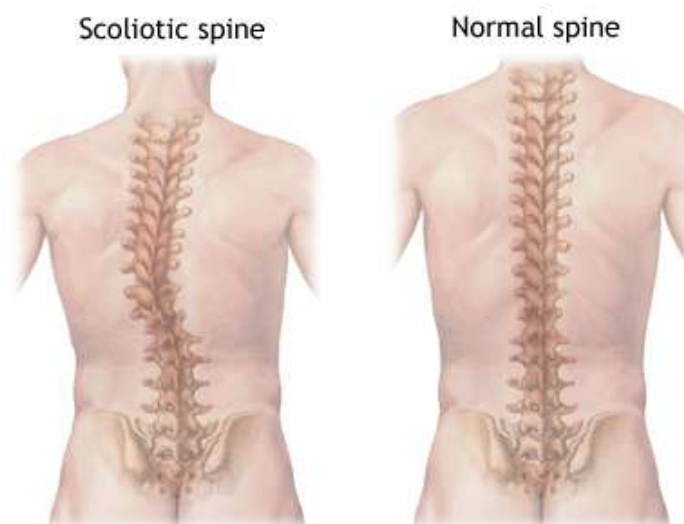
Figure 2.6 Scoliotic spine and normal spine (Mannheim, 2012)

The curvature of scoliosis is usually measured by the Cobb's method (Figure 2.7). The Cobb angle is defined to be the angle between the lines drawn perpendicular to the endplates of the most tilted vertebra above the apex and the most tilted vertebra below the apex. The curve patterns of idiopathic scoliosis can be divided into two

categories: the primary curve and the compensatory curve. The primary curve usually indicates the curves with a larger Cobb angle. The curve with a smaller Cobb angle is called the compensatory curve. The location of curve is identified by the position of the apex of scoliotic curvature. For example, a curve with the apex in the lumbar region is called the lumbar curve.
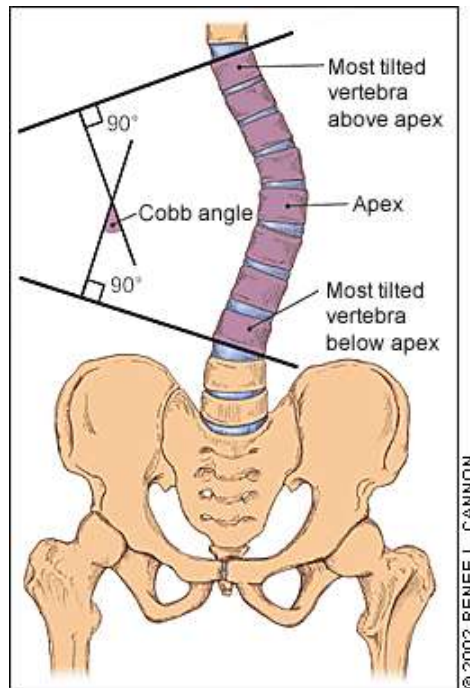
Figure 2.7 The Cobb method of measuring the degree of scoliosis (Greiner, 2002)

thoracic curve   thoracolumbar curve   lumbar curve   double major curve
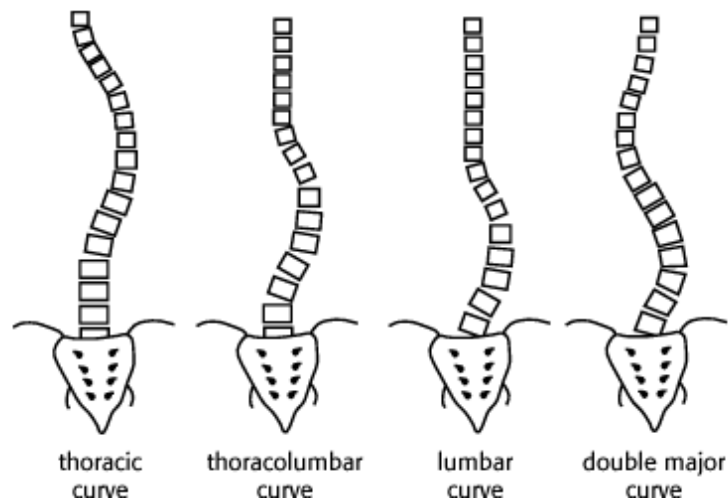
Figure 2.8 Patterns of scoliosis (UWmedicine)

Based on the shape, pattern and location, idiopathic scoliosis curves can be classified into the following four categories (Figure 2.8):

- Thoracic curve: The curve usually extends from T5 or T6 to T11 or T12, with the apex at T10 or higher vertebra;

11

- Thoracolumbar curve: The curve usually extends from T8 to L3, with the apex at the junction between the thoracic and lumbar regions (around T12 or L1);

- Lumbar curve: The curve usually extends from T11 to L4;

- Double major curve: The curve usually extends from T5 to T12 in the thoracic region and from T12 to T4 in the lumbar region, showing two primary curve patterns.

2.2 Sitting Posture

Sitting posture is one of the most important factors in the study of human sitting. Extensive studies have been conducted to evaluate different sitting postures. As early as 1953, Keegan (Keegan, 1953) radiographed 4 subjects in different standing and sitting postures to understand the lumbar spine movements in the sagittal plane. Schoberth (Schoberth, 1962) defined sitting postures into three categories according to the location of center of gravity and the weight transmitted to the ground by feet. In a middle position, the lumbar part is almost straight or appears to be a little kyphosis. A kyphosis of spine or a significant rotation of pelvis is needed in the anterior and posterior sitting postures.

It has been suggested that poor sitting postures can link to pains and other complications for people in daily life in literature (Kirkaldy et al., 1999, Kottke, 1961, McKenzie and May, 1981). Lumbar discomfort is a common problem which has happened to people with prolonged sitting. Results showed that many regular posture changes are an indicator of discomfort of subjects. The two main reasons for an increase of discomfort are found to be lumbar lordotic posture and lower mobility (Vergara and Page, 2002). Adjusting ischial and backrest supports during sitting may be one solution for LBP. A study, including 15 office workers without LBP, showed that sitting with reduced ischial support and fitted backrest to lower back can potentially reduce the onset of LBP (Makhsous et al., 2003).

Some pioneering studies carried out by Nachemson et al. (Nachemson, 1966, Nachemson and Morris, 1964, Nachemson, 1981) have helped to pave the way in direct measurements of pressure in the intervertebral disc. Seventeen postures and related actions were studied including sitting, standing, lying, jumping, etc. In 1999, Sato et al. (Sato et al., 1999) measured both the vertical and horizontal pressures in

L4-L5 disc in a range of postures using an advanced pressure sensor. In the same year, Wilke et al. (Wilke et al., 1999, Wilke et al., 2001) recorded the data of intradiscal pressure among different human body postures through telemetry, with a transducer implanted into the subject's body. All these researches have contributed a lot to the understanding of human body biomechanics and provided data sets for the validation of computational models. It has been suggested that sitting can introduce higher intradiscal pressure than standing, which can cause the disc degeneration and LBP (Andersson and Ortengren, 1974a, Andersson et al., 1974b, Andersson et al., 1974a, Nachemson, 1975, Nachemson and Morris, 1964).
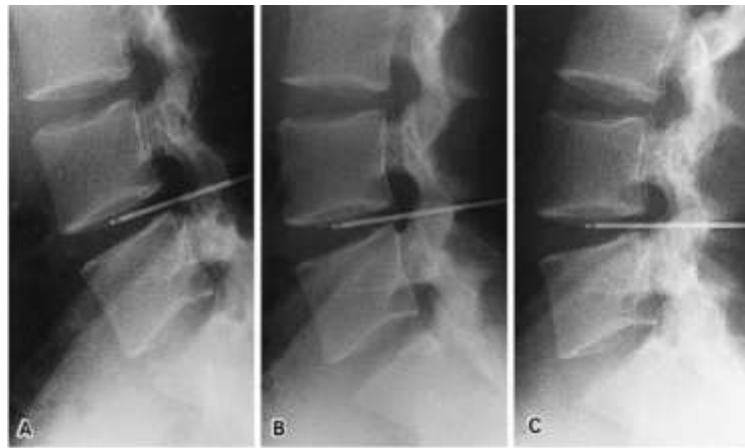
Figure 2.9 Direct measurement by inserting pressure transducer (Sato et al., 1999)

Studies carried out in the past decades, including direct measurements and indirect measurements of the pressure on the intervertebral disc (Levangie and Norkin, 2001), help people gain an insight into the difference between standing and sitting. For the direct measurements, inserted pressure transducers were used to measure the pressure on the intervertebral disc for the *in vivo* experiments, as shown in Figure 2.9. The measured results of intradiscal pressure in sitting and standing postures by direct measurements are shown in Figure 2.10. Table 2.1 shows more information about these studies. It is observed that the mean values of intradiscal pressure in both sitting and standing postures in the earlier studies using liquid-filled transducer for subjects with LBP are higher than in the more recent studies using piezoresistive transducer for subjects without LBP. Besides the large variation among studies, there is also a large variation demonstrated among subjects, such as the results of the study by Sato et al. (Sato et al., 1999). In another more recent study carried out by Wilke et al. (Wilke et al., 1999), the difference of intradiscal pressure between standing and sitting was found not significant. However, the result of this study needs to be considered

with caution, since only one subject was included in the experiments. Generally, it is found that most of the researches using direct measurements (Andersson and Ortengren, 1974a, Nachemson, 1965, Nachemson and Elfstrom, 1970, Nachemson and Morris, 1964, Okushima, 1970, Sato et al., 1999, Schultz et al., 1982) found that the intradiscal pressure in standing is lower than that in sitting.
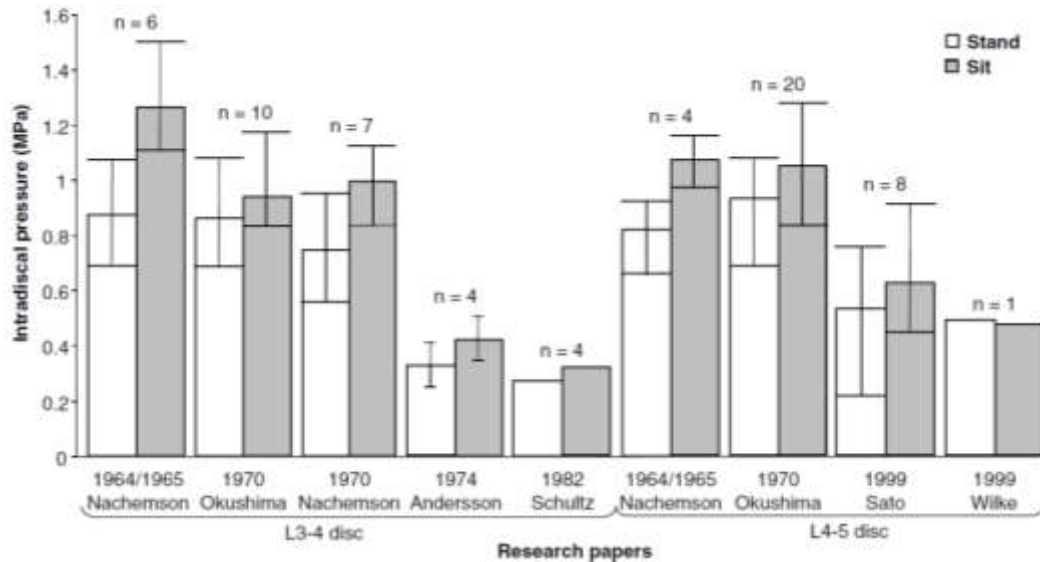
Figure 2.10 The results of mean intradiscal pressure by direct measurements and the number of subjects in researches from 1964 to 1999 (Claus et al., 2008)

Table 2.1 Comparison of subjects and studies by direct measurement (Claus et al., 2008)

Author	Year	L3-4, n	L4-5, n	LBP	Transducer
Nachemson	1964/1965	6	4	Yes	Liquid-filled
Okushima	1970	10	20	Yes	Liquid-filled
Nachemson and Elfstrom	1970	7		No	Piezoresistive
Andersson et al.	1974	4		No	Piezoresistive
Schultz et al.	1982	4		No	Piezoresistive
Sato et al.	1999		8	No	Piezoresistive
Wilke et al.	1999		1	No	Piezoresistive

Different from the direct approach, indirect measurements of intradiscal pressure are inferred by the measurements of spinal shrinkage and load-cell equipped spinal fixators (Claus et al., 2008). The results of these studies (Althoff et al., 1992, Leivseth and Drerup, 1997, Rohlmann et al., 2001) by indirect measurements showed that more intradiscal compression is indicated in standing than in sitting, which is contrary to the findings from the direct measurements. Overall, the results of these

researches provide a conclusion that there have been some disagreements on the comparison of intradiscal pressures in standing and sitting postures for healthy subjects. Based on the literature review, it is also found that the results of intradiscal pressure measurement can be greatly affected by the experimental methodology. Every experimental approach has its own limitation. Direct measurements by *in vivo* experiments depend on the transducer technology and the calibration. On the other hand, indirect measurements suffer from a small size effect (Claus et al., 2008).

In the case of people with scoliosis, the sitting situation is not optimistic. A straight and stable spine is good for functioning, hence the human body is able to support the upper trunk without using arms (Fujita et al., 2005). For a normal sitting, the support of body comes from ischial tuberosities and upper legs. The center of weight is in the midline of upper body (Myhr et al., 1995). Smith et al. (Smith and Emans, 1992) measured the weight distribution of normal and scoliosis subjects in sitting posture with a pressure plate system, and found normal subjects placed up to 60% of the body weight on one side. They defined the asymmetric sitting as greater than 60% of the body weight on one side. It is found in their study that patients with idiopathic scoliosis, especially in the presence of lumbar curves, suffer from the unbalanced sitting when compared with normal subjects. Similar results were also found in another study by Larsson et al. (Larsson et al., 2002). Harms (Harms, 1990) suggested that the key of maintaining a good sitting posture is the proper position of pelvic and the related lumbar spine. Therefore a good understanding of sitting balance is very important and necessary for the assessment of patients with scoliosis and before any surgical treatment (Smith and Emans, 1992).

2.3 Seat Design

Even before 1950, some variables about seat design had been studied by researcher (Staffel, 1884), which included seat-bottom height, seat-bottom incline, seat-bottom contour, seat-bottom width, seat-bottom length, seat-back tilt inclination, seat-back lumbar support, seat-back height, muscle activity, thigh angle to trunk, knee angle and footrest position. The importance of these aspects during seat design were listed by Keegan (Keegan, 1953). According to his conclusion, the importance of design factors (Figure 2.11) are numbered from the most important to least important

in the following order: 1. lumbar support; 2. minimum 105° tilt angle of backrest; 3. open space for posteriorly projecting sacrum and buttocks; 4. convex thoracic support with height to lower scapulae; 5. shoulder support at 105°; 6. any adjustable tilt of seat back pivoted on a point in line with the hip joints; 7. maximum length of seat bottom (16 in); 8. seat-bottom height above floor (16 in); 9. seat bottom curved down under back of knees; 10. free space for feet under seat bottom; and 11. upward tilt of seat bottom of 5° for maintenance of back against back support.
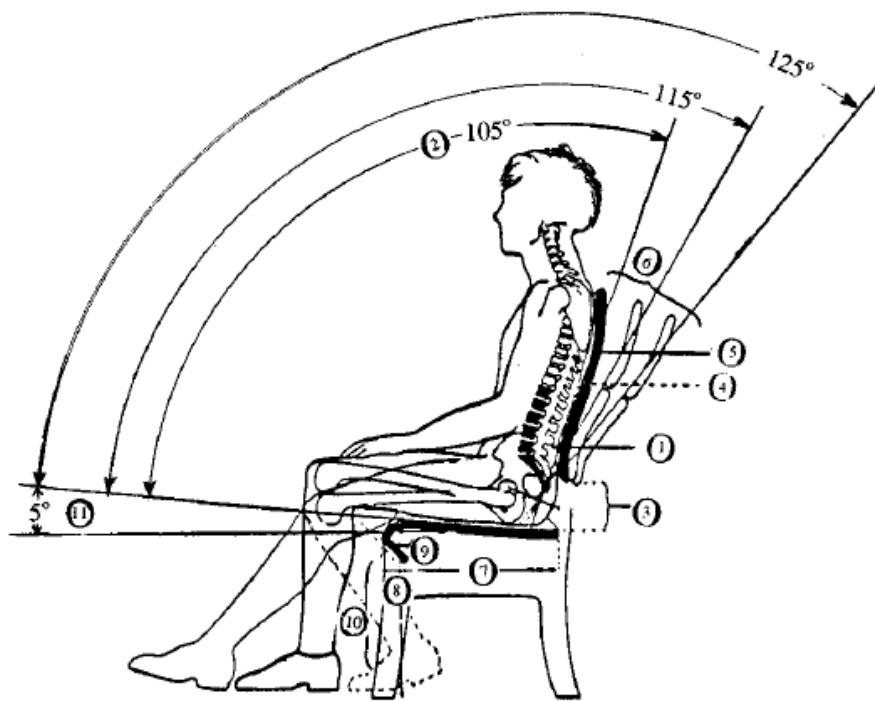
Figure 2.11 Eleven aspects of seat design (Keegan, 1953)

After studying the supporting systems for 104 subjects in 1962, Sweringen et al. (Swearingen, 1962) concluded that 64.8% of body weight is supported by the 8% of seat area under ischium. The remaining 35.2% is for the footrests (18.4%), armrests (12.4%) and backrest (4.4%). Hence the variables related to seat pan are very important in the seat design, such as seat pan inclination, seat pan depth, seat pan height and seat pan contour. Among all these variables, the inclination of seat pan has always been a debatable topic in the past century. Initially, forward slope of seat pan was suggested by Staffel (Staffel, 1884) in 1884. However, later in 1905, Schulthess (Schulthess, 1905) recommended 3° to 5° backward inclination. These different seat pan inclinations were also investigated by other research groups in the following decades. For example in 1958, Floyd et al. (Floyd and Roberts, 1958) suggested that

the inclination of seat pan should be adjusted according to the job requirements. Seat pan depth, if is too long, can make shorter people neglect the backrest and lumbar support (Bennett, 1928, Hooton et al., 1970). There is a same situation when the seat pan is too high (Wilke et al., 1999). It is noted that a short person who sits on a high chair would like to move to the edge of chair and not use the backrest or lumbar support. It is concluded that the dangling legs, caused by the high chair, can lead to the compression stresses on the soft tissues of the posterior thigh and the discomforting feeling to the sitting person. Various contours of seat pan have also been discussed. A flat surface has been proposed to be the optimal design for the seat pan (Bennett, 1928). A seat pan with surface full of vertical elements, which depress linearly by the pressure, was used by Brienze et al. (Brienza et al., 1996) to investigate the pressure distribution of seating interface.

It is believed that stability in sitting was achieved by the backrest of the seat (Swearingen, 1962). A lot of researches have been conducted to study the inclination of backrest. It was suggested that the optimal inclination should be from 90° to 125° (Schulthess, Schede, 1935, Lay and Fisher, 1940, Morant, 1947, Kroemer, 1971). The optimal seat back inclination and size of lumbar support were also researched by Knutsson et al. (Knutsson et al., 1966) by the application of electromyography. The results showed that usually 110° backrest inclination and 1-2 cm of lumbar support are a better fit for people. However, the subjects with serious disc degeneration prefer 100° backrest. It was concluded in a study in 1948 that the lumbar support in sitting posture can provide enough rest for the back muscles (Åkerblom, 1948). In 1984, Majeske et al. (Majeske and Buchanan, 1984) found that the various joint angles are much more normal when the people sit with lumbar support. Reduced LBP and leg pain were recorded in another study in 1997 (Sato et al., 1999).

Adjustable armrests are very useful by decreasing the load on spinal column and helping people change posture. However, they become unnecessary if people need free mobility when sitting (Kroemer, 1971). After 1970, head restraints became a topic in the study of automobile impact. It showed that during whiplash the head restraints are quite useful in reducing the extension strains, which is an important factor in whiplash (Grauer et al., 1997).

Overall, it was suggested that seat design should always be combined with the effect of job requirements, task involved and work space design. Although there is no

perfect seat, according to the research, certain governing rules of chair design remain unchanged (Brunswic, 1984). Lengsfeld et al. (Lengsfeld et al., 2000) investigated lumbar spine curvature by multi-body analysis interfacing a human model with two different office chair models. In that study, it was concluded that from the point of view of the lumbar spine kinematics, a synchro tilt concept with a posterior tilt of seat while the backrest is reclined is more suitable for the human body, because of the evenly distributed lumbar lordosis. Another example is an experiment carried out by Tewari et al. (Tewari and Prasad, 2000) to measure the pressure distribution on different seat pans and backrests of a tractor seat. It was shown that the seat pan, the backrest profile curvature and the backrest inclination have effects on the body pressure distribution.

2.4 Spine Modeling

As one potential risk factor for LBP and disc degeneration, the mechanical load distribution of spine is a crucial research topic in the areas of ergonomics and physiotherapy (Bakker et al., 2009, Hoogendoorn et al., 1999, Marras et al., 1995). Although several researches about *in vivo* measurements (Andersson and Ortengren, 1974a, Nachemson, 1965, Nachemson and Elfstrom, 1970, Nachemson and Morris, 1964, Okushima, 1970, Sato et al., 1999, Schultz et al., 1982, Wilke et al., 1999, Wilke et al., 2001) have been conducted in the past years and significantly contributed to the understanding of spinal biomechanics without doubts, the invasive effects of the inserted load transducers cannot be ignored and the amount of results is limited due to the fact that usually the pressure of only one intervertebral disc is measured and obtained.

For the purpose of a deeper exploration and research of spinal biomechanics, two types of computer models have been developed and applied in the past decades: MBMs and FEMs. Although FEM is definitely very useful for the study of spinal biomechanics and often is the only way in some situations, it is usually applied for the local study of the stress and deformation of segment, in consideration of the effects of one or two motion segments (Belytschko et al., 1974, Bozic et al., 1994, Greaves et al., 2008, Kumaresan et al., 1999, Shirazi-Adl et al., 1986, Teo and Ng, 2001, Yoganandan et al., 1996), or a series of vertebrae (Zander et al., 2002, Seidel et al.,

2001, Schmidt et al., 2008, Pankoke et al., 1998, Zhang et al., 2005, Maurel et al., 1997, Goel et al., 1994). However for the MBM, the detailed musculoskeletal human body calculation model can be established and applied for the simulation of kinematics and kinetics of the whole human body (Roberson and Schwertassek, 1988). This type of model can provide the insight for the whole spine in consideration of the effects of segments, connecting joints, and soft tissues in the whole body during dynamic simulation, which is not able to be obtained easily by the FEMs. It also skips the considerable computational power and convergence problems which FEMs may suffer from.

Several researches (Chaffin, 1969, Bogduk et al., 1992a, Macintosh et al., 1993, McGill and Norman, 1986, Stokes and Gardner-Morse, 1995, van Dieën, 1997) have been done to study the biomechanics of spine by the application of multi-body musculoskeletal models in the past decades. Recently, DeZee et al. (DeZee et al., 2007) presented a generic detailed rigid-body lumbar spine model in 2007. This model was used to investigate the influence of seat pan inclination and friction on the internal forces in seated body (Rasmussen et al., 2009) and study the long-distance driving fatigue (Grujicic et al., 2010). In 2011, Christophy et al. (Christophy et al., 2011) built a musculoskeletal model for lumbar spine, which is able to be applied to predict the joint reactions, muscle forces and muscle activation patterns.

LifeMOD is a commercial human simulation software package based on MD ADAMS (MSC. Software). Numerous studies about the spinal biomechanics have been conducted using LifeMOD. For example, a musculoskeletal human and a wheelchair model were developed to analyze the cervical spine injury in the frontal and side impacts (Kim et al., 2007). A dynamic simulation of cervical spine with a disc implant in the C5-C6 segment was conducted. The obtained results of intradiscal forces, bending moments and vertebrae rotation were compared with the other results in literature (de Jongh et al., 2007).

In the author's research group, a detailed spine model was first developed by Kwang et al. (Kwang et al., 2009), which is able to help develop a design system to simulate kinematic behavior of musculoskeletal forms and generate a human-wheelchair interface to offer effective design solutions for people suffering from long-term sitting. Later, Huynh (Huynh et al., 2013, Huynh, 2010) presented a more detailed spine model. This was obtained by refining the three spine segments (cervical,

thoracic and lumbar regions) into individual vertebra segments, using joints to represent the intervertebral discs, and creating additional ligaments, lumbar muscles and abdominal muscles. This multi-body musculoskeletal human body with detailed spine model has been validated by two comparison studies. The results of these two studies were in consistent with those from the literature. In the first study, with the same extension moment generated in the upright position, the axial and shear forces in the L5-S1 joint calculated in the model were compared to those obtained from the experimental data (McGill and Norman, 1987b) and another spine model (DeZee et al., 2007). In the second study, while a subject holding a crate weighing 19.8kg, the axial force of the L4-L5 joint was computed and compared to the *in vivo* intradiscal pressure measurements (Wilke et al., 2001). Different from the other spine models by other research groups which only include the basic cervical spine (de Jongh et al., 2007, Kim et al., 2007) or the discretized lumbar region of the spine (DeZee et al., 2007, Christophy et al., 2011), Huynh's model (Huynh et al., 2013, Huynh, 2010) is much more detailed, which includes a fully discretized whole spine (cervical, thoracic and lumbar regions) and can be used to study the biomechanics of the whole spine. This multi-body musculoskeletal model has already been applied to the preliminarily investigation of the effects of sitting posture on human body (Huang et al., 2012) and develop musculoskeletal scoliotic spine models (Gibson and Liu, 2013, Hajizadeh et al., 2012b).

In order to simulate the dynamic movements of spine in reality, the motion data of related body segments or the whole body in the three dimensional (3D) space is very important. A complete and accurate motion data can be applied to drive the musculoskeletal model to perform the expected movements for the dynamic analysis. It is suggested that the method of video-based 3D person tracking performs quite well with multiple cameras and background subtraction (Balan et al., 2005). Some researches have been carried out with this method to study the kinematic and kinetics of human spine. A dynamic biomechanical model to determine joint loads was developed by Khoo et al. (Khoo et al., 1995). With the application of Vicon motion analysis system, it was found from their results that the peak lumbosacral loads during walking were between 1.45 and 2.07 times body-weight. The same model was applied later by Goh et al. (Goh et al., 1998) to investigate the effects of varying backpack loads on the peak lumboscral force through experiments using a 5-camera Vicon

motion analysis system. Another whole-body model was created to calculate the compression forces in the lumbar spine during asymmetrical lifting. The kinematic data from the Vicon 3D motion analysis system are served as drivers for the joints (Deuretzbacher and Rehder, 1995). An improved kinematic model of the spine was developed by another research group for the 3D motion analysis in the Vicon system. This model is able to perform dynamic analysis of movements of all the vertebrae (Długosz et al., 2012). The method of optical motion capture system has also been applied to study the biomechanics of spinal deformity. The global posture and kinematic characteristics of scoliotic spines before and after operation were compared using Vicon system (Ployon et al., 1997). A spine and rib cage model is applied to quantify clinical measurements in adolescent idiopathic scoliosis (Tulchin et al., 1999). The repeatability of spinal motion of normal and scoliotic adolescents during walking using the Vicon system was studied (Chan et al., 2006). The measurements of trunk sagittal and fontal plane motion, and spinal frontal plane motion of normal and scoliotic subjects were suggested to be reliable with a single test session. All these examples show that with the help of optical motion capture system, the body model is able to present realistic 3D movements of body segments and perform the analysis of dynamic motion.

2.5 Summary

In summary, the mechanical loading distribution of spine in sitting posture is very important but has not been fully understood yet. There are also seldom quantitative studies about seat design parameters and sitting stability of people with scoliosis in literature. One possible reason can be the limitations of previous experiment approaches. The direct measurements of intradiscal pressure in the *in vivo* experiments suffer from the invasive effect on human body and the dependency on transducer technology and calibration, while the indirect measurements show a small size effect.

Poor sitting posture and improper seat design can lead to discomfort and some health problems with the human body in daily life. Meanwhile, more attention should be paid to the sitting situation of people with scoliosis, who suffer from the unbalanced sitting due to the spinal deformity. As a non-invasive approach, multi-

body musculoskeletal human body modeling can provide a deeper exploration of spinal biomechanics through computational simulation. With the application of 3D motion capture system, accurate movement information of body segments can be coupled with the musculoskeletal body model to investigate the spinal biomechanics during dynamic motion.

CHAPTER 3

ANALYSIS OF COMMONLY ADOPTED STANDING AND SITTING POSTURES

3.1 Introduction

Recently, LBP has emerged as a common healthcare problem (Luoma et al., 2000). Poor sitting posture in daily life is regarded as the main contributing factor in the development of LBP (Kirkaldy et al., 1999, Kottke, 1961, McKenzie and May, 1981). In addition, as discussed previously in Chapter 2, there have been some disagreements on the comparison of intradiscal pressures in standing and sitting postures in literature.

The mechanical loading condition of spine in different postures is a very important research topic but has not been fully investigated yet. Therefore, the objective of this research is to develop a procedure to analyze the effects of the standing and sitting postures on the loading conditions of the intervertebral joint through motion capture and musculoskeletal modeling of healthy subjects. The novelty of this research is the development of human body sitting models based on the combination of the motion capture experiment and the virtual musculoskeletal multi-body modeling.

The general method applied in this chapter is a combination of motion capture using Vicon MX system and musculoskeletal modeling using LifeMOD software, as shown in Figure 3.1. At the beginning of the study, measurements are first conducted to obtain the anthropometric data of subjects. The process of the motion capture experiment is shown in the lift side of Figure 3.1. After attaching the retro-reflective markers on the segments of subject body, the healthy subject performs various postures for the motion capture system to collect dynamic motion data. After data

processing, the segment angles and motion data containing the marker trajectories can be obtained. On the other hand, the musculoskeletal modeling (right side of Figure 3.1) begins with the development of a subject model, including creating segments, connecting joints, soft tissues, etc. After the establishment of the human body model, contacts are defined between the human body model and the environment. Next, the motion data of marker trajectories obtained in the motion capture experiment is imported into the LifeMOD system to drive the human body model in inverse and forward dynamic simulations. After the simulation analysis, results about joint loads can be obtained as the final outputs. The detailed information about the process of this method is provided in the following sections.
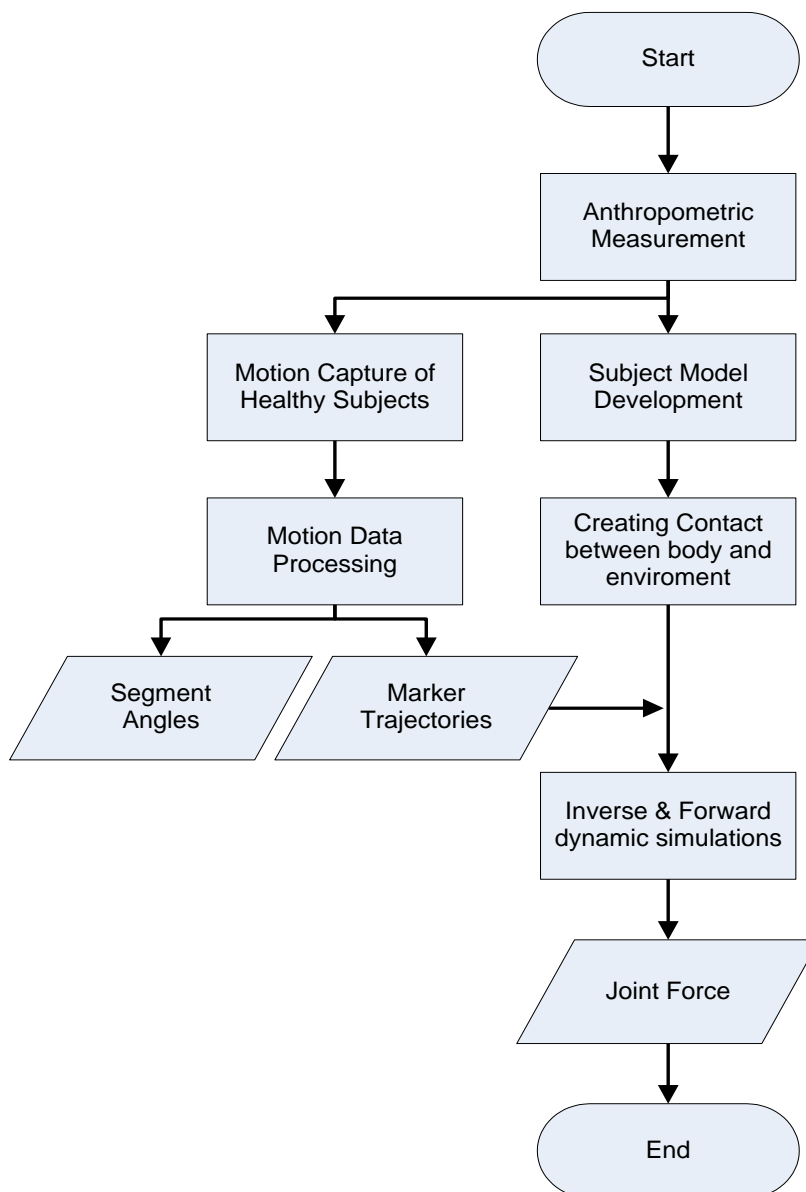
Figure 3.1 Flow chart of method of motion capture and musculoskeletal modeling in the sitting posture study

There are two studies presented in this chapter. The preliminary study on the one subject is to compare the extension and the flexion in standing and sitting postures. The focus of the final study with six subjects is on the compressive loading conditions of lumbar joints in various postures, including upright standing, upright sitting, slumped sitting, cross-legged sitting, flexion sitting and extension sitting. The results of this research may help in furthering the understanding on the difference in spinal loading condition between standing and sitting, and the differences among the common sitting postures adopted in daily life.

3.2 Overview of LifeMOD

As commercial human body modeling and simulation software, LifeMOD provides a basic human body model which can be further modified by editing the anthropometric data such as age, gender, height, weight, etc. The established human body model can be combined with the physical environment for dynamic interaction. The outputs of the simulation can be human motion, contact forces, and internal forces of joints and soft tissues. Generally speaking, there are two types of models in LifeMOD: the passive model and the active model. The passive model, which is reactive to the external environment, is usually applied in the studies of crash dummies and the body's reaction to the external stimuli. In this thesis, the active model, which causes reactions in the environment, is used for the studies of sitting posture and seat design.

The general human modeling paradigm in LifeMOD is shown in Figure 3.2. The development of the human body model starts with the generation of the basic elements, such as body segments, joints, soft tissues, motions and contacts. The detailed information of the basic elements is provided later in the following paragraphs and sections. After the simulations, the test data can be imported and validated to determine whether the result is desired. Otherwise, refinement can be conducted by changing the fidelity of joints, segments, soft tissues or the environment to run the simulations again. If the desired result has been achieved, the study can be further optimized through investigation of design sensitivity, experiment design, etc.
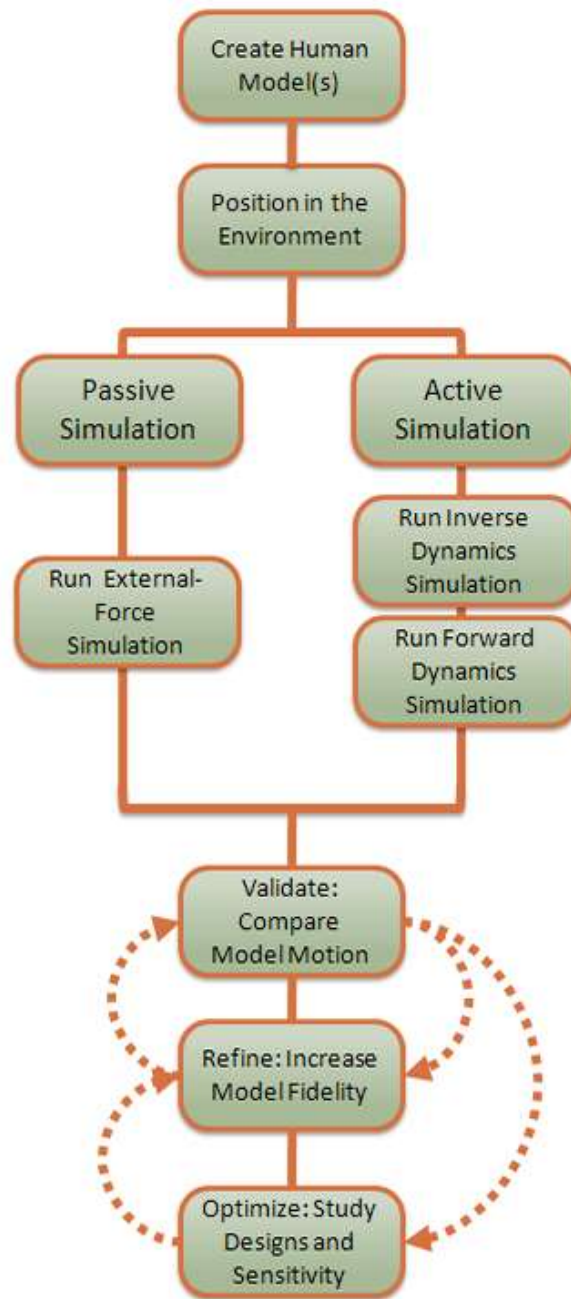
Figure 3.2 The general human modeling paradigm in LifeMOD (LifeModeler)

The body segments are represented by the rigid bodies in LifeMOD, which can be created from the anthropometric databases. The database used in this thesis is the GeBOD database, which is developed by the Modeling and Analysis Branch of the Air Force Aerospace Medical Research Laboratory and the University of Dayton Research Institute. It can create a human body model according to the simple information, such as height, weight, age and gender. As shown in Figure 3.3, the body parameters of the created human body model can also be further modified by the user, including the shoulder height, armpit height, waist height, etc. This is a very useful

26

and necessary tool for developing musculoskeletal models for different experiment subjects in this chapter. The measured anthropometric data of each subject can be used as inputs to generate the individual musculoskeletal body model. Although the measurement process for each subject is quite time-consuming, it can enable the software to generate the most accurate musculoskeletal model for the subject based on the individual anthropometric data.

LifeMOD - Body Segment Measurement Table

BODY MEASUREMENT TABLE (length data displayed in inches)

(•) Male ( ) Female ( ) Child ( ) Non-Human   (•) Hands Gripping ( ) Hands Open

Age (months)	312.0	Waist_Depth	8.9	Left Knee Ht Seated	22.9
Weight (lbs)	178.0	Waist Breadth	12.4	Right Thigh Circum.	22.8
Standing_Height	72.0	Buttock Depth	9.5	Left Thigh Circum.	22.8
Right Shoulder Ht	59.2	Hip Breadth Standing	14.9	Right Upper Leg Circum.	15.3
Left Shoulder Ht	59.2	Right Shoulder To Elbow Ln	14.4	Left Upper Leg Circum.	15.3
Right Armpit Ht	56.2	Left Shoulder To Elbow Ln	14.4	Right Knee Circum.	15.4
Left Armpit Ht	56.2	Right Forearm Hand Length	19.9	Left Knee Circum.	15.4
Waist Height	48.0	Left Forearm Hand Length	19.9	Right Calf Circum.	14.9
Seated Height	39.7	Right Biceps Circumference	12.7	Left Calf Circum.	14.9
Head_Length	7.9	Left Biceps Circumference	12.7	Right Ankle Circum.	8.8
Head_Breadth	6.8	Right Elbow Circum.	12.7	Left Ankle Circum.	8.8
Head To Chin Ht	8.6	Left Elbow Circum.	12.7	Right Ankle Ht Outside	5.1
Neck Circum.	14.1	Right Forearm Circum.	10.6	Left Ankle Ht Outside	5.1
Shoulder Breadth	19.5	Left Forearm Circum.	10.6	Right Foot Breadth	3.9
Chest Depth	9.2	Right Wrist Circum.	7.8	Left Foot Breadth	3.9
Chest Breadth	11.7	Left Wrist Circum.	7.8	Right Foot Length	10.9
		Right Knee Ht Seated	22.9	Left Foot Length	10.9

Close   Apply

Figure 3.3 Further editing the body parameters of the created human body model from GeBOD database

In order to connect two adjoining body segments, the joints are created in LifeMOD. The joint is constituted by a tri-axis hinge and forces acting on each of the three degrees of freedom. In this thesis, passive joints are applied for the inverse dynamic analysis. This type of joint, as a torsional spring force with the user-defined properties such as stiffness, damping, angular limits and limit stiffness, can record the angulation patterns when the model is driven by the motion capture data in the inverse dynamics simulation. Then the trained PD-servo type controller, which can minimize the error between the desired joint angle and the recorded joint angle, is created on the joint axis by multiplying Pgain (or stiffness) by the error and Dgain (or damping) by the derivative of the error. The joint is programmed to repeat those patterns during the forward dynamic simulation, with a user-defined gain on the error between the actual

angle and the commanded error, and a user-defined derivative gain to control the derivative of the error.

There are two types of force-producing soft tissues in LifeMOD: ligaments and muscles. Ligaments are created as passive spring/dampers, and muscles include both trainable and active elements. The parameters in soft tissues include the physiological cross sectional area (pCSA), the maximum muscle force (F_{max}), etc. The data of pCSA is generated from the muscle geometry database compiled by the detailed information in literature (Schumacher and Wolff, 1966, Eycleshymer et al., 1911). It can be scaled based on the height, weight, gender and age of body model using a built-in decision tree algorithm or the allometric scaling (McMahon, 1984). The data of F_{max} is obtained by multiplying the value of pCSA by the value of maximum tissue stress derived from the literature (Hatze, 1981). In this way, the muscle properties of body model with different height, weight, gender and age can be generated by the scaling. This is very useful for the development of human body models of experiment subjects with various anthropometric data in this chapter.

In order to replicate the desired movement of the human body, the muscles generate the necessary forces based on the physiologically-determined equations and stay within individual muscle physiological limit in the meanwhile. The two major types of muscles applied in this thesis are the passive recording muscle (in the inverse dynamic simulation) and the closed loop muscle (in the forward dynamic simulation). The passive recording muscle, with functions based on a user-tunable spring damper, can record the movement patterns during the inverse dynamic simulation driven by the motion capture data. Then the closed loop muscles, including the proportional-integral-differential (PID) controllers, are applied in the forward dynamic simulation. The PID controller creates the muscle activation based on the recorded length/time curve of muscle movements. The closed loop algorithm is shown in the Equation 3.1.

$$F = P_{gain}(P_{error}) + I_{gain}(I_{error}) + D_{gain}(D_{error}) \qquad (3.1)$$

where

$P_{error} = (\text{target value} - \text{current value})/\text{range of motion}$

$I_{error} = \text{time integral of } P_{error}$

$D_{error} = \text{first derivative of } P_{error}$

3.3 Development of the Fully Discretized Multi-Body Spine Model

A basic human body model including 19 segments and 118 muscles (Figure 3.4) can be created by LifeMOD according to the inputs of anthropometric data of the body. However, the spine of the basic human body model is only divided into three segments: cervical, thoracic and lumbar regions. Hence, this basic human body model is not able to fulfill the objective of the detailed investigation of the mechanical loading conditions of spinal joints.
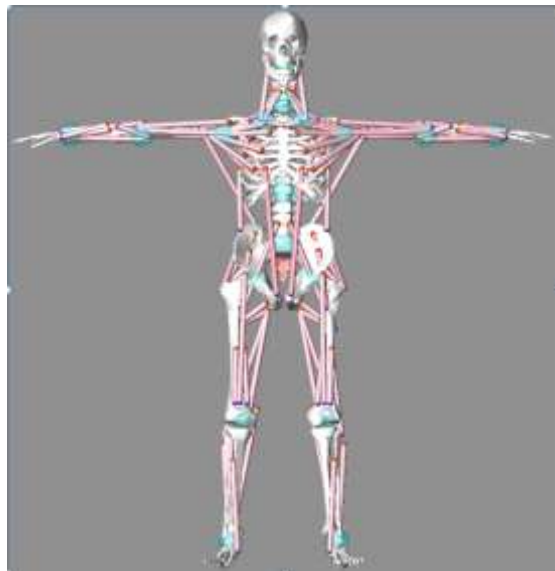
Figure 3.4 Basic human body model in LifeMOD

In order to solve this problem, a bio-fidelity discretized spine model is included in the modeling. The musculoskeletal model applied in this thesis is constituted by the basic human body model and the enhanced discretized spine model. For the discretized spine model, the spine is refined to be 24 individual vertebrae and 25 rotational joints are created to represent the inter-vertebral discs. Five types of ligaments (interspinous ligament, flaval ligament, anterior longitudinal ligament, posterior longitudinal ligament and capsule ligament), four types of lumber muscles (multifidus muscle, erector spinae muscle, psoas major muscle and quadratus lumborum muscle) and two types of abdominal muscles (obliquus externus and obliquus internus) are also implemented. The discretized spine model is developed by referring to the steps in literature (Huynh et al., 2013) and based on the anthropometric data of the experiment subject.

The detailed modeling process is shown in Figure 3.5. The general procedure starts from generating the segments of a basic human body followed by redefining the fidelity of individual segments. The modeling process begins with generating the basic segments, joints and muscle sets of human body in LifeMOD. After the development of a basic human body model, the spine region is discretized into individual vertebra by designating the location of center of mass and the orientation. Spinal joints are created to represent intervertebral discs between two adjacent vertebrae, as shown in Figure 3.6. The spinal joints are modeled as torsional spring forces, which are defined with user-defined properties, including stiffness, damping, angular limits and limit stiffness. The properties of spinal joints are referenced from literature (Table 3.1 and Table 3.2). With the newly created segments of vertebrae, the muscles attached to the original segments also need to be reassigned to the new specific vertebrae segments.

Generate basic segments → Generate basic joints → Generate basic muscle sets ↓ Discretize vertebral bodies ← Create spinal joints ← Create ligament tissue ↓ Reassign muscle attachments → Implement lumbar muscles → Implement abdominal muscles
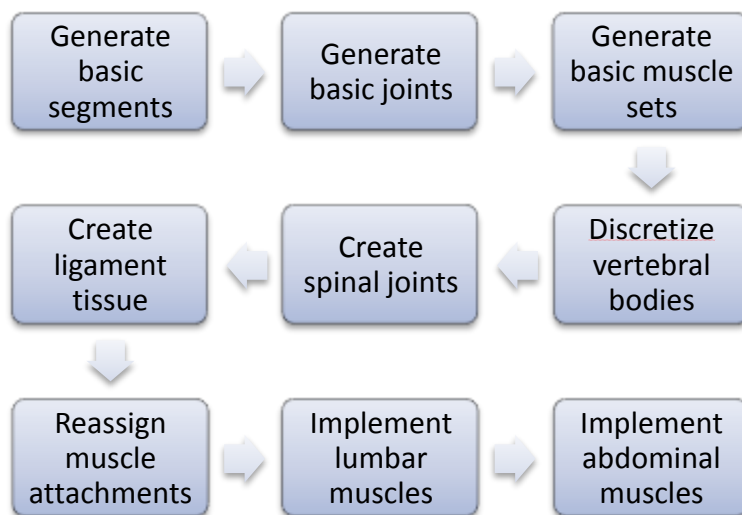
Figure 3.5 Modeling process of the discretized spine model
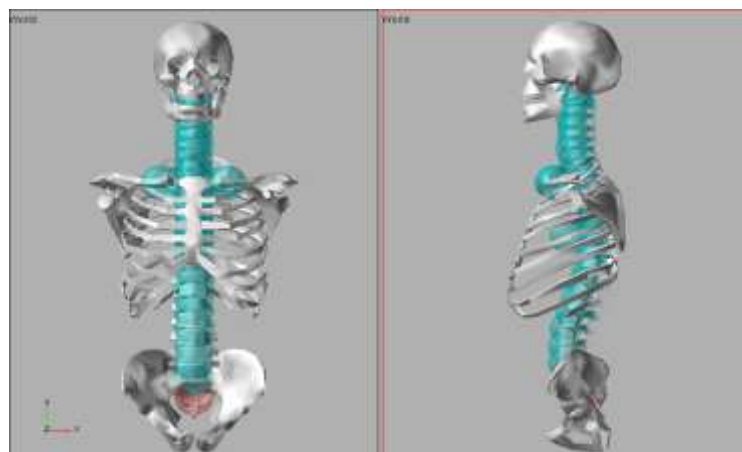
Figure 3.6 Front and side views of spinal joints created in LifeMOD

Table 3.1 Average segmental ranges of motion at each spine level (degree) (Schultz and Ashton-Miller, 1991)

Spine Level	Flexion	Extension	Lateral bending	Torsion
Occ-C1	13	13	8	0
C1-C2	10	9	0	47
C2-C3	8	3	10	9
C3-C4	7	9	11	11
C4-C5	10	8	13	12
C5-C6	10	11	15	10
C6-C7	13	5	12	9
C7-T1	6	4	14	8
T1-T2	5	3	2	9
T2-T3	4	4	3	8
T3-T4	5	5	4	8
T4-T5	4	4	2	8
T5-T6	5	5	2	8
T6-T7	5	5	3	8
T7-T8	5	5	2	8
T8-T9	4	4	2	7
T9-T10	3	3	2	4
T10-T11	4	4	3	2
T11-T12	4	4	3	2
T12-L1	5	5	3	2
L1-L2	8	5	6	1
L2-L3	10	3	6	1
L3-L4	12	1	6	2
L4-L5	13	2	3	2
L5-S1	9	5	1	1

Table 3.2 Mean torsional stiffness values for human spine (N.mm/deg) (Schultz and Ashton-Miller, 1991)

Spine level	Flexion/Extension	Lateral bending	Axial torsion
Occ-C1	40/20	90	60
C1-C2	60/50	90	70
C2-C7	400/700	700	1200
T1-T12	2700/3300	3000	2600
L1-L5	1400/2900	1600	6900
L5-S1	2100/3000	3600	4600

To stabilize the spine model, various types of ligaments are created then attached to the vertebrae in the whole spinal region, as shown in Figure 3.7. The inputs of stiffness values of ligaments are referenced from literature (Yoganandan et al., 2001, Pintar et al., 1992). These newly created ligaments are able to guide the motion of segments and contribute to the stability of the spine by limiting any excessive motion.
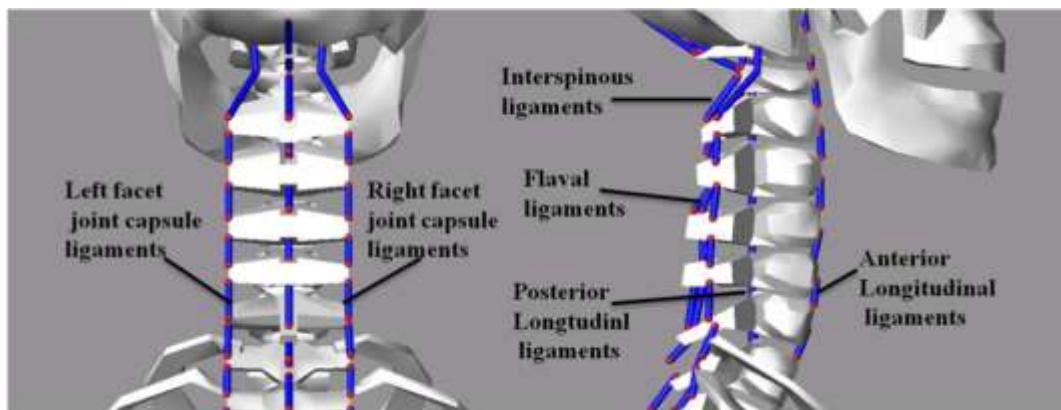
Figure 3.7 Various types of ligaments

Four important types of lumbar muscles are created for the stability of the spine model. As shown in Figure 3.8, the multifidus muscle is divided into 19 fascicles as three layers on each side of body according to literature (Bogduk et al., 1992a, Macintosh et al., 1986). Two divisions of erector spinae (longissimus thoracis pars lumborum and iliocostalis lumborum pars lumborum) are created from the transverse processes of lumbar vertebrae and inserted on the iliac crest close to the posterior superior iliac spine (Macintosh and Bogduk, 1987, Macintosh and Bogduk, 1991). The psoas major muscles originate from lumbar vertebrae and T12 and extend

into the lesser trochanter minor of the femur as 11 fascicles (Andersson et al., 1995, Bogduk et al., 1992b, Penning, 2000). The quadratus lumborum muscles originates from costa 12 and anterior side of spinous processes of lumbar vertebrae and insert into iliac crest as five fascicles (Stokes and Gardner-Morse, 1999). In addition, two types of abdominal muscles are also created in the spine model. An artificial segment with a zero mass and inertia representing the rectus sheath which the abdominal muscles can attach to is developed first. Next, these two types of abdominal muscles are created and divided into 6 fascicles each. The related attachment locations shown in Figure 3.9 can be referenced from literature (Stokes and Gardner-Morse, 1999).

| multifidus muscles | erector spinae muscles | psoas major muscles | quadratus lumborum muscles |
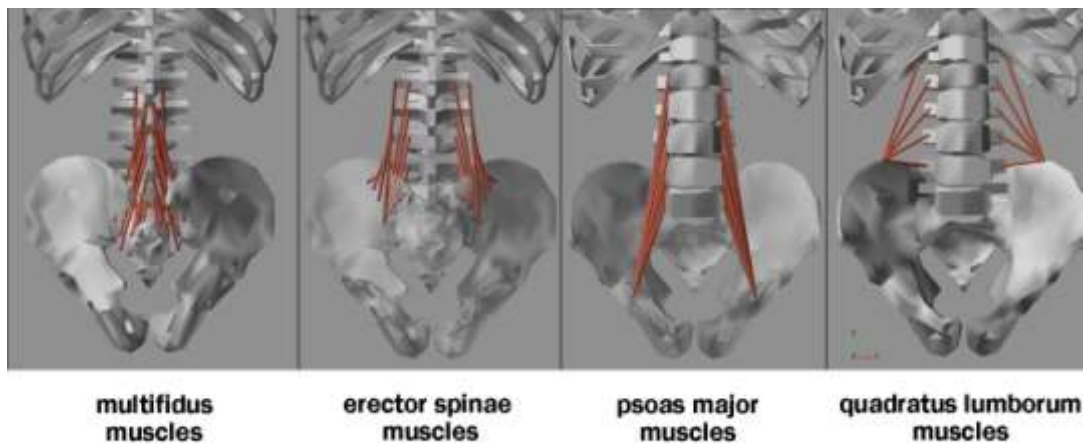
Figure 3.8 Four types of lumbar muscles

| external oblique muscles | internal oblique muscles |
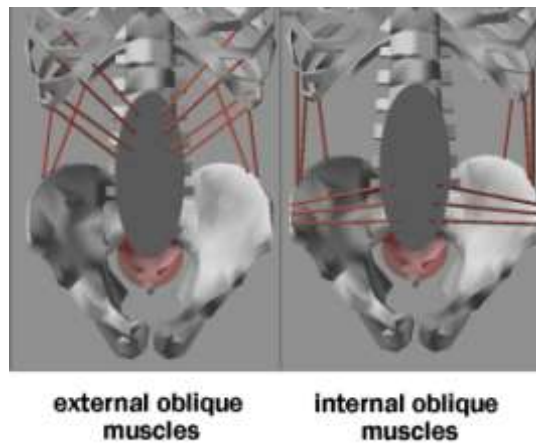
Figure 3.9 Two types of abdominal muscles

The detailed parameters and the locations of the attachments of these soft tissues can be found in the previously mentioned literature. These resources are very useful in developing the customized musculoskeletal models of experiment subjects. Since each subject shows different anthropometric data, the musculoskeletal models

of these subjects also present differences in the sizes of segments, the locations of joints and the attachments of soft tissues. All the customized models for each experiment subject have been built manually by the author, which requires large amount of time.

3.4 Validation of the Spine Model

The developed discretized spine model (Figure 3.10) has been initially proposed by the author's research group and validated by two comparison studies through simulation using LifeMOD (Huynh et al., 2013, Huynh, 2010). In the first study, with the same extension moment generated in the upright position, the axial and shear forces in the L5-S1 joint calculated in the model from the inverse and forward dynamic simulations were compared to those data obtained from the experiment (McGill and Norman, 1987b) and another spine model (DeZee et al., 2007). In the second study, while a human body model holding a crate weighing 19.8kg, the axial force of the L4-L5 joint was computed through the inverse and forward dynamic simulations and compared to that from the *in vivo* intradiscal pressure measurements (Wilke et al., 2001). The results were consistent with findings from literature. This validated enhanced discretized spine model has already been applied for various application using LifeMOD software (Gibson and Liu, 2013, Hajizadeh et al., 2012b, Huang et al., 2012).
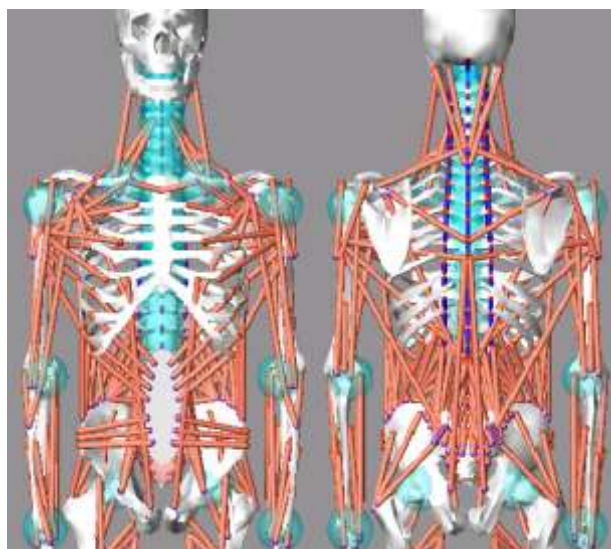
Figure 3.10 Front and back views of the enhanced discretized spine model

3.5 Motion Capture Experiment

The motion capture system involved in this study is Vicon MX, with the location tracing technology on retro-reflective markers. As a validated motion capture system, it is typically used for gait analysis, posture capture, sports performance, etc. The motion capture system applied in this thesis is constituted by eight cameras, the retro-reflective markers, the controlling hardware, the processing software and the host computer. The eight cameras are mounted on the walls of the motion capture lab and located at the specific positions as shown in Figure 3.11. The heights and the orientations of the cameras have been adjusted and calibrated by Vicon technicians to optimize the motion capture performance. The eight cameras can obtain the strobe light reflected by the retro-reflective markers (Figure 3.12) and provide the detailed information about the location of each marker. In this way, the 3D trajectories of markers during the body movements can be calculated accurately and established.
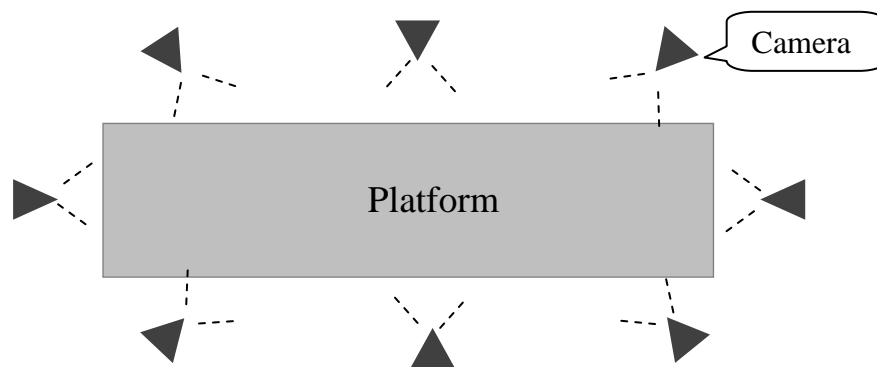
Figure 3.11 Positions of cameras in the motion capture lab

Figure 3.12 Camera obtaining the strobe light reflected by marker

Before the motion capture experiment, the system calibration is required to guarantee the accuracy of experiment results. It enables the software to calculate the relative locations and orientations of the eight cameras of the system. The obtained measurements can be used later to calculate the trajectories of markers during the recorded movements in the space of the capture volume. A calibration of good quality is necessary to obtain accurate results during the motion capture.

There are two steps in the calibration process: the static calibration and the dynamic calibration. The calibration wand, as shown in Figure 3.13, is the calibration tool for these two steps. The static calibration, which is used for the determination of the origin and the orientation of the 3D workspace, is carried out by placing the wand on the platform in the centre of the capture volume and allowing the system to set the origin with the locations of markers on the wand (Figure 3.13). The dynamic calibration involves the movements of the wand. The wand is held and moved in the shape of "8" in the space of the capture volume. After this, the relative locations and orientations of eight cameras can be calculated by the system. Although movements of the cameras are rare, system calibration has still been performed before each capture session of the author's experiments to guarantee the accuracy of captured results.

Figure 3.13 The calibration wand (left) and the static calibration (right)

In this research, the motion capture experiments were carried out with the informed consent of each subject. This work was approved by NUS Institutional Review Board (NUS-IRB).The subjects were instructed to wear minimum clothing for the motion capture experiments: shorts for male, shorts and sports top for female. The anthropometric data of the experiment subject was measured and served as inputs

to generate the human body model in the system, such as leg height, knee width, ankle width, etc. Next, the retro-reflective markers can be attached on the specific locations on the subject's skin (as shown in Figure 3.14) according to the marker protocol. In this chapter, the plug-in gait marker protocol (Figure 3.15 and Table 3.3) was used for the study of healthy people, including 37 marker locations on human segments in the whole body. The plug-in gait marker protocol is a standard marker protocol and is commonly used in the motion capture system and LifeMOD musculoskeletal modeling system to present the detailed motion of the whole body.

Figure 3.14 Subject with attached markers
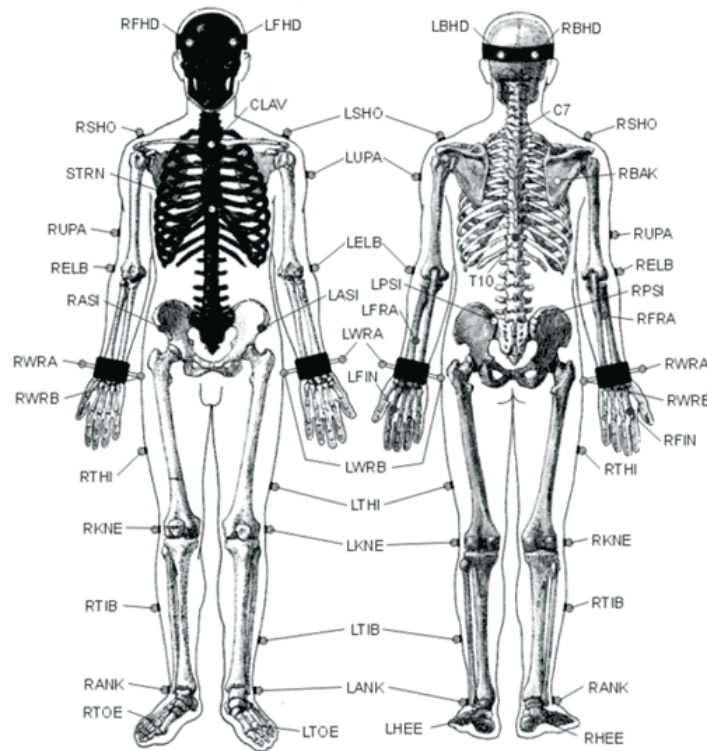
Figure 3.15 Subject with attached markers and the applied plug-in gait marker protocol

Table 3.3 Description of the plug-in gait maker protocol

Marker Label	Description
LFHD/RFHD	Left/Right Front Head
LBHD/ RBHD	Left/Right Back Head
C7	Seventh Cervical Vertebra
T10	Tenth Thoracic Vertebra
CLAV	Clavicle
STRN	Sternum
RBAK	Right Back
LSHO/ RSHO	Left/Right Shoulder
LUPA/ RUPA	Left/Right Upper Arm
LELB/ RELB	Left/Right Elbow
LWRA/ RWRA	Left/Right Wrist Bar Thumb Side
LWRB/ RWRB	Left/Right Wrist Bar Pinkie Side
FIN/ RFIN	Left/Right Finger
LASI/ RASI	Left/Right Anterior Superior Iliac Spine
LPSI/ RPSI	Left/Right Posterior Superior Iliac Spine
LTHI/ RTHI	Left/Right Thigh
LKNE/ RKNE	Left/Right Knee
LTIB/ RTIB	Left/Right Tibia
LANK/ RANK	Left/Right Ankle
LHEE/ RHEE	Left/Right Heel
LTOE/ RTOE	Left/Right Toe

38

The subjects were instructed to perform the designated movements in the capture volume. The Vicon Nexus software can generate the human body models according to the anthropometric inputs and the trajectories of virtual markers which indicate kinematic and kinetic quantities, such as angles, moments, etc. Figure 3.16 shows the plug-in gait model developed by the software. Meanwhile, some processing works usually are also required to be performed with the software, such as deleting the ghost markers in the capture volume, filling the gaps of certain marker trajectories, etc. Finally, the dynamic motion data of subjects (marker trajectories) can be obtained and imported into LifeMOD software in the SLF file format to train the musculoskeletal human body model in the following part.
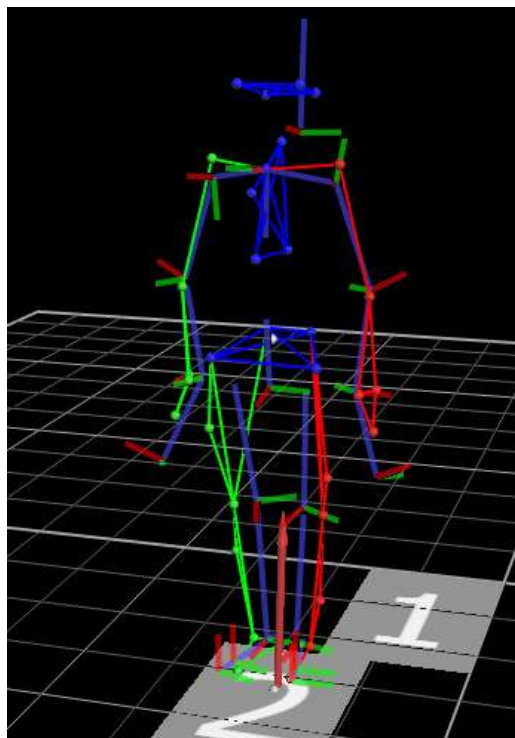
Figure 3.16 Plug-in gait modeling in the Vicon Nexus software

3.6 Integration with Motion Capture Data

The motion data obtained through the motion capture experiments is used to manipulate the human body model during the inverse dynamic simulation in LifeMOD, so that the joints and the muscles can record movement patterns for the following forward dynamic simulation. The motion data is imported into LifeMOD (Figure 3.17) in the SLF file format, which includes the units, the anthropometrics of subject, the trajectories of motion markers, etc. The data of the marker trajectories is

applied to drive the motion agents (the spheres in Figure 3.18) in LifeMOD, which are represented by massless parts and fixed to the body segments by spring attachments. The bigger spheres show the locations of the massless parts governed by the imported motion trajectories. The smaller spheres represent the locations of the segment attachment. These two types of spheres are connected by a bushing spring force with six component springs. Through this connection, the geometric differences between the human subject and the human body model, and the discrepancies of the motion agent locations can be accommodated.
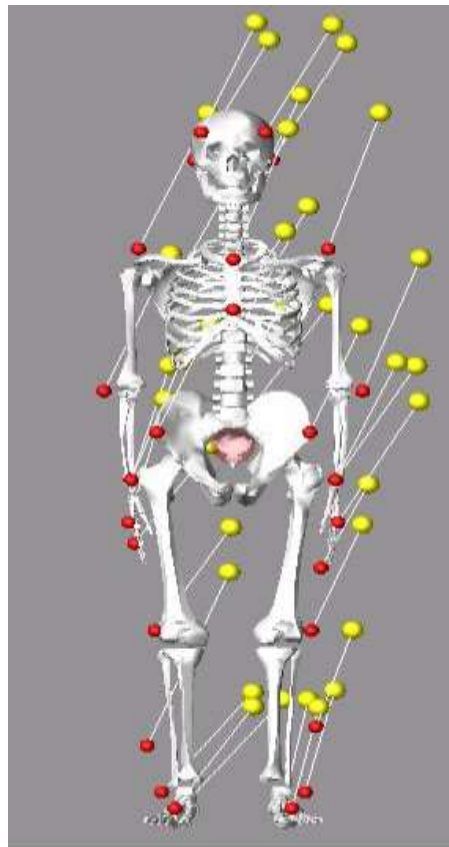
Figure 3.17 Importing motion data into musculoskeletal model in LifeMOD
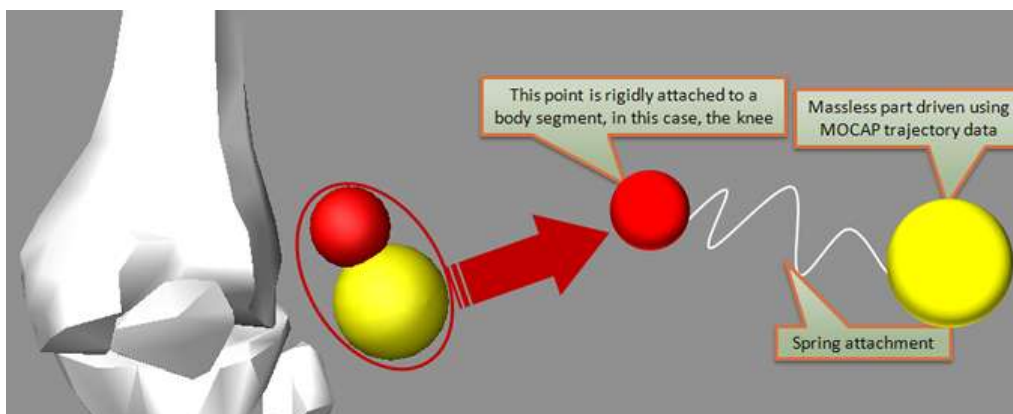
Figure 3.18 Configuration of the motion agent (LifeModeler)

Displacements often occur between the locations of motion capture data and the locations of segment attachment on the human body model, as shown in the left side of Figure 3.19. In order to minimize the discrepancies, an equilibrium analysis is performed before the inverse and forward dynamic simulations. During this analysis, the bigger spheres representing the locations of motion capture data are kept fixed, and the configuration with minimum energy required in the springs of the motion agents is obtained. Fewer discrepancies between the locations of motion capture data and body segment attachment can be observed after the equilibrium analysis, as shown in Figure 3.19. Locations of segment attachments are then synchronized with the locations of motion capture data for the following inverse and forward dynamic simulations.
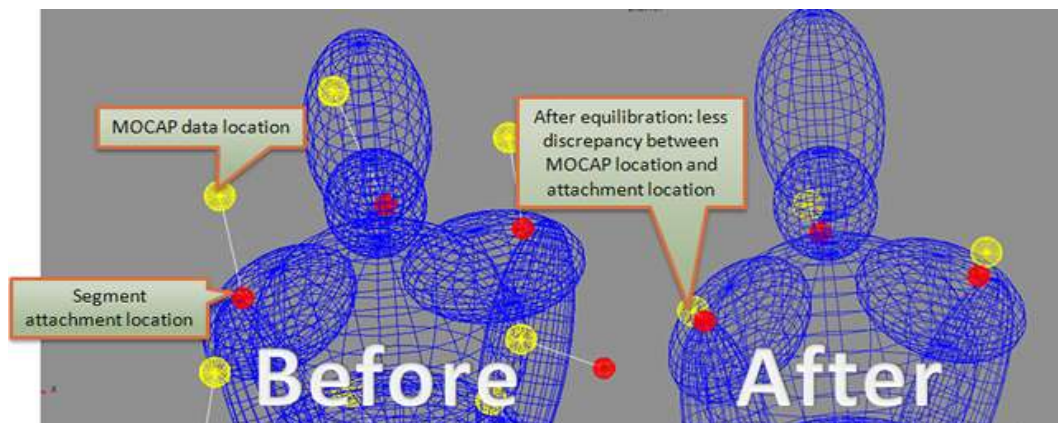
Figure 3.19 Displacements between the motion capture data locations and the segment attachment locations before and after the equilibrium analysis (LifeModeler)

In order to obtain the simulation of dynamic interaction, the musculoskeletal human-body model was combined with the physical environment. Two types of contact elements are applied in this research: the ellipsoid-plane contact elements and the ellipsoid-ellipsoid contact elements. The ellipsoid-plane contact elements are used to create the contact forces between the human body model and the external environment. The contact can generate a normal force and a transverse friction force according to the user-defined parameters. The ellipsoid-ellipsoid contact elements, as a variation of the ellipsoid-plane elements, are used for the contacts between the body segments. In the contact algorithm, eight parameters are served as inputs to calculate the contact force: contact stiffness, exponent, damping coefficient, penetration depth, static friction, dynamic friction, friction transition velocity and stiction transition velocity. Figure 3.20 shows the contact force generated between the upper leg of body

model and the seat model. The contact parameters and the overlapping area of the two contacting bodies are used to calculate the resulting contact force, which is then applied on the surface of each body. An impact force algorithm is employed in the contact algorithm, as shown in Equation 3.7. The penetration is determined by the distance between the related markers on the body segments and the seat during the dynamic motion in LifeMOD. The penetration velocity is a ratio of the penetration variation and the time variation. In this Equation, $Step(x, x_0, h_0, x_1, h_1)$ is a cubic polynomial function, with x being the independent variable, x_0 and x_1 being real variables that specifies the x value at which the lower and upper end saturation starts, and h_0 and h_1 being the values of the function at the lower and upper saturation point.

$$F_n = k * (g ** e) + Step(g, 0,0, dmax, cmax)dg/dt \qquad (3.1)$$

where

g= the penetration of one geometry into another

dg/dt= the penetration velocity at the contact point, as a ratio of penetration variation and time variation.

e= a positive real value denoting the force exponent

dmax = a positive real value specifying the boundary penetration to apply the maximum damping coefficient cmax, with damping coefficient specifying a ratio of damping force and velocity.
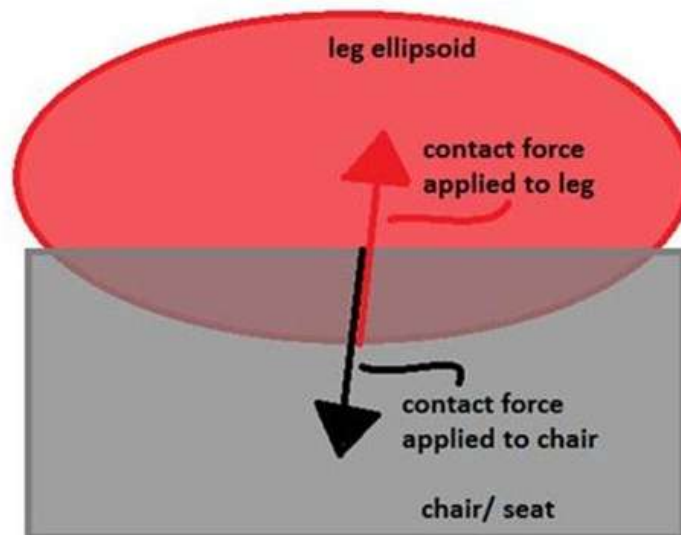
Figure 3.20 Contact forces between the upper leg of body model and the seat model

In this research, a planar surface representing the floor and a rigid-body model of the seat were developed to create the contact forces between the human body and the physical environment. Contact elements were defined between the human body

42

and the physical environment to obtain the contact forces, which are computed with the overlapping area of two contacting bodies and other parameters, such as stiffness, damping, coefficient of friction, and stictional and frictional transition velocities. Stiffness of contact represents resistance offered by the ground to deformation. Friction transition velocity of human/chair contact means the velocity above which the dynamic friction coefficient takes effect. Different values of stiffness and friction transition velocity are used for the two types of contact (Table 3.4).

Table 3.4 Parameters for human-environment contact

parameter	Human/chair contact	Human/Ground contact
Stiffness	20 N/mm	200 N/ mm
Damping coefficient	2 Ns/mm	2Ns/mm
Static friction coefficient	1	1
Dynamic friction coefficient	0.8	0.8
Stiction transition velocity	1 mm/s	1mm/s
Friction transition velocity	10 mm/s	1mm/s

The computational analysis is based on the inverse and forward dynamic simulations. For the inverse dynamic simulation, the motion capture data from the previous experiments was used to train the musculoskeletal human-body model by recording the movements of muscles and joints (Figure 3.21). In the forward dynamic simulation, the motion agents were disabled. The movements of muscles and joints achieved in the inverse one were applied to drive the human-body model behaving in the same way during the forward dynamic simulation. In other words, for the forward dynamic simulation, the human-body model was driven by the recorded joint torques and muscle contractions, and affected by the gravity and contact forces. Since the spinal joints were created as torsional spring forces, joint forces can be obtained after the inverse and forward dynamic simulations. All the values of compressive loads on spinal joints are averaged results over 2 seconds after the body changes posture and reaches a new equilibrium state. The average values of joint compressive forces in different postures are shown in the following section.
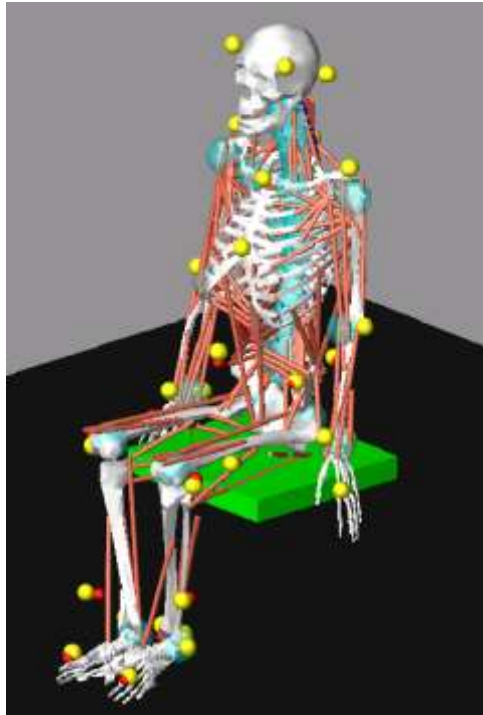
Figure 3.21 The musculoskeletal human body model trained by the motion capture data in the inverse dynamic simulation

3.7 Analysis of Flexion and Extension Postures

A healthy 24 years old, height 178cm and weight 70kg male Asian adult with no history of back pains is the subject of this study. The subject was asked to perform the motion from flexion to extension continuously in both standing and sitting postures, as shown in Figure 3.22. The motions of flexion and extension are defined by the angle between the thoracolumbar junction and the sacrum of the subject, with flexion defined as the positive direction. The detailed process of applied method has been introduced in the previous sections. Five separate trials of each motion of the subject were taken during the motion capture experiment. The plug-in gait modeling in the Vicon Nexus system generated the human body modeled segments according to the anthropometric inputs and the virtual marker trajectories. After data processing, the output data of marker trajectories can be obtained and applied to drive the developed subject's musculoskeletal model in LifeMOD for the inverse and forward simulations. The compressive loads of spinal joints can be obtained after simulations.
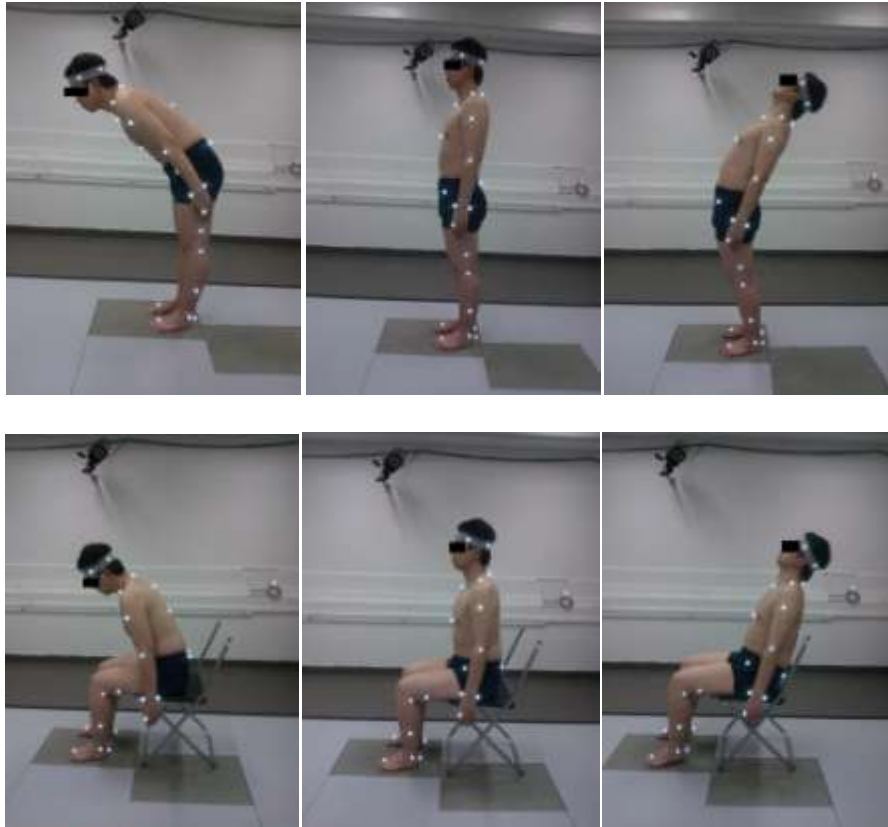
Figure 3.22 The subject performing flexion and extension in standing and sitting

The results of compressive loads of lumbar joints from flexion to extension in standing and sitting postures of the subject are presented in Figure 3.23. It is found that the compressive loads on L3-L4, L4-L5 and L5-S1 joints in both standing and sitting increase not only with flexion, but also with extension. However, the compressive loads on L4-L5 joint in sitting are higher than the ones in standing during the whole motion. The opposite situation is shown for L5-S1 joint. The compressive loads on L3-L4 joint in sitting are higher than the ones in standing from the extension angle of -15° to 0° and at the flexion angle of 20°. Generally, it is clear that the most significant increase of the compressive loads occurs at the flexion angle of 35°. There are also increases in extension, with the maximum forces at the extension angle of -25°. It is observed that the compressive loads from flexion to extension in standing change in a curvilinear fashion, with the minimum values at the extension angle of -5°.

For the postures of flexion and extension in standing and sitting, the line of gravity (LoG) is more anterior or posterior to the spinal joint axes than that in the upright posture, as shown in Figure 3.24. Greater distance between the LoG and the axes of spinal joints creates larger moments at the spinal joints. Thus more muscle activities and higher tension in ligaments are required to keep a stable posture, leading

to more energy expenditure and higher spinal compressive loads (Levangie and Norkin, 2001).
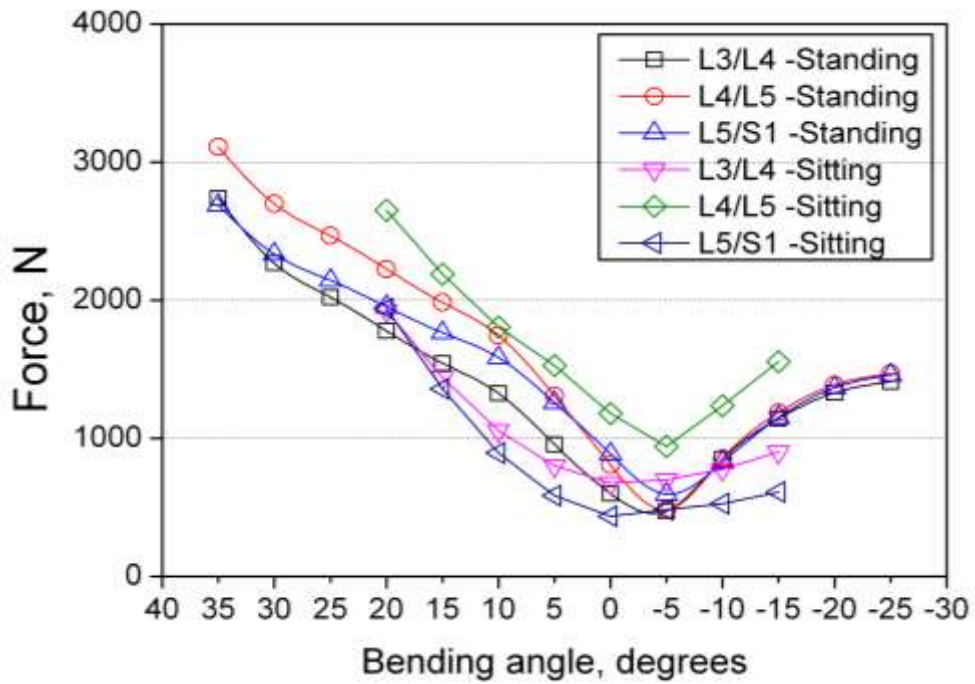
Figure 3.23 The compressive loads on intervertebral joints in flexion and extension
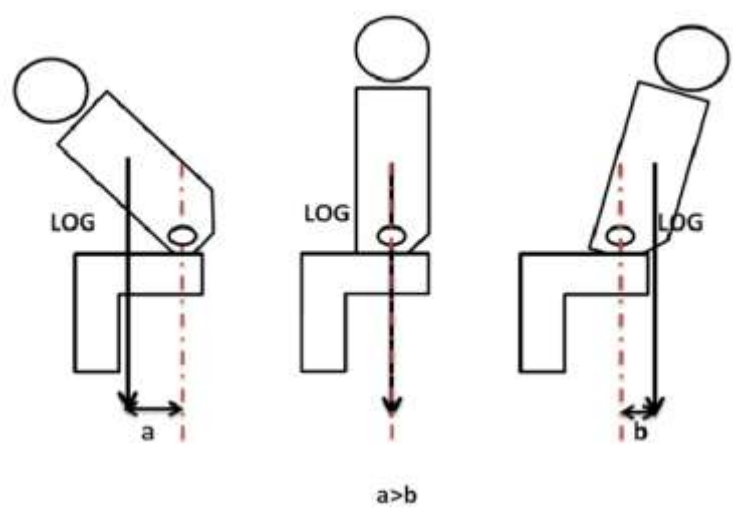
Figure 3.24 The distances between the LoG and the axe of spinal joint in flexion sitting, upright sitting, and extension sitting

3.8 Analysis of Sitting Postures

Six Asian adults with no previous or ongoing back pains are involved in this study. These subjects were asked to perform a series of the following postures continuously in one capture (Figure 3.25): upright standing, upright sitting, slumped

46

sitting, cross-legged sitting, flexion sitting and extension sitting. In order to ensure the subjects performing similar flexion and extension sitting postures to each other, the angle between the vertical line and the line connecting the thoracolumbar junction and the sacrum of subject is set to be mean +20° (SD 5°) in the flexion sitting, and mean -15° (SD 5°) in the extension sitting. Five separate trials of each action were taken for each subject. Subjects' basic information is shown in Table 3.5. The mean age was 24.3years, the mean height was 166cm, and the mean body weight was 57kg.
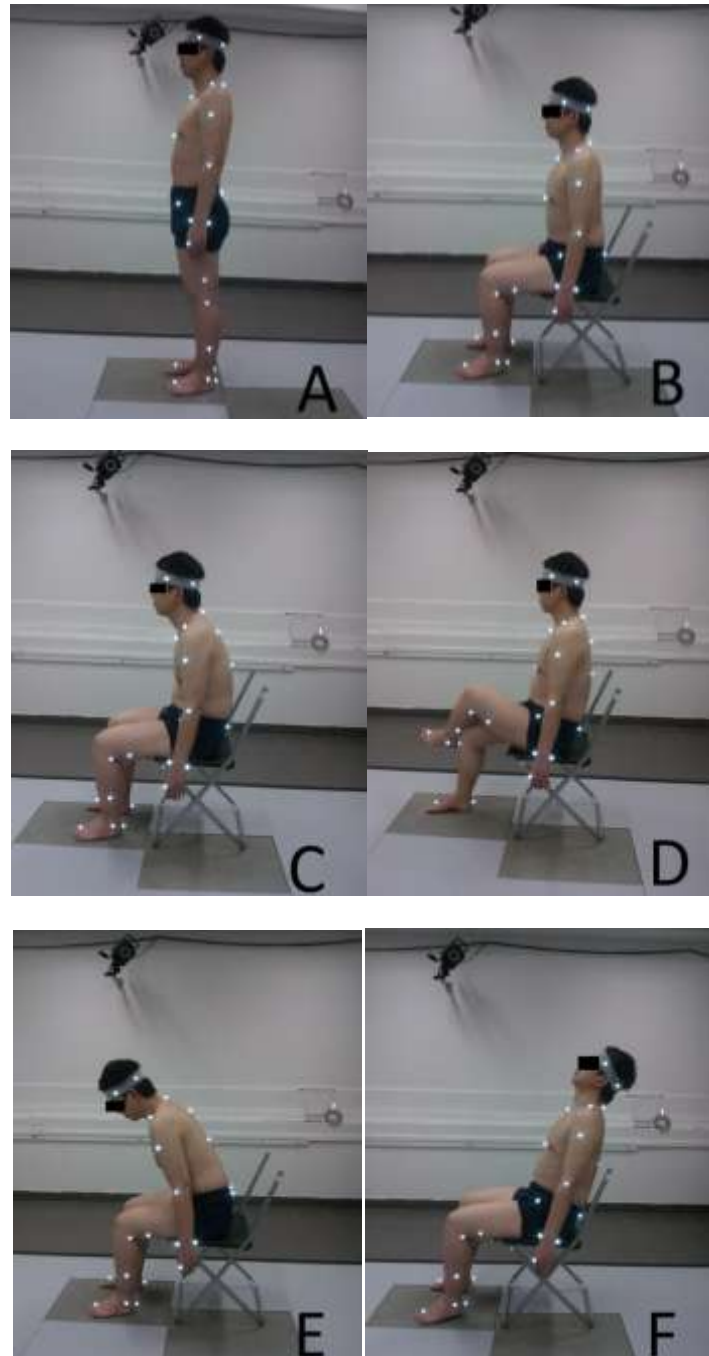
Figure 3.25 The subject performing postures: A, Upright standing; B, Upright sitting; C, Slumped sitting; D, Cross-legged sitting; E, Flexion sitting; F, Extension sitting

Table 3.5 Basic information of subjects

Subject	Gender	Height(cm)	Weight(kg)	Age (years)
1	M	178	70	26
2	M	173	69	26
3	F	170	60	24
4	M	159	55	25
5	F	159	40	21
6	F	157	48	24
Mean		166	57	24.3

After the motion capture experiments and the data processing, the segment angles and marker trajectories were obtained. The outputs of spine angles in the sagittal plane of human body were measured and calculated by comparing the relative orientations of the two related segments in the plug-in gait mode. As shown in Figure 3.26, the spine angle is defined as the angle between the thorax axis and pelvis axis, with the positive direction following the spine tilting forwards (flexion).
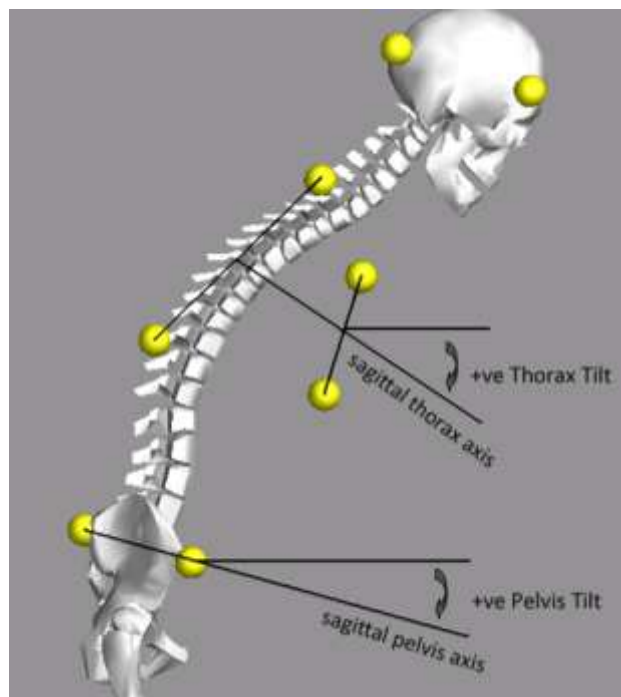
Figure 3.26 Definitions of spine angle

The spine angles in the sagittal plane of six subjects in various postures are shown in Figure 3.27. It is observed that the spine angles of six subjects all increase when subjects change from upright standing to upright sitting. This finding indicates that there is an obvious reduction of lumbar lordosis (inward curvature of lumbar region) from standing to sitting, which matches the literature (Harrison et al., 1999).

48

Compared to upright sitting, the other four types of sitting postures (slumped sitting, cross-legged sitting, flexion sitting and extension sitting) generate more reduction of lumbar lordosis.
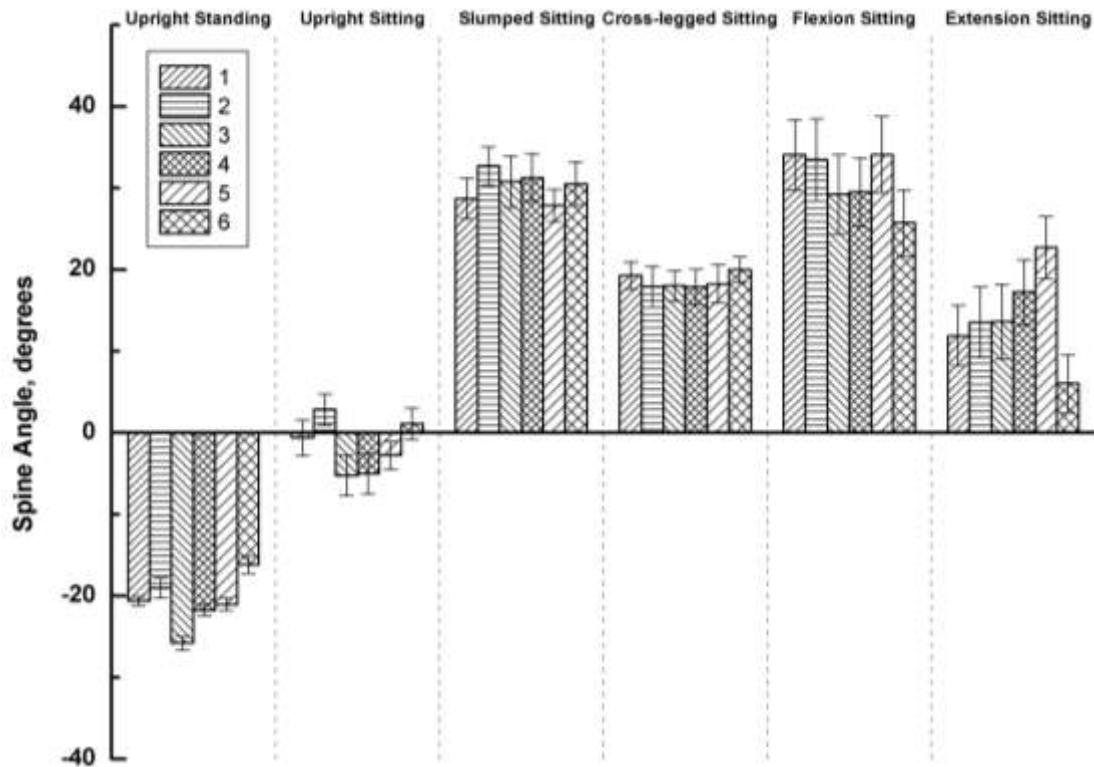
Figure 3.27 Spine angles of six subjects in various postures

Six customized musculoskeletal multi-body models were developed according to the individual anthropometric data of the subjects. The process of modeling has been described in detail in the previous sections, including generating basic body model, refining the spine into individual vertebrae, creating spinal joints and various types of soft tissues. The motion data of marker trajectories of subjects was imported into LifeMOD to drive the musculoskeletal models accordingly for computational analysis. After the inverse and forward simulation, the compressive loads of lumbar joints can be obtained as final outputs.

The compressive loads of L3-L4, L4-L5 and L5-S1 joints are shown in Table 3.6, Table 3.7 and Table 3.8 respectively. The mean compressive loads of these joints for healthy subjects with an average body weight of 57kg, body height of 166cm and age of 24.3years are also provided additionally. It is found from the results that the average compressive loads on the L3-L4 joint of subjects are within the range of 0.82 to 2.86 times body weight, with the minimum value in upright standing and maximum value in flexion sitting. The average compressive loads on the L4-L5 joint are within

the range of 0.84 to 4.72 times body weight with the minimum value in upright standing and maximum value in flexion sitting. The average compressive loads on the L5-S1 joint are within the range of 0.87 to 3.30 times body weight with the minimum value in upright sitting and maximum value in flexion sitting.

Table 3.6 The compressive loads (N) on L3-L4 joint

Subject	Upright standing	Upright sitting	Slumped sitting	Cross–legged sitting	Flexion sitting	Extension sitting
1	570	714	1087	1217	1927	901
2	527	727	1134	1264	1912	970
3	412	948	1180	1108	1261	829
4	449	950	1039	1126	1369	941
5	390	462	862	843	1352	744
6	413	535	906	933	1778	908
Mean	460	723	1035	1082	1600	882

Table 3.7 The compressive loads (N) on L4-L5 joint

Subject	Upright standing	Upright sitting	Slumped sitting	Cross–legged sitting	Flexion sitting	Extension sitting
1	569	957	1766	1641	2652	1554
2	497	1030	1702	1863	2491	2053
3	442	848	1666	1828	2551	1750
4	515	927	1443	1677	2493	1896
5	382	903	1515	1426	2835	2136
6	420	911	1452	1570	2782	1603
Mean	471	929	1591	1668	2634	1832

Table 3.8 The compressive loads (N) on L5-S1 joint

Subject	Upright standing	Upright sitting	Slumped sitting	Cross–legged sitting	Flexion sitting	Extension sitting
1	550	509	758	895	1941	612
2	746	684	1114	967	1808	933
3	431	406	772	851	1823	1021
4	416	374	753	623	1726	834
5	364	530	760	912	1938	1197
6	410	389	940	1002	1813	600
Mean	486	482	850	875	1842	866

The mechanical loading condition of spine is highly complicated. The compressive force along the long axis of the spine is affected by many factors,

including gravity, ground reaction forces, and forces generated by the ligaments and muscle contraction (Levangie and Norkin, 2001). Some variance is observed among the subjects in the same posture. For example, significantly higher compressive loads of L4-L5 and L5-S1 are found for Subject 5 than Subject 6 (with greater gravity, similar height and same gender) in extension sitting. The reason can be that Subject 5 bent backwards too much for the extension sitting during the motion capture experiment compared with Subject 6.

Despite the variance among subjects in the same posture, the correlation between spine angle and spinal load in various postures shown in Figure 3.28 is found to be approximately linear after polynomial curve fitting: Y (spinal load) = 32.8 X (spine angle) + 1128.6. As there is almost no difference in the correlation with order 1 and order 2 polynomials, order 1 is chosen in the curve fitting to simplify the expression. It is demonstrated that there is an increase in the compressive load, as the spine angle increases. This is because the reduction of lumbar lordosis as spine angle increases can introduce higher disc loads (Hedman and Fernie, 1997, Harrison et al., 1999).
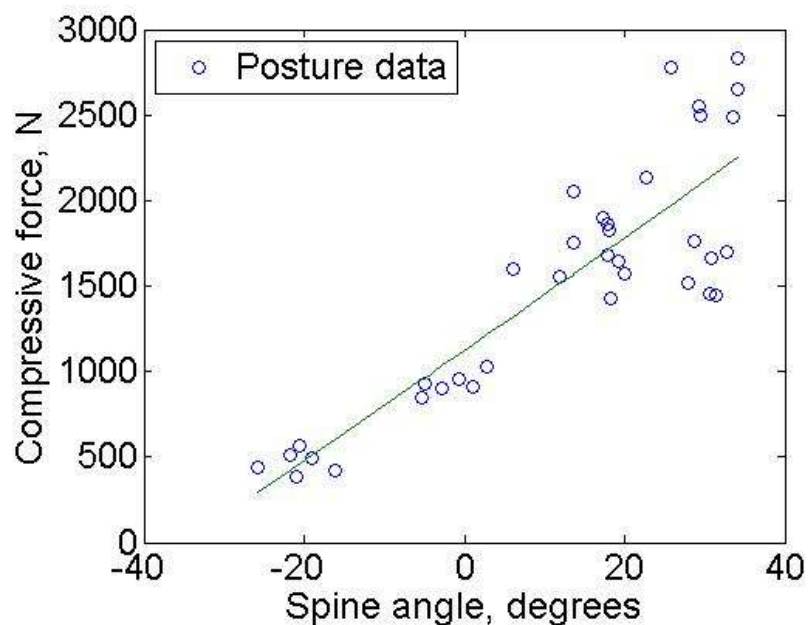
Figure 3.28 Correlation between spine angle and spinal load

It is found from the results that the compressive load on L5-S1 joint in upright standing is 486N, which is 0.85 times the mean body weight. This is consistent with the conclusion that lumbosacral loads in upright standing posture were in the range of 0.82 to 1.18 times body weight (Khoo et al., 1994). Differences in the compressive

51

loads between upright standing and upright sitting are also observed from the results. Existing literature has shown some disagreements on the comparison of pressures in the intervertebral disc in the standing and sitting postures (Claus et al., 2008). It is also known from the literature that the intervertebral disc resists about 84% of the intervertebral compressive forces in upright standing, and 100% of the intervertebral compressive forces in upright sitting (Adams and Hutton, 1980). Hence from the results of the current study, it is calculated that the mean compressive loads on L3-L4, L4-L5, and L5-S1 discs are 386N, 396N and 408N respectively in upright standing; and 723N, 929N, and 482N respectively in upright sitting. At least these findings suggest that there are differences among the compressive loads on intervertebral discs in upright standing and upright sitting. Higher compressive loads on L3-L4, L4-L5 and L5-S1 discs are exhibited in upright sitting than in upright standing. It can be explained by the fact that the pelvis tilts backwards in sitting, causing a reduction in the lumbar lordosis and an increase in compressive loads compared with that in standing (Harrison et al., 1999). These results support those from the *in vivo* experiments (Nachemson, 1966, Nachemson, 1981, Okushima, 1970, Sato et al., 1999), which found that the measured pressure of L3-L4 and L4-L5 intervertebral discs in upright sitting are higher than those in upright standing.

Compared to upright sitting, slumped sitting and cross-legged sitting both lead to higher compressive loads on spinal joints. Furthermore, the compressive loads in cross-legged sitting are slightly higher than the ones in slumped sitting. It is also found that the compressive loads in upright sitting are lower than those in flexion and extension postures. In other words, the compressive loads increase not only with forward bending, but also with backward bending in sitting posture. This is in consistent with the finding of the study in previous section (Figure 3.24) that flexion and extension postures can introduce higher compressive forces on lumbar joints with greater (forward and backward) bending angles.

Generally, slumped sitting, cross-legged sitting, flexion sitting and extension sitting, which are all very common postures in daily life, introduce higher compressive loads on spinal joints compared to upright sitting. This finding is in consistent with the conclusion from the studies in literature (Sato et al., 1999, Andersson et al., 1974a, Andersson and Ortengren, 1974a, Andersson et al., 1974b). From their studies, lower disc pressure was observed in upright sitting compared to

other sitting postures, including relaxed sitting, posterior sitting, anterior sitting, etc. Compared to upright standing or upright sitting, many commonly adopted postures can reduce the lumbar lordosis (Dolan et al., 1988). It has been concluded in literature that the loss of lordosis in sitting can increase the load in discs and muscles (Hedman and Fernie, 1997, Harrison et al., 1999). The same finding is observed in the current study. Since the loading concentrations in the posterior annulus caused by prolonged spine flexion can be a common reason for disc pain (Adams et al., 1996), these commonly adopted sitting postures are likely to pose a threat to the lumbar intervertebral discs and to be the cause of LBP.

3.9 Summary

In summary, this study has developed a procedure to investigate the compressive loads on intervertebral joints in common standing and sitting postures through the approach of motion capture and musculoskeletal modeling. The results of this study indicate that the compressive loading conditions of spinal joints are highly dependent on human body posture. Differences among the compressive loads on the intervertebral joint in upright standing and upright sitting are observed. Greater compressive loads on lumbar discs are shown in upright sitting than in upright standing. Some commonly adopted postures in daily life, including slumped sitting, cross-legged sitting, flexion sitting and extension sitting, introduce higher compressive loads on spinal joints, which are likely to be harmful to the intervertebral discs and may cause LBP.

This chapter seeks to help the understanding of the spinal load in different postures. The study is the first attempt in literature to apply the current method which is a combination of motion capture experiment and the virtual musculoskeletal multi-body modeling and simulation to investigate spine biomechanics. The motion data of subjects were applied to train the musculoskeletal multi-body models in the inverse and forward dynamic simulations. The enhanced bio-fidelity discretized spine model plays a very important role by providing spinal joints connecting adjacent vertebrae and additional soft tissues in the abdomen and back regions. Through this approach, the loading conditions of each intervertebral joint throughout the spine during the whole motion can be obtained. In literature, some researches have been conducted to

investigate the relations between the spinal load and the posture through *in vivo* pressure needle measurements (Nachemson, 1966, Nachemson and Morris, 1964, Nachemson, 1981, Sato et al., 1999, Wilke et al., 1999, Wilke et al., 2001). However, due to the invasive effect of this method, only one intervertebral disc can be considered in the experiment, and the number of subjects may be limited. Through the proposed procedure in this chapter, load conditions of any intervertebral joint can be obtained. The procedure can also be applied to more subjects or body postures in the future. This can help people get more insights into the spinal load from the view of musculoskeletal modeling and simulation.

However, this study has some limitations. The motion capture experiments have been carried out based on a relatively hard seat with no contours. Other types of seat were not explored. The marker protocol used in this study is the plug-in gait marker protocol. More markers on the subject's spine may be included in the future to record more detailed trajectories of spine segments. Another problem in the motion capture experiments is that it was not always possible to determine whether the subjects were repeating the same exact body posture, because each subject has his/her own specific body type and preferred body behaviors.

CHAPTER 4

INVESTIGATION OF THE INFLUENCE OF VARIOUS SEAT DESIGN PARAMETERS

4.1 Introduction

Seat design plays a very important role in the study of human sitting. Poor or unsuitable seat design is related to discomfort and other healthcare problems, such as LBP. In literature, there are few quantitative studies of the relationship between spinal loads and seat design parameters. Hence in this chapter, the effects of seat design variables on spinal joints forces are investigated through the approach of musculoskeletal modeling and simulation.

Intra-abdominal pressure (IAP) is a pressure within the abdominal cavity which are formed by the diaphragm above, the musculo-aponeurotic perineum below, the lumbosacral spine posteriorly and the walls of the abdominal cavity anterolaterally. In the study with dynamic motion data in Chapter 3, IAP of human body was not included as a continuous stabilizing and compression-reducing mechanism, since the detailed kinematic trajectories of body segments were provided by the motion capture data of subjects. The musculoskeletal model without IAP shows its ability to reach an equilibrium state for the expected posture and reasonable compression of spinal joints. This conclusion is also in accordance with the finding from another study (McGill and Norman, 1986).

For the study with a designated static posture in this chapter, it is hypothesized that there is a need to involve IAP into the musculoskeletal model as a stabilizing and compression-reducing mechanism, due to the fact that no motion data is used and the musculoskeletal model has to maintain the equilibrium state in designated posture by its own muscle tension in simulation. Hence in this chapter, the effects of elevated

IAP were studied first to validate the necessity of IAP in musculoskeletal human model with static posture. The human body model with adequate IAP was applied in the following study to investigate the influence of seat design parameters on the spinal joint loads.

The role of elevated IAP as a mechanism of unloading and stabilizing the spine has been the subject of debate for many years. It was proposed that IAP could produce a trunk extensor moment, and thus reduce the activity of the erector spinae muscles and the loading of spine (Bartelink, 1957). However, some researchers argue that the contraction of the abdominal muscles to generate the IAP also leads to a flexor moment, which may negate the extensor moment produced by the IAP. It has been suggested that the IAP may only be a by-product of trunk muscle activation (McGill and Norman, 1987a) and contribute to the stabilization of spine, instead of unloading (Cholewicki et al., 1999). However studies carried out in recent years found that the elevated IAP without concurrent abdominal and back muscle contraction could generate an extensor torque (Hodges et al., 2001) and increase the stiffness of lumbar spine (W Hodges et al., 2005). Overall, the results of these researches provide a conclusion that there has been some disagreement on the role of the elevated IAP.

Overall, the objective of the study in this chapter is first to investigate the effects of elevated IAP on the head displacements and the spinal joint loads, and the influence of various seat design parameters on the spinal joints loads of the musculoskeletal human body sitting model. The flow chart of method in this chapter is shown in Figure 4.1. In order to validate the necessity of including IAP, elevated IAP was added to the musculoskeletal human body model, which was built using the same procedures in Chapter 3. The body model was adjusted to be in the static upright sitting posture, with the spine angle in upright sitting obtained from the previous motion capture experiment in Chapter 3. Meanwhile, the ratio of hip flexion and spine flexion is maintained as 2.2:1, as suggested by another experimental study (Bell and Stigant, 2007). After the adjustment of static sitting posture, a chair model was created and contacts were defined between the feet and the ground and between the body and the chair. The musculoskeletal computational analysis was based on the inverse and forward dynamic simulations. After the study of necessity of including IAP, this sitting model with adequate IAP was applied to study the influence of seat

design variables on the compressive loads of spinal joints. The involved seat design variables include backrest inclination, seat pan inclination, seat pan height, seat pan depth and backrest height. This study may help gain a better understanding of the role of IAP and provide the quantitative analysis of seat design parameters to fill the gap in literature.
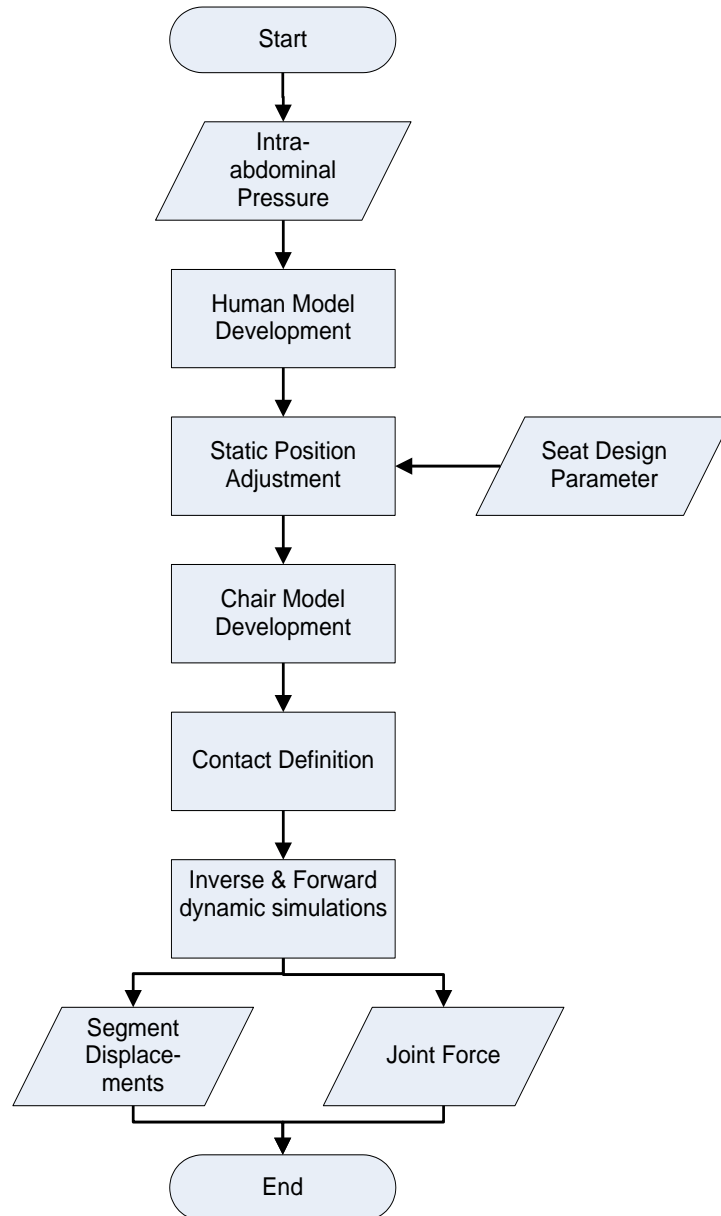
Figure 4.1 Flow chart of method of musculoskeletal modeling in the seat design study

4.2 Implementation of Intra-Abdominal Pressure

The implementation of IAP is accomplished by adding a bushing element in the abdominal cavity of the musculoskeletal model in LifeMOD, as shown in Figure

57

4.2. The general method to include IAP introduced here is based on a research in literature (Huynh, 2010).
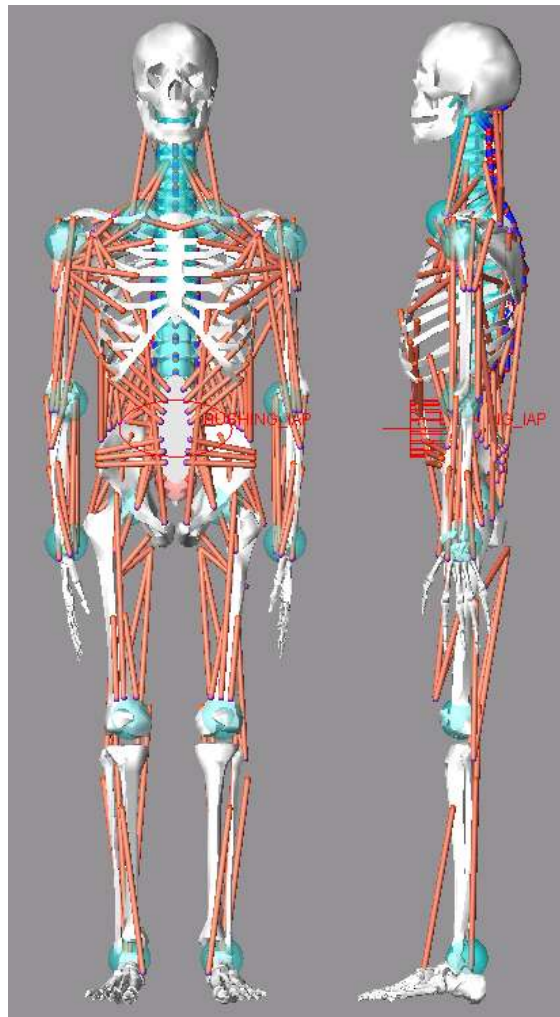
Figure 4.2 An equivalent bushing element implemented in the musculoskeletal model

First, a spring structure (Figure 4.3) to simulate all the mechanical properties of IAP, such as tension/compression, anterior/posterior shear, lateral shear, flexion/extension, lateral bending and torsion, is created. Then the translational and torsional stiffness of the spring structure are determined according to the abdominal volume and the mean section area. Finally, an equivalent bushing element which can specify all the stiffness properties of the spring structure is added in the human body in LifeMOD. The mechanical properties of the spring structure and the equivalent bushing element are obtained using Equation 3.8 to 3.15. The detailed IAP calculation procedure can be found in literature (Huynh et al., 2013, Huynh, 2010).
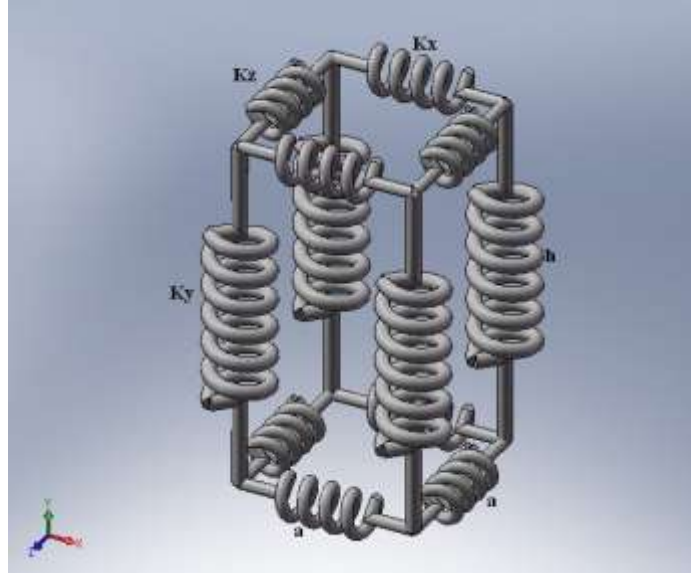
Figure 4.3 The spring structure which is able to mimic the mechanical properties of IAP (Huynh, 2010, Huynh et al., 2013)

$$k_y = \frac{1}{2}Pa^2 \qquad (3.2)$$

$$k_x = k_z = \frac{1}{2}Pah \qquad (3.3)$$

$$M_x = M_z = k_y \frac{\pi}{180} a^2 \qquad (3.4)$$

$$M_y = k_x \frac{\pi}{180} a^2 = k_z \frac{\pi}{180} a^2 \qquad (3.5)$$

$$k_x' = k_z' = 4k_x = 4k_z \qquad (3.6)$$

$$k_y' = 4k_y \qquad (3.7)$$

$$M_x' = M_z' = k_y \frac{\pi}{180} a^2 \qquad (3.8)$$

$$M_y' = k_x \frac{\pi}{180} a^2 = k_z \frac{\pi}{180} a^2 \qquad (3.9)$$

Where

P= Intra-abdominal pressure

a= Length of the spring structure

h= Height of the abdomen

k_x= Translational stiffness of the spring structure in X direction

k_y= Translational stiffness of the spring structure in Y direction

k_z= Translational stiffness of the spring structure in Z direction

M_x= Torsional stiffness of the spring structure in X direction

M_y= Torsional stiffness of the spring structure in Y direction

M_z= Torsional stiffness of the spring structure in Z direction

k_x'= Translational stiffness of the bushing element in X direction

k'_y= Translational stiffness of the bushing element in Y direction

k'_z= Translational stiffness of the bushing element in Z direction

M'_x= Torsional stiffness of the bushing element in X direction

M'_y= Torsional stiffness of the bushing element in Y direction

M'_z= Torsional stiffness of the bushing element in Z direction

4.3 Effects of Intra-Abdominal Pressure

In order to understand the effects of intra-abdominal pressure in the human body model, different levels of IAP were implemented into the musculoskeletal human body model. Since the measured range of IAP in sitting posture was from 10mmHg to 21mmHg in the *in-vivo* experiment (Cobb et al., 2005), the influence of elevated IAP from 0mmHg to 30mmHg with increment of 5mmHg was studied. After the model development and combination with environment, inverse and forward dynamic simulations were carried out to obtain the head displacements and loadings of lumbar joints of the human body musculoskeletal model.

Generally, the first step to validate the performance and the accuracy of the musculoskeletal human body model is to evaluate its stability. In this study, the human body model was set in the upright sitting posture for the inverse dynamic simulation. During this simulation, the joint angles and muscle tensions required to maintain this posture were recorded. It is expected that the multi-model can reach a new equilibrium state of upright sitting during the forward dynamic simulation with the recorded data of joints and muscles.

Figure 4.4 shows the initial positions before simulations and final position after simulation of the sitting human body with 0mmHg IAP. It is found when the IAP is 0mmHg, which means there is no IAP implemented into the model, the human body model is able to achieve a stable state but not able to maintain the exact same posture after simulation. There are very obvious displacements of body segment after simulations, especially the head. Thus, the displacements of the head between the initial position before simulation and the final position after simulation with elevated IAP in Y and Z directions are obtained as shown in Figure 4.5. It is observed that when IAP increases from 0mmHg to 30mmHg with increment of 5mmHg, the

displacements of the head in both Y and Z direction decrease, with the most significant changes from 0mmHg to 5mmHg. The displacement in Y direction becomes stable from 10mmHg to 30mmHg. The displacement in Z direction keeps decreasing as IAP increases, with decreasing slopes. Figure 4.6 shows the results of compressive forces of lumbar joints with elevated IAP after simulations. It is found that all compressive forces decrease with elevated IAP.
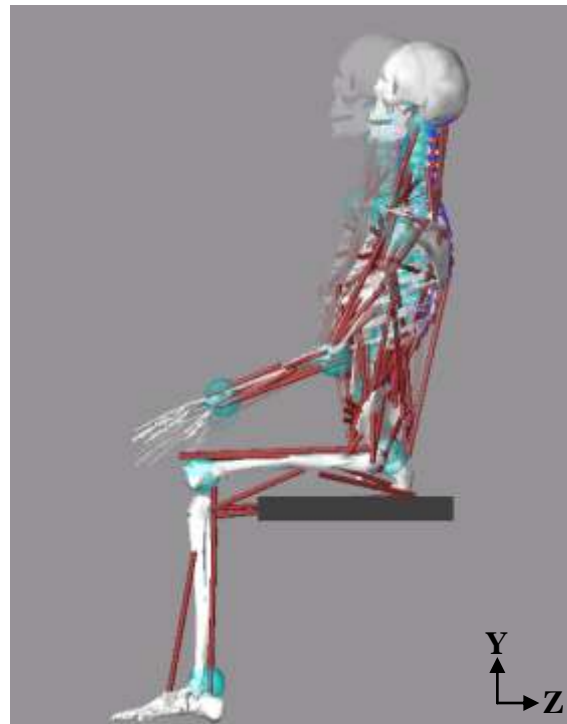
Figure 4.4 The initial position (light colour) and the final position (deep colour) of sitting human body with 0mmHg IAP during simulations
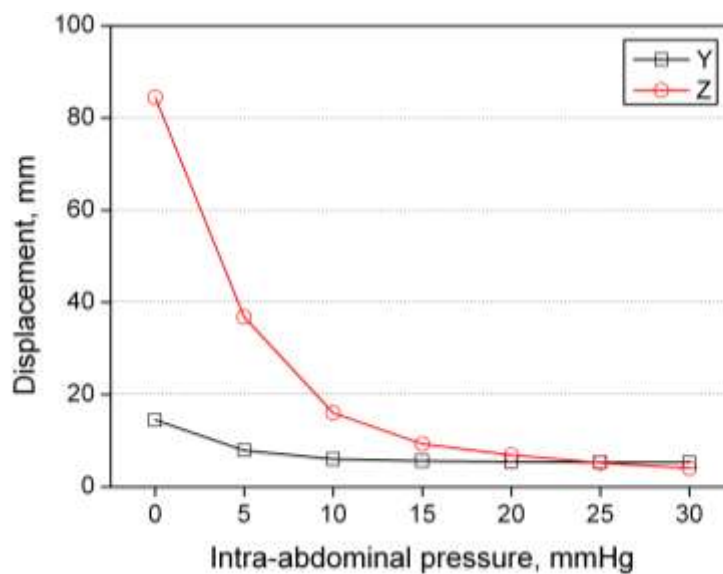
Figure 4.5 The displacements of head between the initial position and final position in Y and Z directions after simulations with elevated IAP
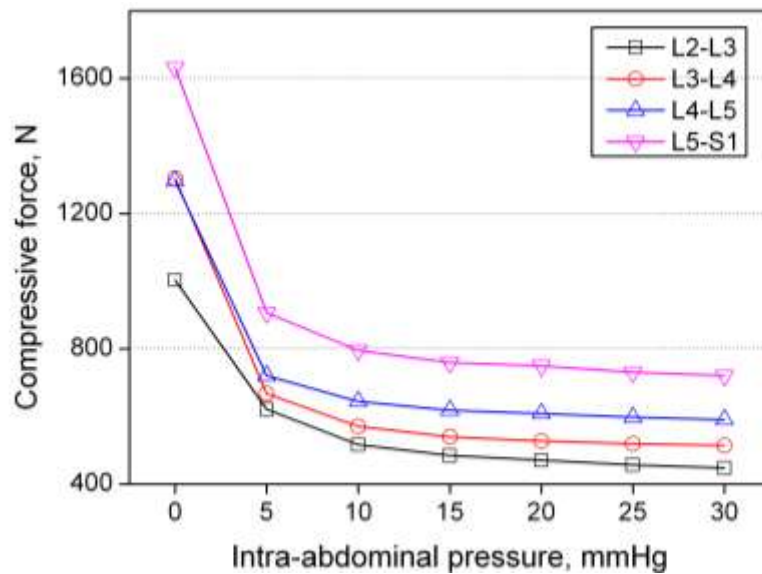
Figure 4.6 The compressive loads of intervertebral joints with elevated IAP

The results of this study indicate that elevated IAP helps stabilizing the human body model with less head displacements. In the absence of IAP, the head displacements in both Y and Z directions are highly obvious. The human body model is not able to maintain the same upright sitting posture after simulations with the upper torso bending backwards. After implementing elevated IAP in the body model, the head displacements in both directions decrease, indicating the musculoskeletal model is more stabilized and is more capable to maintain the same upright sitting posture with no obvious backward bending of upper torso.

On the other hand, the results show that the implementation of elevated IAP reduces the compressive loading on the lumbar joints. It is noted that the compressive forces of L3-L4, L4-L5 and L5-S1 joints without IAP are 1304N, 1297N and 1631N respectively, which are all higher than the mean values obtained from the simulation with dynamic motion data of upright sitting posture presented in Chapter 3.

Since the normal average IAP of subjects in sitting was 16.7mmHg (Cobb et al., 2005), the body model with IAP of 15mmHg in this study is considered as the real case in sitting. In this real case, the head displacements in both Y and Z directions are less than 15mm, which are acceptable for simulation. The compressive forces of L2-L3, L3-L4, L4-L5 and L5-S1 are 484N, 539N, 618N and 759N respectively, which are less than half of those without IAP.

Overall, it can be concluded that IAP is necessary as a continuous stabilizing and compression-reducing mechanism in the study of static posture when the detailed

kinematic trajectories are not provided. Since IAP is modeled as a bushing element in this study, there is no need to be concerned with the compressive effects of abdominal muscle forces required to produce the IAP, which was discussed in literature (McGill and Norman, 1987a). Hence in the following simulations of static sitting with various seat design parameters, the musculoskeletal multi-body model with a normal IAP (16.7mmHg) was applied.

4.4 Integration with Seat Model

A seat model was developed and integrated with the musculoskeletal multi-body model in LifeMOD as shown in Figure 4.7 to provide a new basis for the investigation of sitting biomechanics. The seat design parameters involved in this research (Figure. 4.8) include backrest inclination, seat pan inclination, seat pan height, seat pan depth and backrest height. For the parameters related to the inclination of seat surface, such as backrest inclination and seat pan inclination, the effects of friction coefficient of the seat surface have also been studied.

Contacts were created on the sitting interfaces. Figure 4.9 and Figure 4.10 show the contact points defined in the study. There are 24 contact points defined between the backrest and the upper body, 3 contact points defined between the seat pan and the lower body, and 2 contact points defined between the footrest and the feet. For better visualization, the graphics of muscles, ligaments, connecting joints and seat are hidden in these two figures to show the locations of contact points. The contact forces are calculated based on the overlapping area of the two contacting bodies and other parameters, such as stiffness, damping, coefficient of friction, and stictional and frictional transition velocities. The values of these parameters can be obtained from Table 3.4 in Chapter 3. The inverse and forward dynamic simulations were conducted to study the effects of various seat design parameters. The resulting outputs are the compressive forces of lumbar joints.
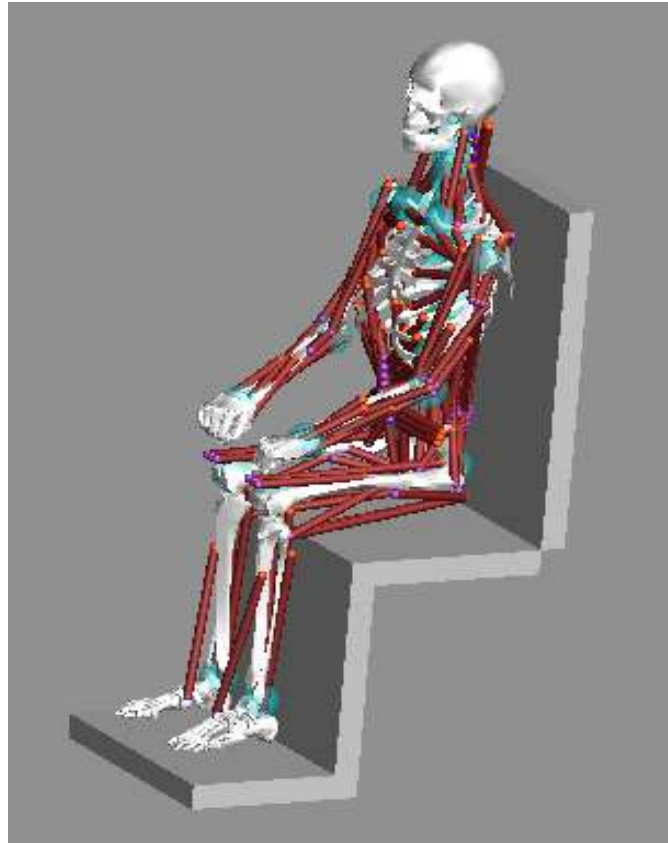
Figure 4.7 Musculoskeletal multi-body model integrated with a seat model
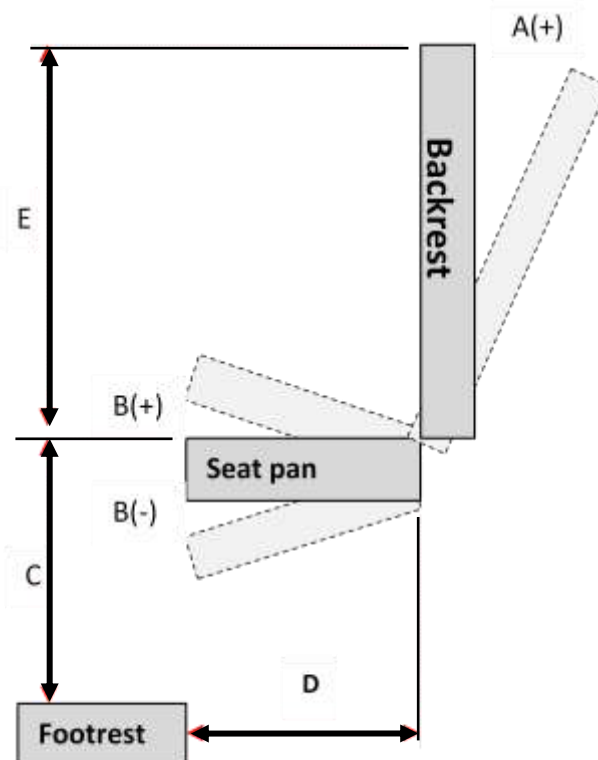
Figure 4.8 Variables of seat design: A, backrest inclination; B, seat pan inclination; C, seat pan height; D, seat pan depth; E, backrest height.
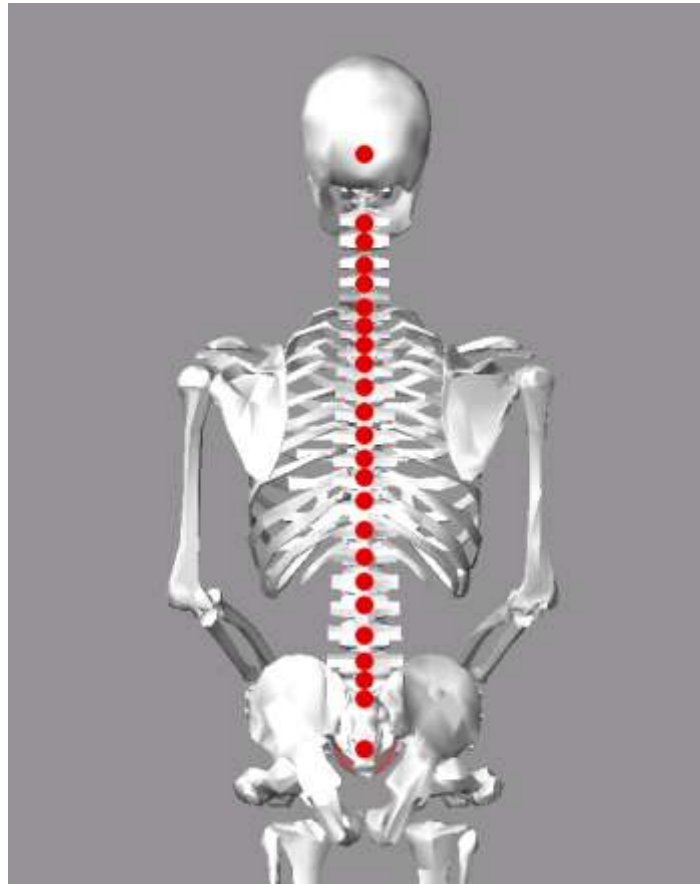
Figure 4.9 Contact points defined between backrest and body (back view)
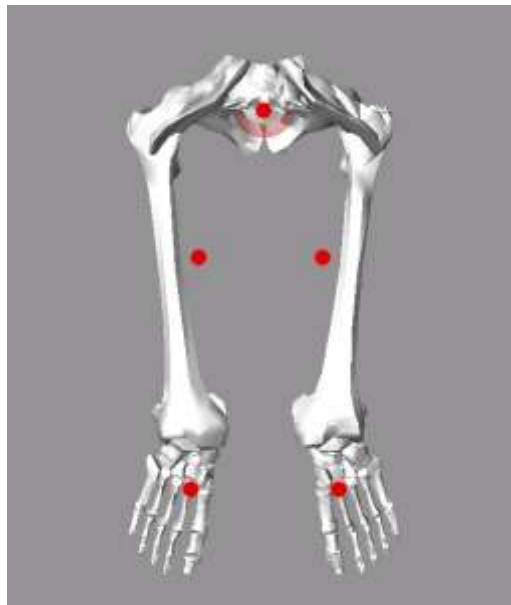
Figure 4.10 Contact points defined between seat pan, footrest and body (top view)

4.5 Backrest Inclination

Backrest inclination (Figure 4.8 A) describes the angle between the backrest and the vertical line. The inclination angle of an upright backrest is 0°. When the backrest inclines towards the seat pan, the inclination angle is defined to be negative; when the backrest inclines away from the seat pan, the inclination angle is defined as positive. Since the backrest with a positive inclination angle is much more common in daily life, the effects of varying backrest inclination angle from 0° to 20° with increment of 5° and friction coefficient of seat surface from 0.2 to 0.8 in the increments of 0.2 were studied.

The variation of compressive forces of joint L2-L3, L3-L4, L4-L5 and L5-S1 over the backrest inclination and the friction coefficient are shown in Figure 4.11, 4.12, 4.13 and 4.14 respectively. Overall, the results show that the biomechanics of sitting is very complicated. It was expected that all the compressive joint forces would decrease as the backrest inclination increases, due to the fact that a higher portion of body weight can be supported by the backrest. However, only the joint force of L4-L5 with a friction coefficient of 0.8 and the joint force of L5-S1 with friction coefficients of 0.6 and 0.8 follow this trend. It is interesting to notice that the compressive joint forces depend on the backrest inclination and the friction coefficient of seat surface in a complicated way. Greater backrest inclination can cause greater compressive forces on spinal joints in certain situations, such as a low friction coefficient of seat surface (0.2 or 0.4).
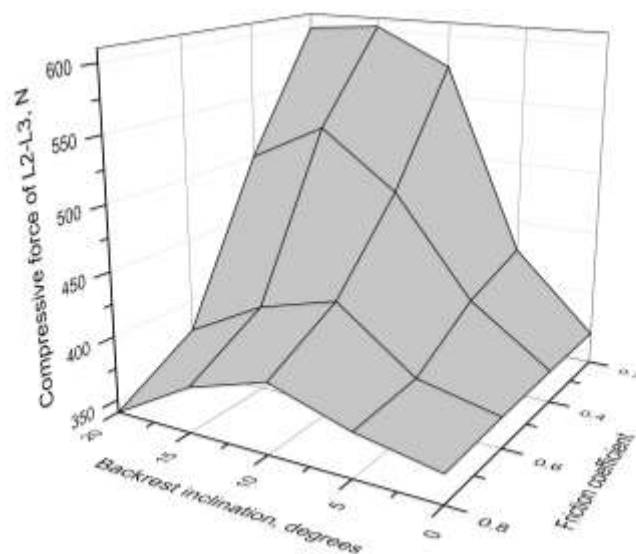
Figure 4.11 Compressive forces of L2-L3 joint over the backrest inclination
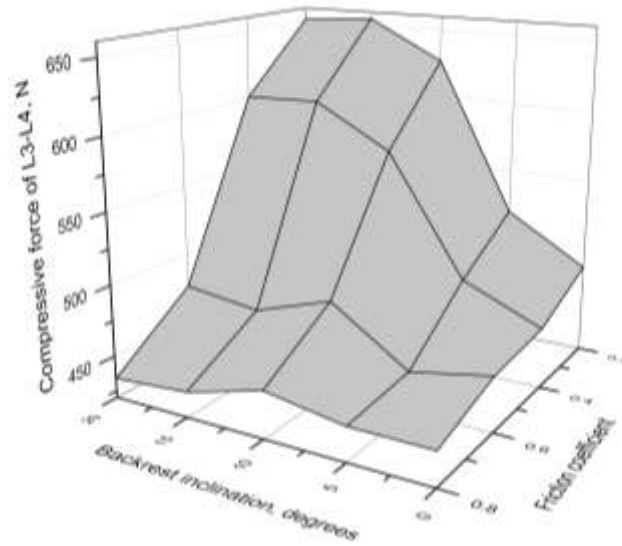
Figure 4.12 Compressive forces of L3-L4 joint over the backrest inclination
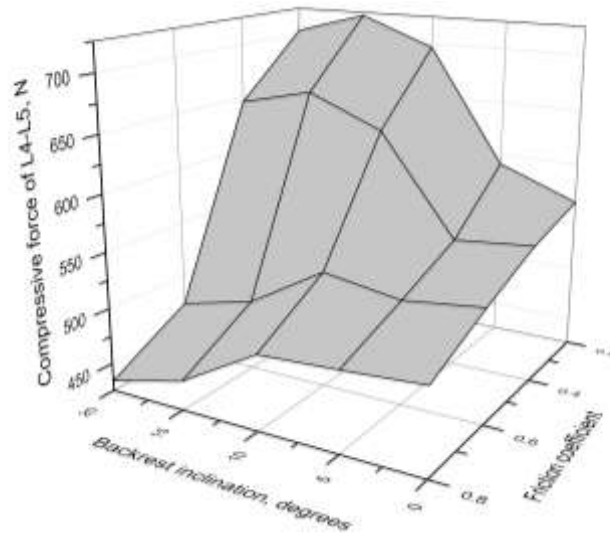
Figure 4.13 Compressive forces of L4-L5 joint over the backrest inclination
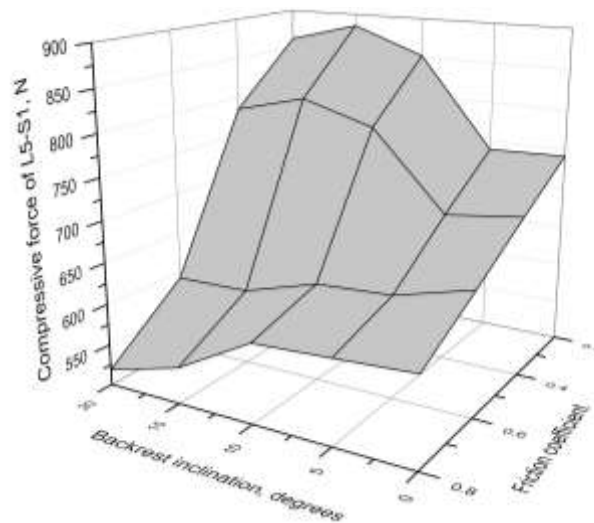
Figure 4.14 Compressive forces of L5-S1 joint over the backrest inclination

Overall, the simulation results show that a greater backrest inclination may or may not decrease the compressive joint forces is dependent on other conditions, such as the friction coefficient of seat surface. When the coefficient is large enough to prevent slip (0.6 or 0.8), greater inclination of backrest can lead to less compressive forces on joints L4-L5 and L5-S1. This finding is in consistent with the results from literature that the decrease of disc pressure is caused by the increase of backrest inclination (Andersson and Ortengren, 1974a, Andersson et al., 1974b, Andersson et al., 1974a). When the coefficient is low (0.2 or 0.4), greater inclination of backrest can cause more compressive forces on all those joints. This is due to the low friction coefficient of seat surface with low resistance to motion, making the human body a tendency sliding off the chair. In literature, there is one study about the dependency of compressive joint force with the friction coefficient in a certain backrest inclination using musculoskeletal multi-body modeling (Grujicic et al., 2010). From that study, the compressive force of L4-L5 joint increases when the coefficient changes from 0.5 to 0.2 with a 10° backrest inclination. It is obvious that the results from the current study in Figure 4.13 are in consistent with the findings in literature. This also supports the conclusion that the lumbar disc pressure is higher if the lumbar lordosis is maintained by muscle activity other than back support (Andersson and Ortengren, 1974b). Further study can be carried out to evaluate the variation of related muscle activity in sitting in an inclined chair with a low friction coefficient.

4.6 Seat Pan Inclination

Seat pan inclination (Figure 4.8 B) describes the angle between the seat pan and the horizontal line. The inclination angle of a horizontal seat pan is 0°. When the seat pan inclines towards the floor, the angle is defined as positive; when the seat pan inclines away from the floor, the angle is defined as negative. In this study, the effects of varying seat pan inclination angle from -10° to 10° with increment of 5° and friction coefficient of seat surface from 0.2 to 0.8 in the increments of 0.2 were examined.

The variation of the compressive force of joints L2-L3, L3-L4, L4-L5 and L5-S1 over different seat pan inclinations and friction coefficients are shown in Figure 4.15, 4.16, 4.17 and 4.18 respectively, with the positive inclination meaning the

forward tilt of seat pan. In this study, all these joints show the maximum compressive forces at the seat pan inclination angle of -10° and the minimum at 10°. The effects of friction coefficient with the forward inclination of seat pan on spinal loads are not significant, but very significant with the backward inclination of seat pan. For example, it is obvious that with the backward seat pan inclination, the compressive forces of spinal joint at friction coefficient 0.2 are much higher than those at 0.4.
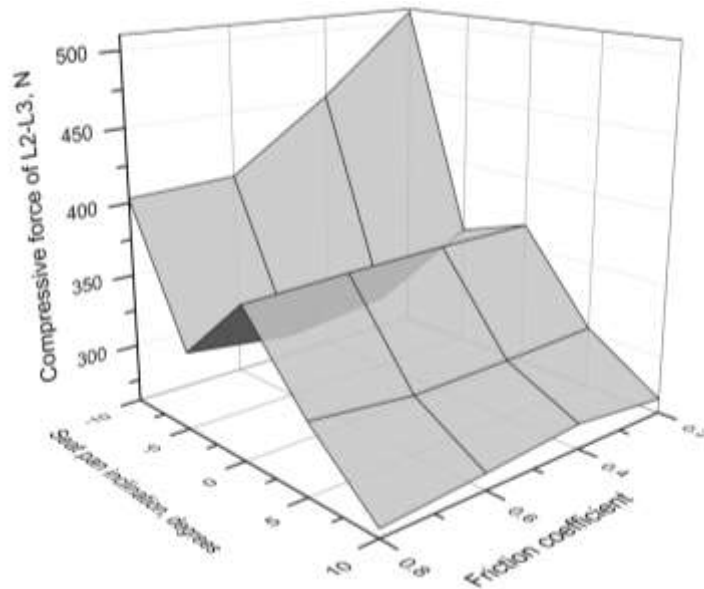
Figure 4.15 Compressive forces of L2-L3 joint over the seat pan inclination
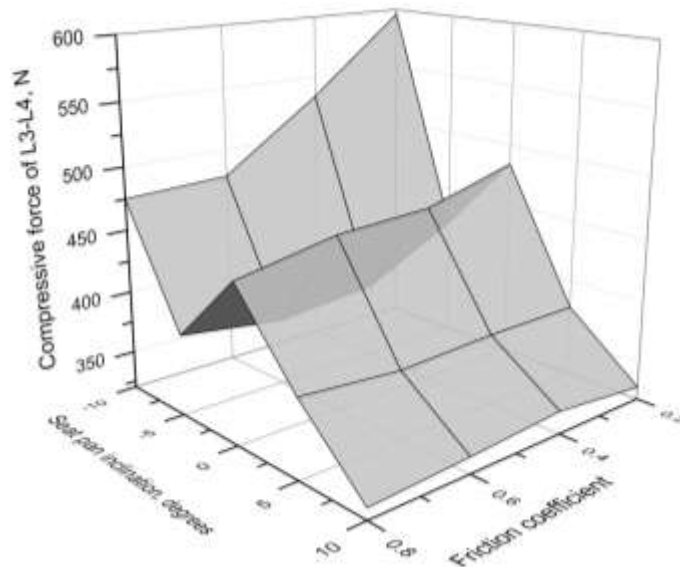
Figure 4.16 Compressive forces of L3-L4 joint over the seat pan inclination
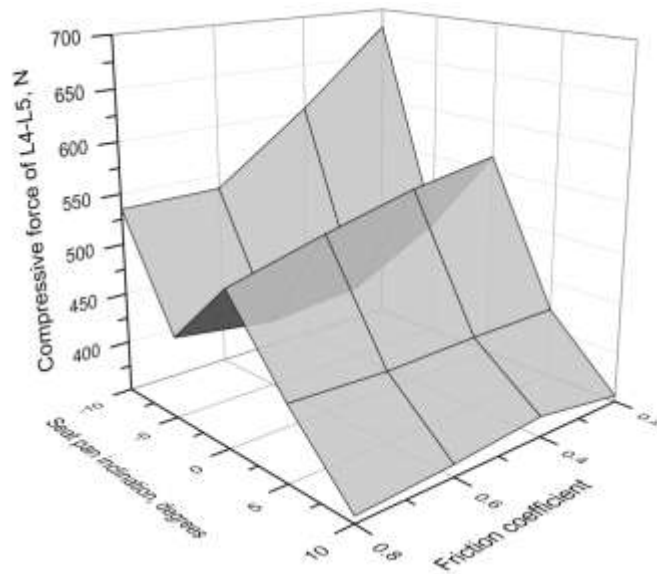
Figure 4.17 Compressive forces of L4-L5 joint over the seat pan inclination
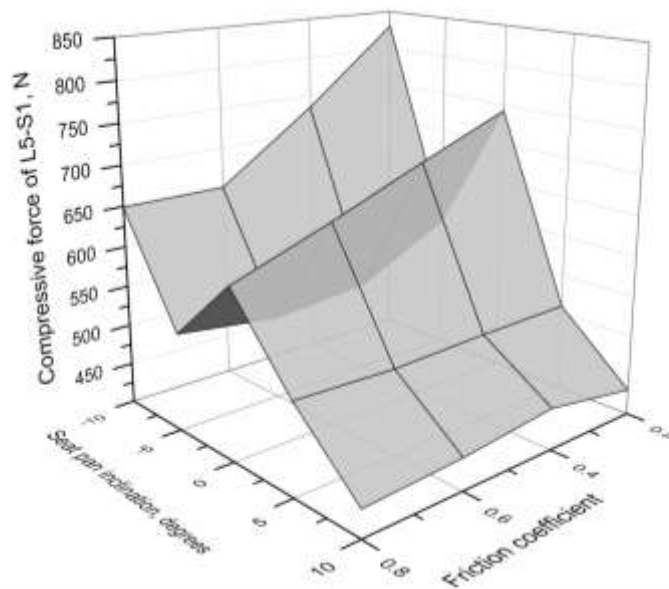
Figure 4.18 Compressive forces of L5-S1 joint over the seat pan inclination

In literature, there are some disagreements on the optimal inclination of seat pan, as discussed in Chapter 2. From the results of this study, it is found that the forward tilt of seat pan can decrease the compressive forces of joints, which is beneficial to the human body. This can be explained by an increase of lumbar lordosis with a forward increase of seat pan inclination (Bendix and Biering-Sørensen, 1982). As the seat pan inclination increases from 0° to 10°, the concurrent increased thigh-trunk angle can cause an increase of lumbar lordosis (Keegan, 1953). As a consequence, the reduction of lordosis in the horizontal seat pan leads to greater compressive force of the spinal joints thus may cause LBP in the long run. However,

the backward tilting seat pan may or may not decrease the compressive force of spinal joints depending on the backward inclination angle. For example, a backward seat pan inclination of -10° can increase the compressive loading of lumbar spinal joints. However, with a backward inclination of -5°, the compressive forces of joints are lower than the ones with no inclination. It was expected that the backward inclination of seat pan would increase the load at the lumbar spine, due to the findings of the reduction of lordosis or the appearance of kyphosis of the lumbar spine when the thigh-trunk angle is changed from 200° to 50° (Keegan, 1953). The support from the backrest of seat can be a reason for the decrease of compressive forces with the backward seat pan inclination. When the seat pan tilts backwards, the human body is also pushed backwards, which forms better contact between the back and the backrest. A deeper investigation can be carried out to focus on the spinal loads and the contact forces with the backward seat pan inclination in the increments of 1° in future.

4.7 Seat Pan Height

Seat pan height (Figure 4.8 C) is the distance from the seat pan to the footrest. The medium-level seat pan height, which should be adjusted according to the height of the sitting subject, is defined to enable a knee angle of 90°. In this study, the medium-level seat pan height is 463mm for the sitting body model. The low-level seat pan height was set as 363mm, with the knee angle of the sitting body model less than 90°. The high-level seat pan height was set as 563mm, while the knee angle of 90° and the dangling feet of the sitting body model. In this study, the effects of seat pan with low-level height, medium-level height and high-level height were examined.

The effects of varying seat pan heights on the compressive forces of lumbar joints from L2-L3 to L5-S1 are shown in Figure 4.19. It is found from the results that the compressive forces with different seat pan heights increase in the following order: medium-level, high-level and low-level.

When the human body sits on a seat pan with the medium-level height, which means the knee angle is 90° and the feet are in contact with the footrest, the seat is able to provide good support to the lower torso, upper legs and feet. However, for the seat pan with the low-level height, only parts of upper legs are supported by the seat pan and a higher portion of the body weight than usual is transferred to the lower

torso and the feet as the knee angle of the sitting body is less than 90°. As the knee angle decreases, the thigh-trunk angle also decreases. It is found from the results of another study that as the thigh-trunk angle decreases from 200° to 50°, the lumbar curvature changes from lordosis to kyphosis (Keegan, 1953). It has also been concluded in another study that the loss of lordosis of the lumbar spine can increase the compressive forces on the lumbar joints (Harrison et al., 1999). This should be the reason that the seat pan with the low-level height causes the highest compressive forces in this study. On the other hand, the seat pan with the high-level height can maintain the same knee angle (90°) as the medium-level height, but can incur the dangling feet of the sitting body (Keegan, 1953). This leads to the neglect of support from footrest, which was found to be able to bear 18.4% of the body weight (Swearingen, 1962). Thus this explains why the seat pan with the high-level height causes greater compressive loads on the lumbar joints as compared to the medium-level height seat pan.
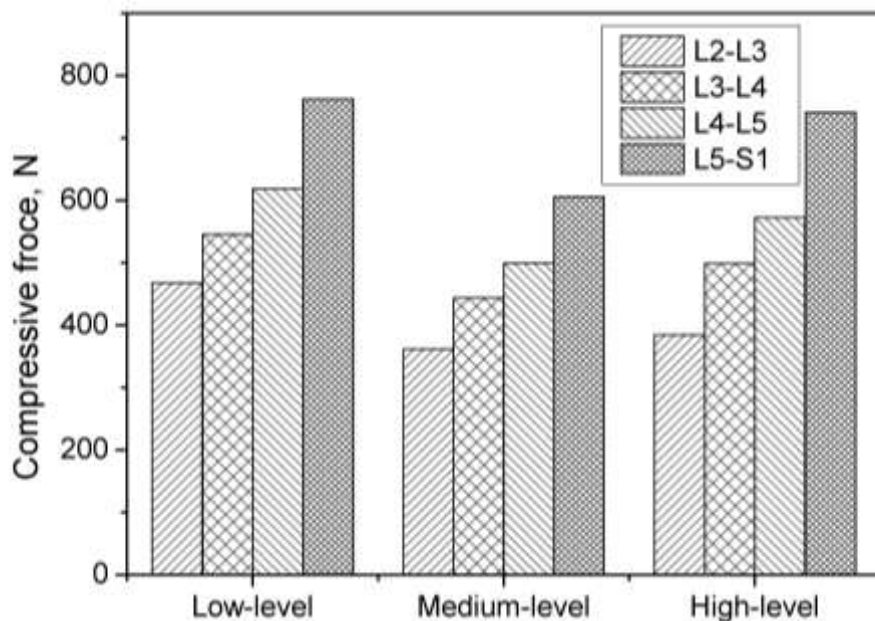
Figure 4.19 The variation of compressive forces of lumbar joints over the seat pan height

4.8 Seat Pan Depth

Seat pan depth (Figure 4.8 D) is the distance from the front edge to the back edge of the seat pan in the sagittal plane of sitting body. The seat pan with the medium-level depth can support almost full of upper legs with four fingers space (70mm) between the knees and the front edge of the seat pan, and allow the sitting body making use of the backrest. In this study, the medium-level depth of the seat pan was set as 400mm; the low-level depth was set as 300mm, with a distance of 170mm between the knees and the front edge of the seat pan; The high-level depth was set as 500mm, with a distance of 70mm between the knees and the front edge of the seat pan, thus the sitting body is not able to utilize the backrest to support the upper torso. In this study, the effects of seat pan with low-level depth, medium-level depth and high-level depth were examined.
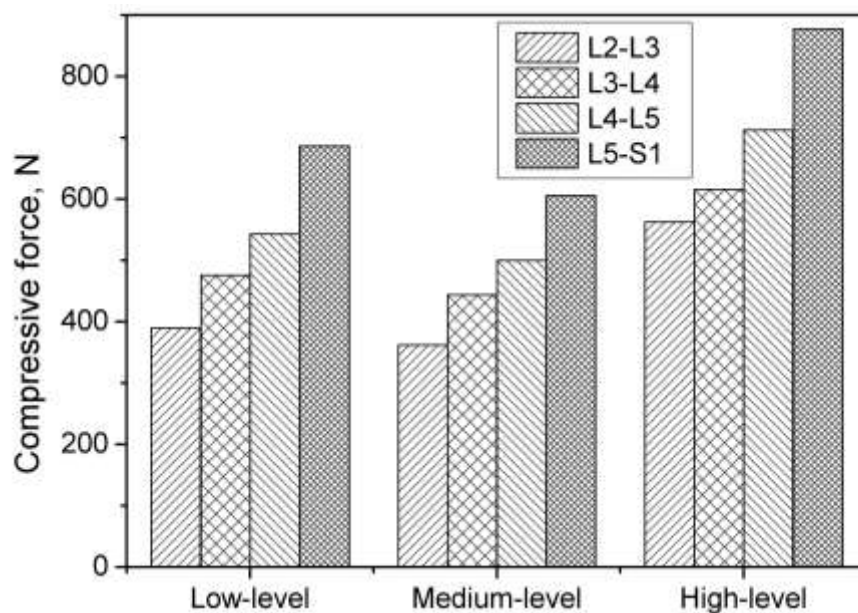
Figure 4.20 The variation of compressive forces of lumbar joints over the seat pan depth

The influence of different seat pan depths on the compressive forces of lumbar joints from L2-L3 to L5-S1 is shown in Figure 4.20. Three types of seat pan depths have been studied, including low-level, medium-level and high-level. From the figure, the compressive forces with different seat pan depths increase in the following order: medium-level, low-level and high-level. Interestedly, the seat pan with the high-level

depth leads to highest compressive loads on the lumbar joints than the other two levels.

Compared to the medium-level depth, the seat pan with the low-level depth is not able to provide full support for the upper legs. In this case, more energy is required to maintain the sitting posture. Thus higher compressive forces are observed in the low-level depth than the medium-level. When the depth of seat pan is at the high-level, the body can only sit on the frontal part of the seat pan, with full support for upper legs. However, this type of seat pan depth causes the sitting body neglecting the backrest. Since there is no contact between the body and the backrest, the human body needs to maintain the lumbar curvature by its own muscle activation instead of the support from backrest. This explains the significantly great compressive forces observed in the seat pan with the high-level depth. This result is also in agreement with other studies (Andersson and Ortengren, 1974b, Wilke et al., 2001) with the conclusion that the lumbar disc pressure with lumbar lordosis maintained by the muscle activity is higher than the one maintained by the lumbar support.

4.9 Backrest Height

Backrest height (Figure 4.8 E) is the distance from the top edge to the bottom edge of the backrest in the sagittal plane of sitting body. The backrest with the medium-level height means it is able to provide the full shoulder support for the sitting body, which was 650mm in this study. The low-level height is defined to be able to support only the lumbar region, which was set as 300mm. The high-level height is defined to be able to fully support the head and neck, which was set as 950mm. Seats without backrest are another common type of seats in daily life. Thus, in this study, the effects of seat without backrest, and with low-level, medium-level and high-level heights of backrests were examined.

Figure 4.21 shows the results of compressive forces of lumbar joints over the different backrest heights. Four types of backrests were included: no-backrest, low-level height backrest, medium-level backrest and high-level backrest. From the figure, the seats with no backrest and the low-level height backrest can cause higher compressive forces on lumbar joints than the medium-level height backrest and the

high-level height backrest. It is also observed that almost same compressive forces are found in backrests with the medium-level height and the high-level height.
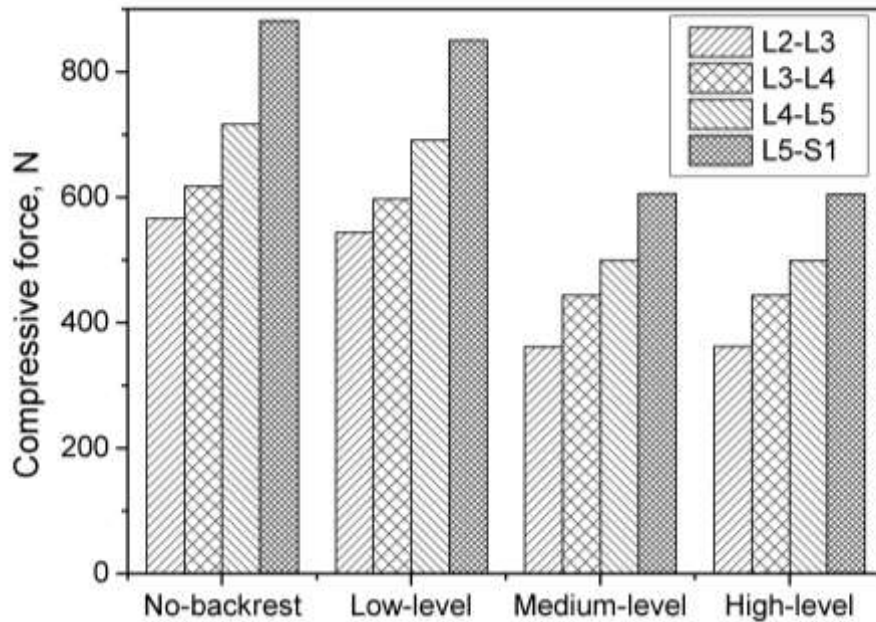
Figure 4.21 The variation of compressive forces of lumbar joints over the backrest height

In this study, the seat with no backrest causes the highest compressive forces on the lumbar joints. The reason is that the sitting body has to maintain the spine curvature by its muscle activity thus leading to higher compressive loads on the lumbar joints (Andersson and Ortengren, 1974b), same as the case of high-level seat pan. For the backrest with the low-level height, it can only provide support for the lumbar part of spine. Hence the compressive forces are lower than the seat without backrest but higher than the seat with the medium-level height of backrest. The backrest with the medium-level height can provide support from the shoulder to the lower torso. It helps relax the muscles on the back and reduce the energy expenditure. It was expected that the backrest with the high-level height can lead to the minimum compressive loads, since it supports the body from head to lower torso. However, the compressive forces with the high-level height and the medium-level height are quite similar. This may be explained by the fact that the placement of the backrest in this study is upright with 0° inclination angle. Due to the natural curvature of spine, when people sit upright on the seat with the high-level height backrest, little or even no contact exists between the head and the backrest. Thus the effects of backrest height with certain positive inclination of backrest on the spinal loads can be included in future.

4.10 Summary

The objective of this study is to investigate the influence of various seat design parameters on the compressive forces of lumbar joints. The seat design parameters which have been studied include backrest inclination, seat pan inclination, seat pan height, seat pan depth and backrest height. Before conducting the simulations for these seat design parameters, it was suggested that the IAP may be necessary to be implemented in the musculoskeletal human body model, since no motion trajectories were applied to train the body model. Thus at the beginning of this chapter, the effects of elevated IAP on the displacements of head and the spine loadings were studied, from 0mmHg to 30mmHg with increment of 5mmHg. Results show that the body model without IAP (0mmHg) introduces the greatest head displacements in Y and Z directions in the sitting posture and the highest compressive loads on lumbar joints. The elevated IAP can help stabilize the human body model in sitting by decreasing the head displacements and reducing the compressive loads on lumbar joints. The findings of this study can contribute to a better understanding of the biomechanics of IAP, and provide some suggestions for the rehabilitation of patients with back pain and other back problems. It is suggested that people can make better use of IAP through regular exercise, which can help reduce the loadings on spinal joints and thus relieve LBP.

Based on the findings, it is also concluded that the IAP should be implemented in the musculoskeletal body model for the simulations of static posture, as a stabilizing and compression-reducing mechanism. Thus the musculoskeletal body model with a normal IAP in sitting (16.7mmHg) was applied in the investigation of the effects of various seat design parameters in the following studies of seat design parameters.

Overall, the results of this study provide some general rules of seat design and provide some guidelines on choosing parameters for optimal seat design parameters. However, other factors should always be considered in the seat design, such as the requirement of individuals and related jobs. For example, people with problems on their L2-L3 or L3-L4 joint are not recommended to choose a backrest with inclination angle of 10°, when the friction coefficient of seat surface is high. Because it is found

from the results that the backrest inclination angle of 10° can introduce higher compressive forces on these two lumbar joints than other inclination angles.

Being an exploratory study, the posture of upright sitting has been used to study the seat design parameters. Therefore, one limitation of this study is that only one specific sitting posture has been investigated. But in daily life, there are many other commonly adopted sitting postures apart from upright sitting. In addition, the anthropometric data of the model may also have some effects on the resulting joint forces. Thus it is suggested that other types of sitting postures and different sizes of musculoskeletal models can be involved in the future study.

CHAPTER 5

STUDY OF SITTING STABILITY WITH SCOLIOSIS SPINE MODEL

5.1 Introduction

In the previous two chapters, sitting posture and seat design for people with healthy spine have been investigated. A straight spine is good for function in sitting (Fujita et al., 2005). However, the sitting situation for people with scoliosis is not optimistic, as discussed previously in Chapter 2. People with scoliosis may suffer from unbalanced sitting, with the center of weight not in the midline of the upper body (Smith and Emans, 1992, Larsson et al., 2002). A good understanding of the sitting stability is very important for the assessment and the surgical treatment of patients with scoliosis (Smith and Emans, 1992).

Thus, the main objective of this chapter is to investigate the sitting stability of people with scoliosis through musculoskeletal multi-body modeling with scoliosis spine and computational simulation in LifeMOD. The flow chat of the method is presented in Figure 5.1. Since the Cobb angle of scoliosis defines the severity of spinal deformity (as introduced in Chapter 2), the effects of various Cobb angles of scoliotic spines on sitting stability and the spinal loads were studied first using three hypothetical scoliosis body models. Next, three scoliosis patient models with different curve patterns of scoliosis were applied to study the influence of various backrests and muscle activities of related lumbar muscle group on the sitting stability and spinal loads. In these studies, the developed musculoskeletal multi-body models were adjusted to be in the static sitting position. After creating the corresponding chair model, contacts were defined between the body and the chair. Inverse and forward simulations were run to obtain the final results, such as the head displacements and

spinal joint forces. The studies in this chapter may help the evaluation of sitting stability of people with scoliosis and provide possible strategies to improve the stability in sitting.
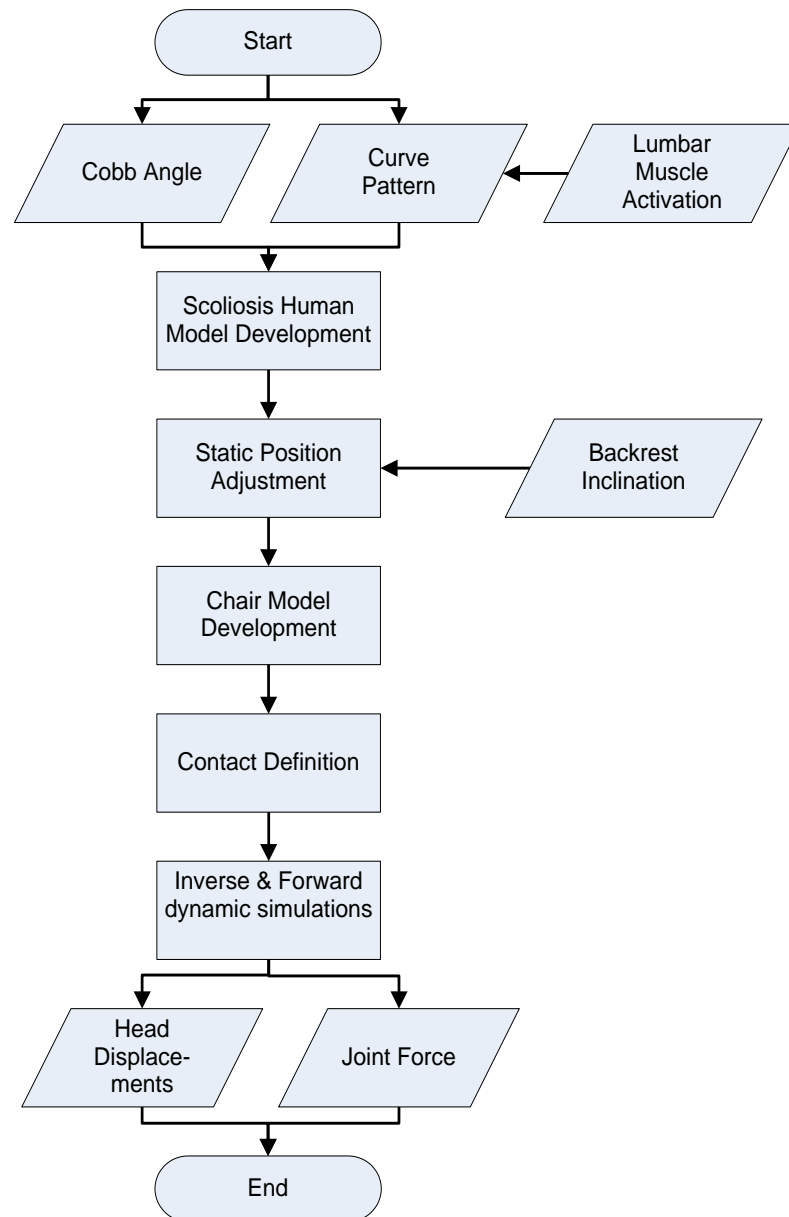
Figure 5.1 Flow chart of method of study of sitting stability with scoliosis spine model

An additional study about sitting posture of patients with scoliosis through motion capture and musculoskeletal modeling is presented in Section 5.9. The method is similar to the one applied in Chapter 3. However, the experiment subject in this study is the patient with scoliosis, instead of healthy people in Chapter 3. The dynamic motion data obtained in the motion capture experiments were used to drive the developed musculoskeletal multi-body model (with the discretized scoliosis spine)

in LifeMOD to run the inverse and forward dynamic simulations. This preliminary study with only one patient subject can work as a basis for future research about sitting posture on more patient subjects.

5.2 General Method of Scoliosis Spine Modeling

The general method of scoliotic spine modeling used in this chapter is introduced here. The development of the scoliotic spine model starts with the creation of a human body model with an enhanced normal spine in LifeMOD according to the procedures described in literature (Huynh, 2010, Huynh et al., 2013). The body model with a normal spine is the basis for developing scoliosis models. The curvature of scoliosis is created by properly displacing and rotating the related vertebrae and joints in the frontal plane to form the desirable Cobb angle, as shown in Figure 5.2. The attachment points of related soft tissues are also relocated according to the curvature of scoliotic spine. For better visulization on the shapes of a normal and a scoliosis spine, some segments, joints and muscles in the musculoskeltal models are hidden in this figure. In this thesis, the only difference between the scoliosis body model and the healthy body model is the shape of spine structure (locations and orientations of vertebrae and joints). The other properties assigned during the modeling process are the same for the scoliosis and healthy models, such as torsional stiffness of spinal joint (Table 3.1), segmental ranges of motion (Table 3.2), etc.
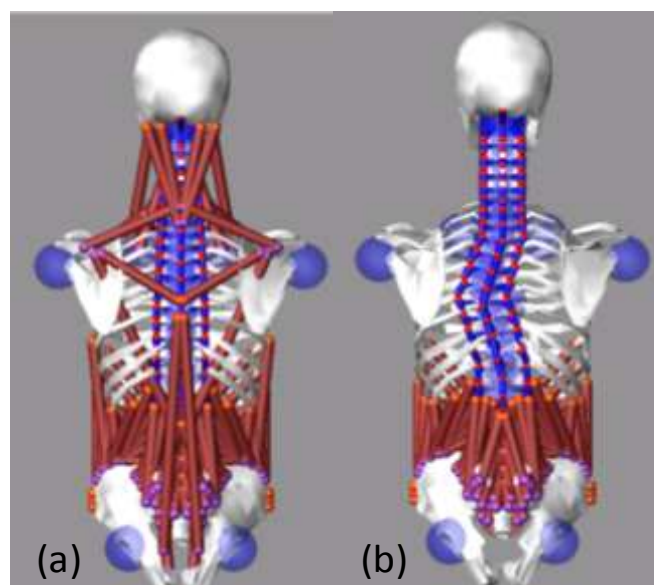
Figure 5.2 Healthy spine model (a) and scoliosis spine model (b)

5.3 Development of Three Hypothetical Scoliosis Spine Models

In order to investigate the effects of various Cobb angles of scoliotic spine on sitting stability and spinal biomechanics, three multi-body models (178cm height, 70kg weight and 24 years old) with hypothetical scoliosis (Cobb angles of 38°±2, 52°±2 and 62°±2 in the thoracic region) from T4 to T10 with the apex on T7 were developed (Hajizadeh et al., 2012a) and used. These scoliosis models with the Cobb angle of 38°, 52° and 62° are referred to as Case I, Case II and Case III respectively in this chapter. Figure 5.3 shows the posterior view of these three hypothetical scoliosis models with different Cobb angles. For better visualization, unrelated body segments and muscle sets in the cervical and thoracic regions are hidden in the figure.
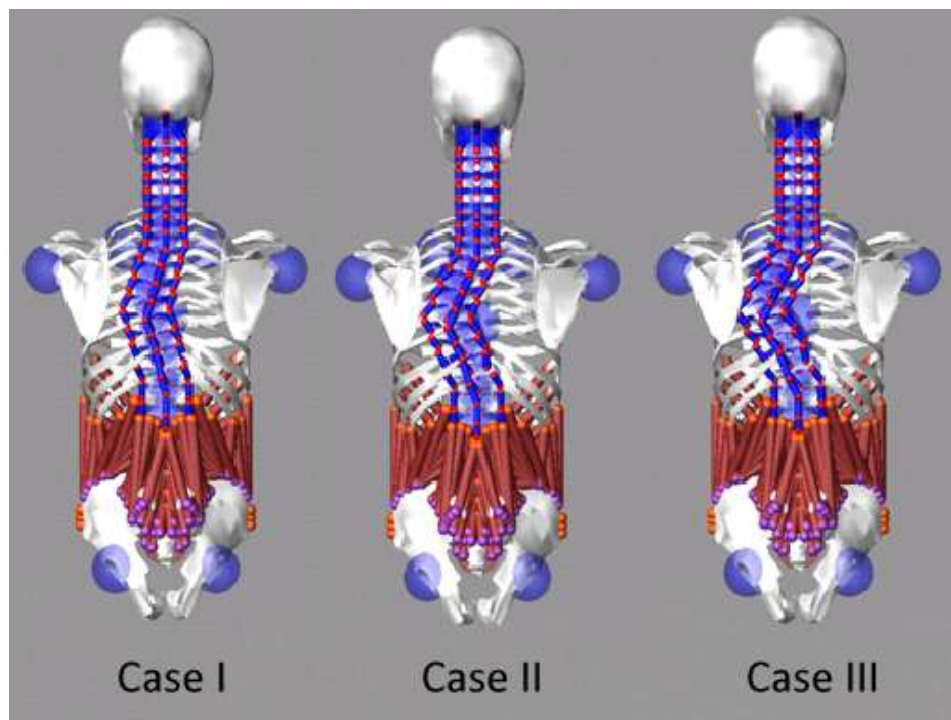
Figure 5.3 The posterior view of scoliosis models with 38° Cobb angle (Case I), 52° Cobb angle (Case II) and 62° Cobb angle (Case III)

These three scoliosis models were set in upright sitting for the study in static posture. In order to study the sitting stability, the support of seat backrest was neglected. Seat pan, footrest and contact points between the support system and the human body (refer to Figure 4.10) were created. The definition of contact between body and seat for scoliosis body model is the same as the one for the healthy body

model (refer to Table 3.4). After the inverse and forward dynamic simulations, the head displacements and the mechanical loading condition of lumbar joints can be obtained.

5.4 Effects of Various Cobb Angles

Lateral head displacements of Case I, Case II and Case III in the sitting posture are shown in Figure 5.4. It is clear that all the values of head displacements become constant after 1 second, which indicates that all the three hypothetical scoliosis models reach a new equilibrium state in the sitting posture. These findings help evaluate the stability of these hypothetical scoliotic models. Due to the asymmetry structure of scoliosis spine, the models may lean to one side and lead to a certain head displacement between the initial and final head locations. It is found from the results that the lateral head displacement is 1.9mm for Case I, 3.4mm for Case II, and 4.4mm for Case III. So the value of head displacement increases as the Cobb angle of scoliosis increases.
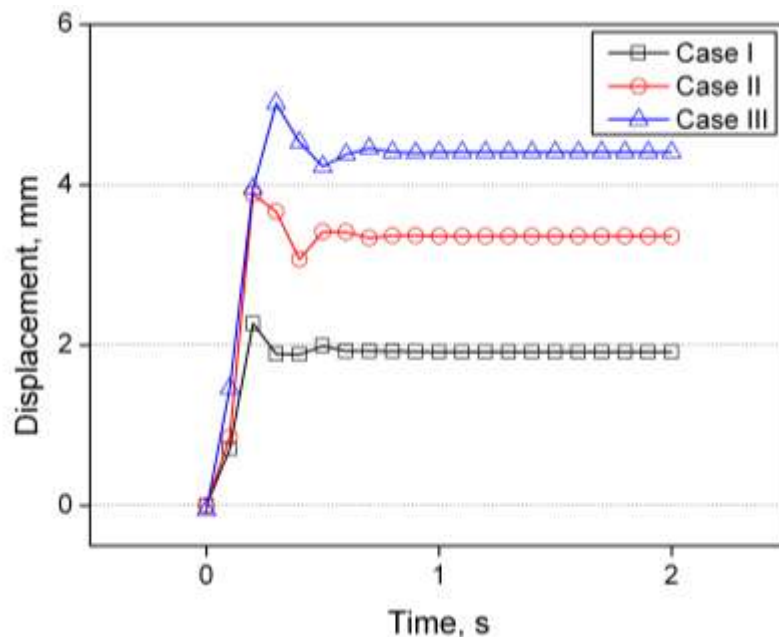
Figure 5.4 The lateral head displacements of Case I, Case II and Case III
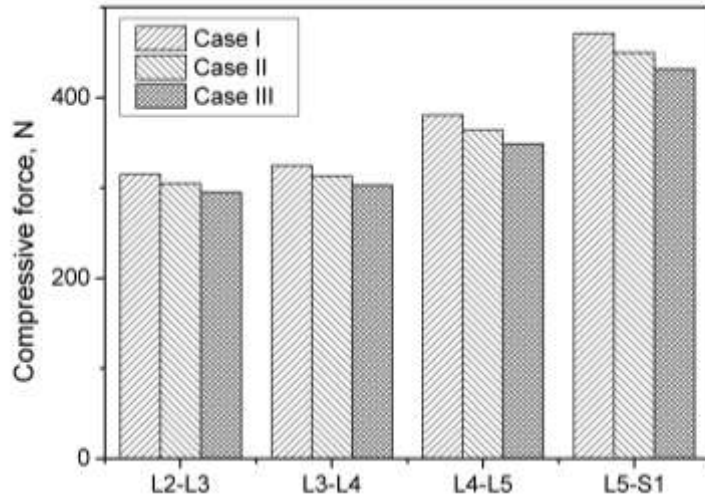
Figure 5.5 The compressive forces of lumbar joints of Case I, Case II and Case III
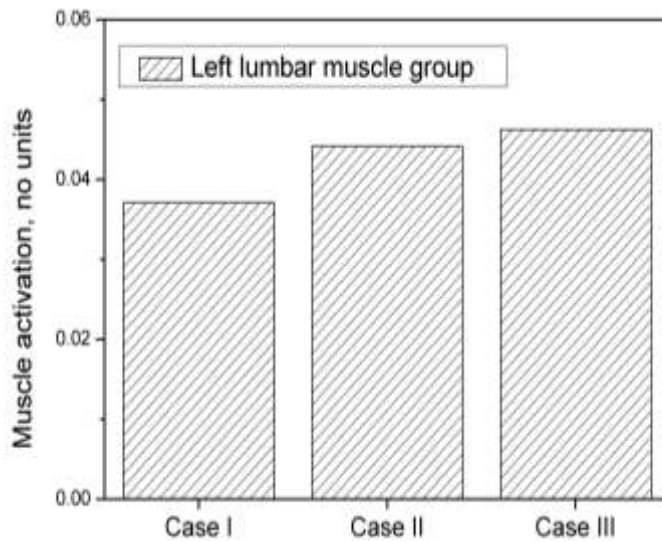
Figure 5.6 The mean activations of left lumbar muscle group of of Case I, Case II and Case III

The values of compressive force of lumbar joints (Figure 5.5) are found to decrease in the following order: Case I, Case II and Case III. It is interesting to find that the scoliotic model with the greatest Cobb angle presents the smallest compressive load. One reason could be the change of the weight distribution due to the spinal deformity. It can be observed from Figure 5.3 that the curvatures of scoliosis all start from T4 to T10 with the apex on T7 in the thoracic region. The "C" shape of the thoracic spine may change the force distribution in the lower torso. Meanwhile, the sitting stability has some effects on the loading conditions of spine. The scoliosis model leans more to the left side in sitting as the Cobb angle increases. A larger portion of force inside the body is likely to be distributed to the muscles on

the left side, especially to the left lumbar muscles. In fact it has been demonstrated that higher muscle activation of left lumbar muscle group was found in the scoliosis model with greater Cobb angle, as shown in Figure 5.6. The muacle activity represents the percentage of the maximum force that the muscle is producing. The lumbar muscle group (refer to Figure 3.8) includes multifidus muscle, erector spinae muscle, psoas major muscle and quadratus lumborum muscle in the lumbar region of human body.

Since the sitting stability in this chapter is evaluated by the head displacement in lateral plane, it is observed from the results that the Cobb angle of scoliosis curvature have some effects on the sitting stability of scolisos model. It is found that with greater Cobb angle, the sitting stability of scoliosis model is worse by introducing greater head disaplacement. On the other hand, greater Cobb angle of scoliosis model shows the least compressive forces on the lumbar joints, due to the situation that more portion of internal force is distributed to the left lumbar muscle group. It can be concluded from the results of current study that one of the strategies to improve the sitting stability of people with scoliosis is to reduce the Cobb angle of scoliosis curvature. The general suggestions for reducing Cobb angle include treatment by surgery, wearing brace during sitting, etc. However, this study only focuses on the specific curvature from T4 to T10 with the apex on T7. The findings may not apply to other types of scoliosis curvatures. Since the biomechanics of scoliosis is very complicated, more research is needed for deeper exploration.

5.5 Development of Models of Scoliosis Patients from X-Ray Images

In order to investigate the influence of various backrests on sitting stability of people with scoliosis, three scoliosis patient models developed based on the X-ray images of patients in the erect posture in the frontal plane from National University Hospital (NUH) in Singapore (Hajizadeh, 2013) were applied in the following study. Before the musculoskeltal modeling of scoliosis spine, the information about the location and the orientation of each vertebra were obtained by measurement using Computerised Patient Support System (CPSS) in NUH, as shown in Figure 5.7. The

musculoskelatal modeling of these three patients started by developing the normal spine models and followed by displacing and rotating the related vertebrae and joints to form the specific scoliotic curvature according to the measurement information.
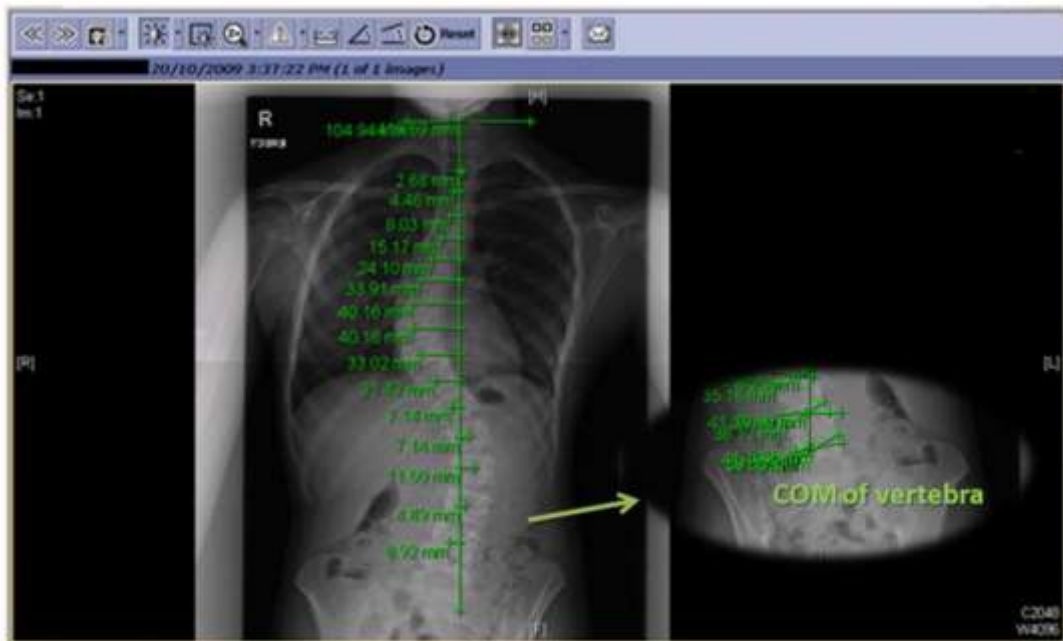
Figure 5.7 Location of the COM (center of mass) of the vertebrae in X-ray image
(Hajizadeh, 2014)

Table 5.1 shows the basic information of the three patients with scoliosis. The X-ray images and corresponding multi-body models of patient 1, 2 and 3 in erect posture are shown in Figure 5.8, 5.9 and 5.10 respectively. Patient 1 (P1) has the thoracolumbar scoliosis with the convexity to the left in the thoracic region. The scoliotic curvature starts from T4 to L4, with the apex on T10. Patient 2 (P2) also shows the thoracolumbar scoliosis with an obvious curvature from T7 to L3 and the apex on T10 on the left side of body. Patient 3 (P3) has the double scoliotic curvatures with the convexity to the right in the thoracic region and to the left in the lumbar region. The curvatures begin with T4 and end with L5, with the apex on T9 and L2.

Table 5.1 Basic information of patients

Patient	Gender	Height (cm)	Weight (kg)	Age (years)	Scoliosis curve pattern
1	F	151	41.0	15.0	Thoracolumbar
2	M	158	77.0	14.5	Thoracolumbar
3	F	161	45.5	15.5	Double

Figure 5.8 The front and back view of X-ray images and 3D model of P1

Figure 5.9 The front and back view of X-ray images and 3D model of P2
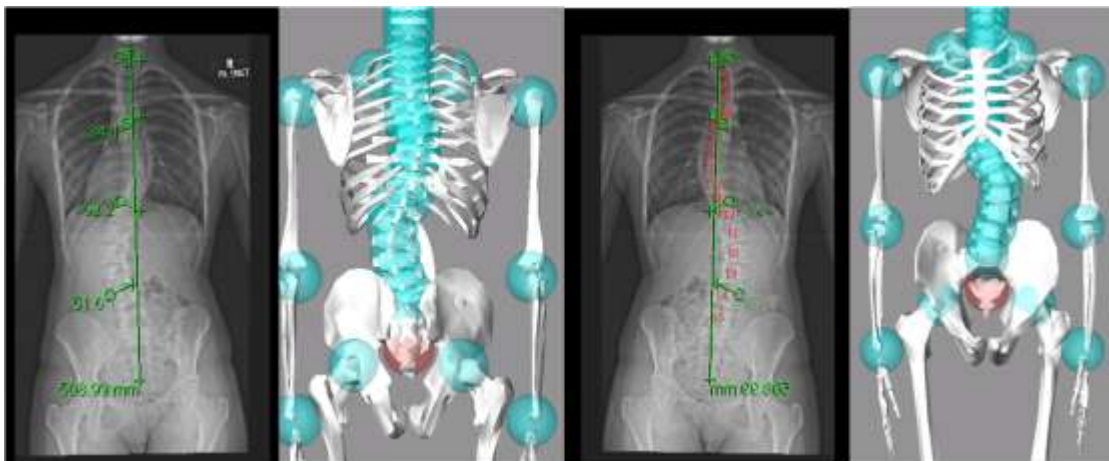
Figure 5.10 The front and back view of X-ray images and 3D model of P3

5.6 Effects of Various Backrests

The three patient models were set in upright sitting posture with hands resting on upper legs. In order to evaluate the effects of various backrests on sitting stability, three types of supporting systems were included in the current study: seat with no backrest, upright backrest and inclined backrest. The angles between seat pan and backrest (refer to Figure 4.8 A) were set to be 90° and 100° for the upright and inclined backrests respectively. After defining the contact points (refer to Figure 4.9 and 4.10) between the human body and the supporting system, the outputing results of head displacements and lumbar joint loads can be obtained by running the invers and forward dynamic simulations.
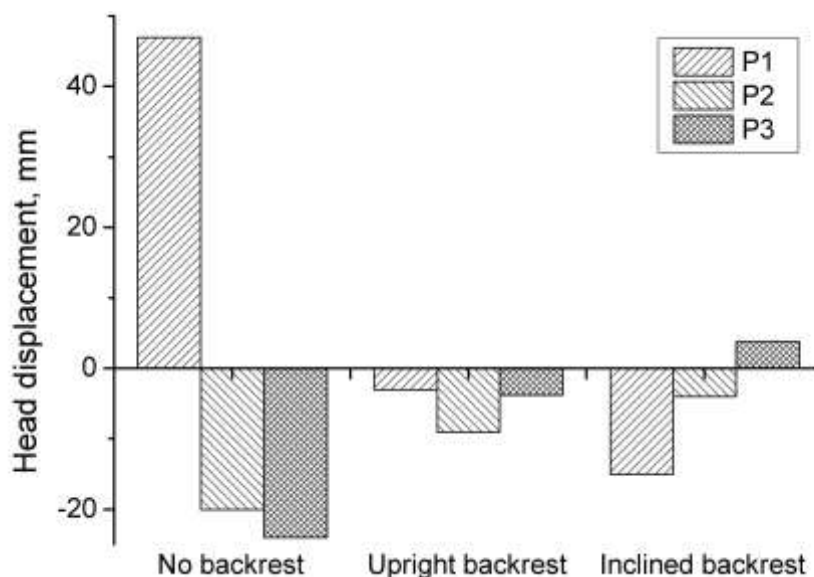
Figure 5.11 The head displacements in the lateral plane of P1, P2 and P3

All three patient models show that the greatest head displacement in the lateral plane is observed in the seat with no backrest (Figure 5.11). Due to the lack of support for the back, the upper body of scoliosis model without backrest is likely to lean to one side in the sitting posture. It is observed that the head of P1 leans to the opposite side with the greatest displacement compared to P2 and P3. It is because the scoliosis curvature of P1 is on the right side of body showing the most serious spine asymmetry in thoracolumbar area while the curvatures of P2 and P3 are on the left side of the body according to the X-ray images of patients. When the type of seat changes from no backrest to upright backrest, the values of head displacement decrease significantly. This finding corresponds to the belief that stability in sitting is achieved by the

backrest of seat (Swearingen, 1962). When the backrest inclines to 100°, the head displacement of P2 decreases, and the heads of P1 and P3 lean to the opposite side. One of the reasons can be that the inclined backrest can help to locate the centre of mass of scoliosis model near to the midline of body to enable a better sitting balance. As shown in Figure 5.12, there is a distance (a) between the centre of mass of the scoliosis model and the midline of the body, due to the scoliotic curvature of spine. The distance is found to decrease with the inclined backrest (b). This means that although the inclined backrest may lead to the head displacement in the opposite direction of scoliotic convexity, it is able to help locate the centre of mass near to the midline of body. Further studies can be carried out to find the detailed effects of inclination angle on the sitting stability of people with scoliosis.
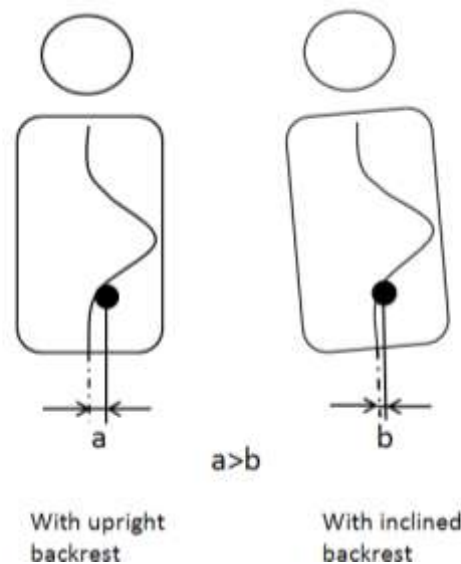
Figure 5.12 The distances between the centre of mass and the midline of body with upright backrest and inclined backrest

The compressive forces of lumbar joints L3-L4, L4-L5 and L5-S1 joints for P1, P2 and P3 are shown in Figure 5.13. It is found from the results the greatest compressive forces of lumbar joints of three patients happen in the case with no backrest. The compressive loads all decrease when the type of seat changes from no backrest to upright backrest. Differences are also observed between the results with upright backrest and inclined backrest. Inclined backrest can lead to slightly less compressive forces than upright backrest. From the results, it can be concluded that the application of backrest, especially the inclined backrest, can help improve the sitting stability of people with scoliosis and relieve the compressive loading conditions on lumbar joints in the meanwhile.
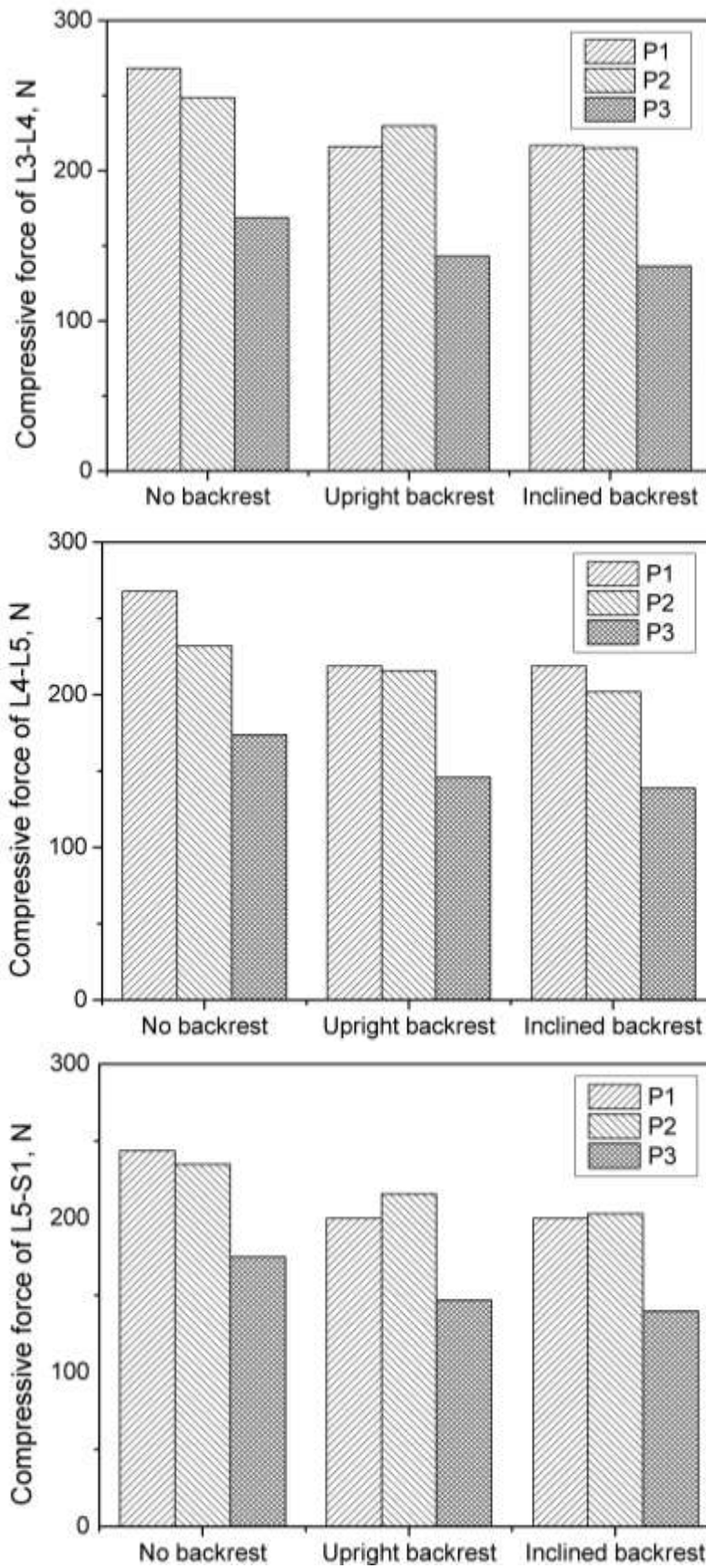
Figure 5.13 Compressive forces of lumbar joints L3-L4, L4-L5 and L5-S1 joints of P1, P2 and P3

5.7 Application of Hill-Based Muscles

In the last study, the activations of left and right lumbar muscle groups of P1 and P2 are found almost the same in sitting without backrest. However for P1 who leans to the left side with 47mm of head displacement, there is a significantly higher activation of right lumbar muscle group. Hence a study has been carried out to investigate the effects of lumbar muscle activation on the sitting stability.

In order to ensure the lumbar muscle activation value is constent during the simulation, the Hill-type muscle instead of the recording-type muscle was used in the modeling of the specific lumbar muscles. The Hill-based muscles are applied in the right lumbar muscle group (including multifidus muscle, erector spinae muscle, psoas major muscle and quadratus lumborum muscle, as shown in Figure 3.8), while the other muscles in the body are still of the passive recording type. The Hill-based muscle (Figure 5.14) is constituted by a contractile element (CE), a series elastic element (SEE) in series and a passive element (PE) in parallel. This type of muscle model is generated based on the material behavior of the muscle model from the literature (Hill, 1938). It is assumed that the CE is totally stress-free and freely distensible in the resting condition. The SEE and PE are elastic, and the muscle is comprised of the same sarcomeres in series and parallel when the muscle is activated. The SEE (the grey element in Figure 5.14) is usually neglected after adding a series of tendon. Therefore when neglecting the SEE, the total muscle force calculated based on the Hill formulation equals to the sum of the forces of PE and CE (Equation 3.2). The force of CE (Equation 3.3) is a function of time dependent activation (A(t)), instantaneous muscle lengthening velocity (v_r) and muscle length (I_r). The force of PE (Equation 3.4 to 3.6) depends on the instantaneous muscle length (I_r). It is very obvious the value of muscle activation serves as an input for the Hill-based muscle to generate the corresponding muscle force. In this study, the activation of right lumbar muscle group of P1 was set from 0 to 1 with increment of 0.25. The reuslts can be onbtaind by running the inverse and forward dynamic simulations.
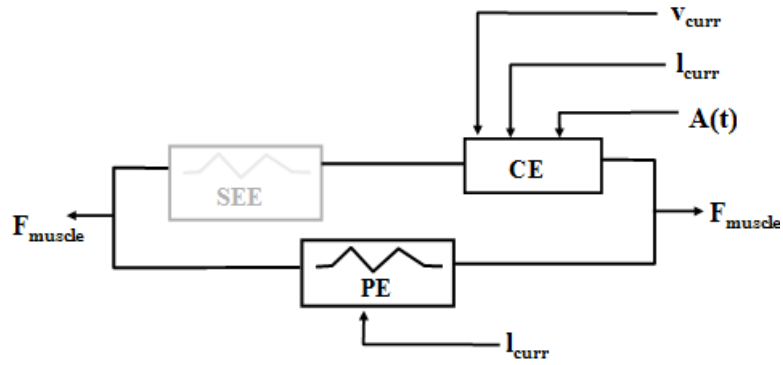
Figure 5.14 Components of the Hill-based muscle model (LifeModeler)

$$F_{MUSCLE} = F_{CE} + F_{PE} \tag{5.1}$$

where

F_{CE} = force of CE

F_{PE} = force of PE

$$F_{CE} = A(t) \cdot F_{max} \cdot f_H(v_r) \cdot f_L(I_r) \tag{5.2}$$

where

$A(t)$ = activation state (normalized between 0 -resting to 1 -maximum activation)

F_{max} = muscle force at maximum activation isometric conditions

f_H = the normalized active force-velocity relation (Hill-curve)

f_L = the normalized active force-length relation

v_r = dimensionless lengthening velocity

I_r = dimensionless muscle length

$$F_{PE} = \sigma \cdot pCSA \tag{5.3}$$

where

σ = passive muscle stress

pCSA = physiological cross sectional area

$$\sigma = (k \cdot \varepsilon)/(1 - //asym) \tag{5.4}$$

where

k = strain defined as the elongation relative to the resting length of the muscle

ε = passive muscle stiffness

asym = strain asymptote

$$\varepsilon = (I_{curr} - I_{free})/I_{free} \tag{5.5}$$

where

I_{curr} = current (instantaneous) length of the muscle

I_{free} = free length of the muscle at rest when it is removed from the body

91

5.8 Effects of Various Related Lumbar Muscle Activations

Due to the relatively significant asymmetry of lumbar muscle activation on the left and right sides of the body observed in the sitting of P1 with no backrest after analysis, a study of the effects of elevated lumbar muscle activation on the sitting stability and the spinal loading was carried out. The Hill-type muscle was applied for the first time in this thesis. It is found that this type of muscle is very useful for the analysis with the constant muscle activation. In this study, the muscle activation of the right lumbar muscle group (refer to Figure 3.8) increases from 0 to 1 in the increment of 0.2 for P1 for the analysis.

The results show that the head displacement of P1 decreases from 48.7mm to 10mm as the right lumbar muscle activation increases from 0 to 1 (Figure 5.15). This finding indicates that a higher activation of right lumbar muscle group can enable better sitting stability of patient with scoliosis, because greater tension forces to maintain the sitting stability is generated by the lumbar muscle group. On the other hand, the compressive forces of lumbar joints (Figure 5.16) all increase due to the elevated right lumbar muscle activation. This is because greater muscle tension can lead to higher compressive loads of spinal joints (Levangie and Norkin, 2001). Hence geneally it is suggested that patient with scoliosis can improve sitting stability by a better functioning of lumbar muscles which can be achieved by regular exercise.
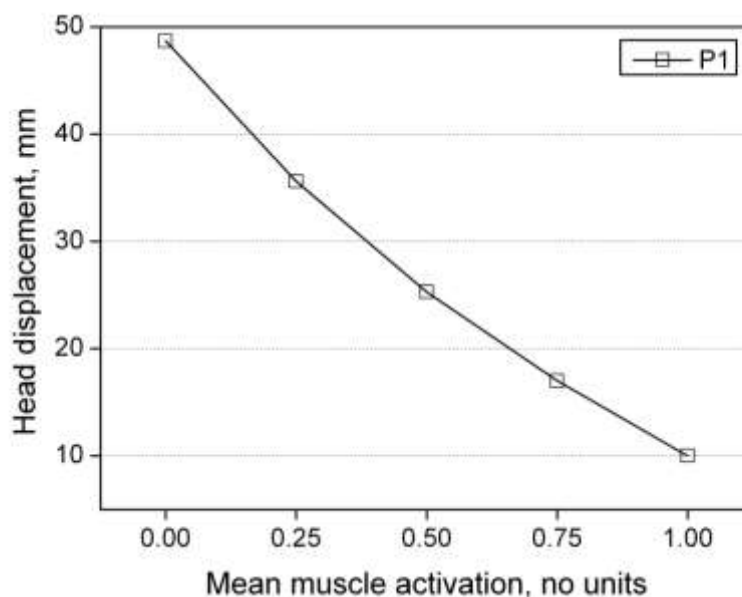
Figure 5.15 The head displacements of P1 with elevated lumbar muscle activation
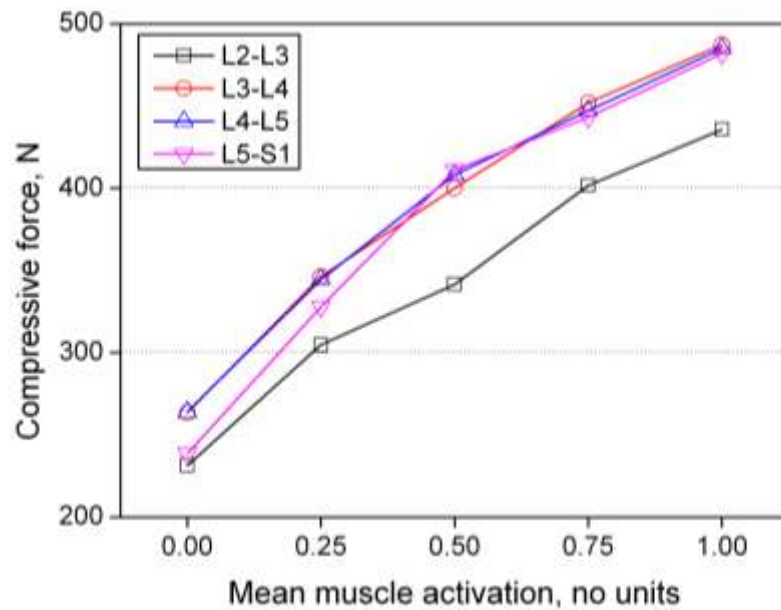
Figure 5.16 The compressive forces of lumbar joints of P1 with elevated lumbar muscle activation

5.9 Sitting Posture of Patient with Scoliosis

In this section, an additional study of sitting posture of patient with scoliosis is presented. The method in this study is a combination of motion capture and musculoskeletal modeling applied previously in Chapter 3 as shown in Figure 3.1. Different from the study in Chapter 3 based on healthy subjects, the study in this section focuses on the patient subject with scoliosis. A female patient (159mm height, 40kg weight and 16 years old) with scoliosis was included in this preliminary study. From the X-ray image in Figure 5.17, her spine shows double scoliotic curves: one is from T7 to T10 with Cobb angle of 22° and convexity to the right side, and the other is from T11 to L3 with Cobb angle of 26° and convexity to the left side.

The study began with the measurements of the anthropometric data of the patient. Next, the retro-reflective markers were attached on the skin of the subject. The motion data of the subject performing different postures were recorded using the motion capture system (Vicon MX). The postures include upright standing, upright sitting, slumped sitting, flexion sitting and extension sitting (refer to Figure 3.25). The detailed procedures of the experiment are explained in Chapter 3.
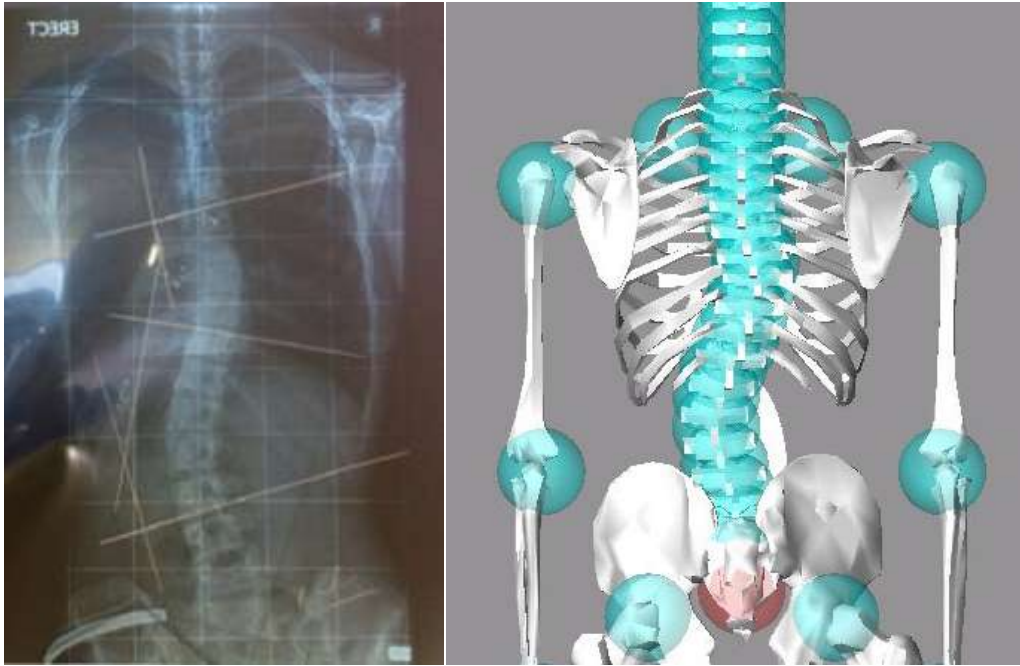
Figure 5.17 The back view of X-ray image and the 3D body model of the subject
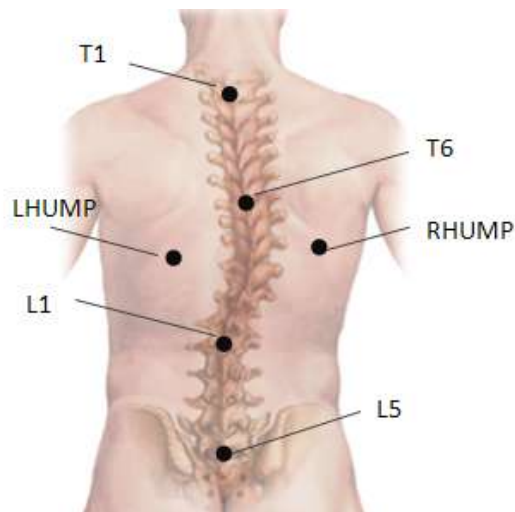
Figure 5.18 The enhanced customized marker set for the subject with scoliosis

Table 5.2 Description of the enhanced customized marker set

Marker Label	Description
T1	First Thoracic Vertebra
T6	Sixth Thoracic Vertebra
L1	First Lumbar Vertebra
L5	Fifth Lumbar Vertebra
LHUMP/RHUMP	Left/Right Hump

Unlike the study in Chapter 3, the motion marker protocol applied in this study was improved to be more appropriate for the patient with scoliosis. Since the patient exhibits an asymmetrical spinal structure, the plug-in gait marker protocol (Figure 3.15) was not detailed enough for the body with scoliosis. A customized augmented marker set was added in the basic plug-in gait marker protocol. Hence in this study, not only the plug-in gait marker protocol, but also an enhanced customized marker set (Figure 5.18 and Table 5.2) with 6 marker locations on the subject's back was applied to capture the more detailed movements of the asymmetrical spine of the subject with scoliosis. The enhanced customized marker set had been initially proposed and applied in the study of the behavior of patients with scoliosis by the author's research group (Hajizadeh, 2013). The number of markers in the customized marker set on the subject's back is determined based on the scoliosis of experiment subject. In the study, the customized markers have been added on vertebra T1, T6, L1, L5, left and right hump of the subject, as shown in Figure 5.18.

The musculoskeletal multi-body model with the discretized scoliotic spine was developed according to the anthropometric data of the patient in LifeMOD. The scoliotic curvature on the back was created based on the information from the X-ray image of the patient, as shown in Figure 5.17. Contacts were defined between the body and the seating system (refer to Table 3.4). The motion data obtained from the motion capture experiment was applied to drive the motion agents on the musculoskeletal model during the inverse dynamic simulation. During the forward dynamic simulation, the motion agents were disabled, and the model was trained by the recorded joint angles and muscle movements.

The spine angles in the sagittal plane of the patient with scoliosis were obtained by the measurement using the motion capture system. Because five actions were conducted for each series of motion, the mean angles were derived from the average values of these five sets of data collected in the motion capture experiments. The angle definitions have been described previously in Chapter 3 as illustrated in Figure 3.26. The values of spine angle are shown in Figure 5.19, with the positive value indicating the anterior tilt of the spine. Compared to upright sitting, upright standing and flexion sitting show more spinal extension, while slumped sitting and extension sitting show more spinal flexion.
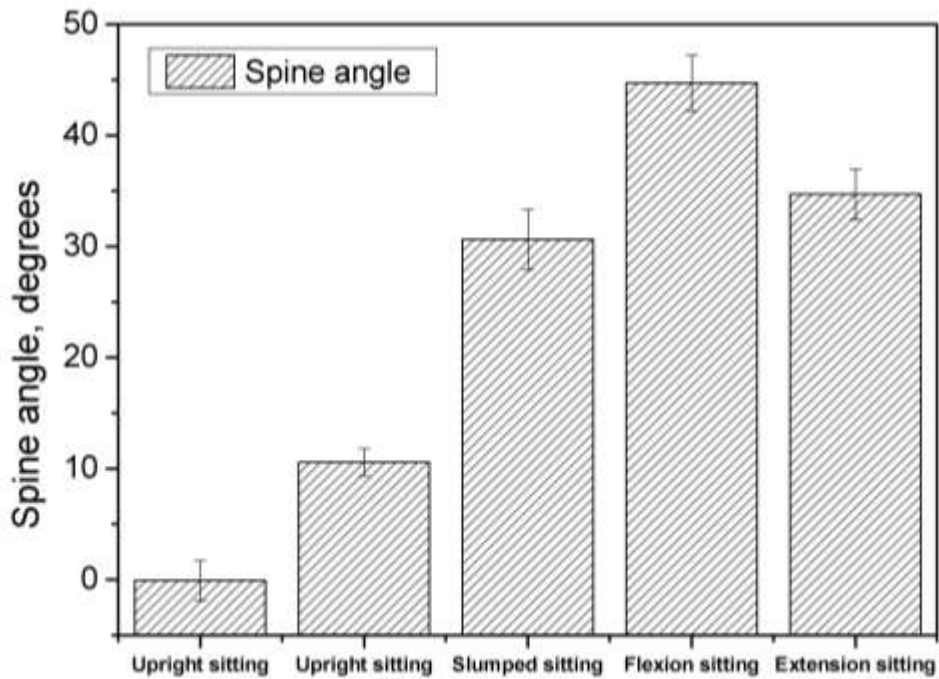
Figure 5.19 The mean angles for pelvis, thorax and spine in the sagittal plane of the patient with scoliosis
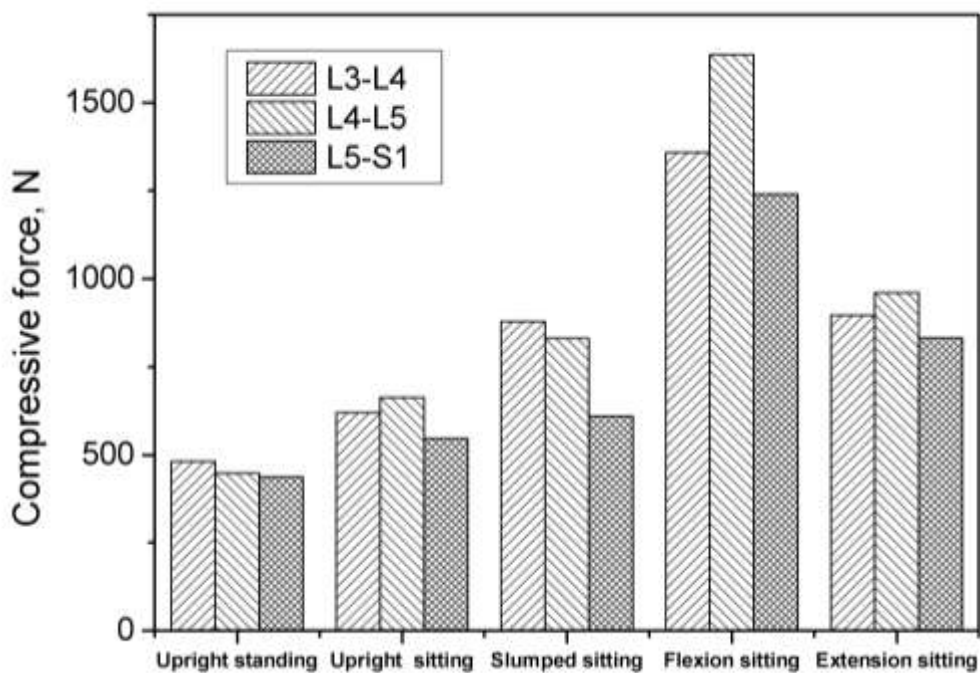
Figure 5.20 The mean compressive forces of L3-L4, L4-L5 and L5-S1 joints over the weight of the patient with scoliosis

The mean compressive forces of L3-L4, L4-L5 and L5-S1 joints in various postures are shown in Figure 5.20. All the values of compressive loads increase in the following order of body postures: upright standing, upright sitting, slumped sitting, extension sitting and flexion sitting. Results show that the compressive loads of

lumbar joints increase as the spine angle increases. This is due to the reduction of lumbar lordosis which can lead to higher compressive loads on the spine (Hedman and Fernie, 1997, Harrison et al., 1999). Since this study only involves one patient subject at the moment, the specific correlation between spine angle and compressive joint load of patient with scoliosis is not yet fully understood. More patient subjects can be included in future to understand the relationship in detail.

Compared to the mean results of healthy subjects in Chapter 4, there are some differences in the exact values of segment angels and joint compressive loads in patient with scoliosis. However no conclusion can be made based on this information at the moment, because of the limitation in the number of subject. Six healthy subjects were included in the study of Chapter 4. In this section, only one patient with scoliosis was included due to the limitation of time and consent from patient. Although there is no statistical significance of this preliminary study, it helps pave the way for future study of sitting postures of patients with scoliosis through motion capture and musculoskeletal modeling.

5.10 Summary

In this chapter, the sitting stability of people with scoliosis is the main focus and has been investigated. The results show that the Cobb angle of scoliosis has some effects on sitting stability and spinal biomechanics. The scoliotic model with the greatest Cobb angle shows the worst sitting stability and the least compressive loads on lumbar joints. Backrest, especially the inclined backrest can help relocate the center of mass of people with scoliosis near to the midline of upper body, as well as greater activation of lumbar muscle group. In summary, sitting stability of patient with scoliosis can be improved by the reduction of Cobb angle of scoliosis, application of backrest and better function of the lumbar muscle group. In literature, there are few quantitative studies about the sitting stability of patient with scoliosis. The results of the current research contribute to a deeper understanding about the unbalanced sitting of people with scoliosis. The approach through musculoskeletal modeling can be applied for further studies about sitting stability in the future. Strategies to improve the sitting stability have been proposed, such as reduction of the Cobb angle, usage of backrest and better function of lumbar muscles. The results

provide doctors and therapists with more suggestions to patients with scoliosis who suffer from unbalanced sitting.

An additional study of sitting posture of patient with scoliosis is presented at the end of this chapter. The experiments of motion capture and the simulations of dynamic motion are all based on one patient with double scoliotic curves. Different from the study of healthy subjects in Chapter 3, the marker protocol applied for the patient in this chapter includes both the basic plug-in marker set and a customized marker set on the patient's back. With this more detailed marker protocol, accurate movements of the back with scoliotic spine can be recorded and applied in the musculoskeletal analysis. Since the situation of scoliosis varies with different patients, the enhanced marker set on back can also be customized based on individual situation of patient with scoliosis in the future study. Until now, this study has only involved one subject. More patient subjects can be included in the future to conduct a deeper investigation.

During the research process, a study of the correction of scoliotic curvature by external forces was also conducted by the author. However the result is not optimistic, due to software limitations. LifeMOD software is only able to present the real time response in short time frames, but cannot simulate the degradation effect of the model. Hence in order to perform the simulation on the correction of scoliotic curvature by external forces, other simulation tools may be needed, such as finite element analysis.

CHAPTER 6

CONCLUSION

6.1 Contributions

LBP is a common healthcare problem in nowadays and has a strong relationship with the degeneration of intervertebral disc (Luoma et al., 2000). It has been suggested that poor sitting postures in daily life can introduce LBP to people with the lower back being forced away from the natural lordotic curvature (Kirkaldy et al., 1999, Kottke, 1961, McKenzie and May, 1981, Vergara and Page, 2002). The reduction of lumbar lordosis of human spine can lead to higher loads on the intervertebral disc (Hedman and Fernie, 1997, Harrison et al., 1999).

Mechanical loading distribution of spine, as a potential risk factor for LBP and disc degeneration, is a very important factor in the areas of ergonomics and physiotherapy (Bakker et al., 2009, Hoogendoorn et al., 1999, Marras et al., 1995). In the past decades, two measurement methodologies have been applied to investigate the spinal biomechanics: direct measurement with insertion of pressure transducer (Andersson and Ortengren, 1974a, Nachemson, 1965, Nachemson and Elfstrom, 1970, Nachemson and Morris, 1964, Okushima, 1970, Sato et al., 1999, Schultz et al., 1982, Wilke et al., 1999) and indirect measurement inferred by other measurements (Althoff et al., 1992, Leivseth and Drerup, 1997, Rohlmann et al., 2001). There is no doubt that all these researches contribute significantly to the understanding of spinal biomechanics. However, each experimental approach has its own limitations: direct measurement depends highly on the specification and calibration of the transducer, and is also an invasive experimental procedure; on the other hand, the outcome of indirect measurement has a small size effect.

Due to the limitations of the above mentioned research approaches, the mechanical loading distribution of human spine has not been fully understood yet.

99

Hence in Chapter 3 of this thesis, a novel research procedure to study spinal loads in various postures has been developed. The method is based on musculoskeletal modeling and motion capture. The motion data obtained from motion capture experiment was imported into LifeMOD to drive the developed musculoskeletal model for the inverse and forward dynamic simulation. The musculoskeletal model of the experimental subject, established based on individual anthropometric data, includes a basic human body model and an enhanced bio-fidelity discretized spine model. This is the first study in literature that a musculoskeletal discretized whole spine model was applied to study the sitting biomechanics. Because the current research aims to understand LBP, the mechanical loads of lumbar joints are presented as the final results for discussion in this thesis. However, since the spine model was refined into individual vertebrae and rotational joints were created to connect two adjacent vertebrae in the whole spine region, the mechanical loading distribution of every spinal joint in the spine could be obtained after the computational analysis. This proposed approach with the discretized whole spine model avoids the limitation of results in direct measurement by inserting transducer, in which only the pressure of one intervertebral disc can be obtained after the *in vivo* experiment.

Moreover, this research has covered a wide variety of postures, including upright standing, upright sitting, slumped sitting, cross-legged sitting, flexion sitting and extension sitting. All these postures are commonly adopted in daily life. In literature, there are some disagreements about the comparison of spinal loads in standing and sitting, as discussed previously in Chapter 2. From the results of current research, greater compressive loads on lumbar joints are found in sitting than those in standing. It is because when the body changes from standing to sitting, the reduction of lumbar lordosis can increase the spinal loads (Harrison et al., 1999). This finding contributes to the understanding of spinal loads in standing and sitting postures through the approach of musculoskeletal modeling. It is also found that the other sitting postures, such as slumped sitting, cross-legged sitting, flexion sitting and extension sitting, can introduce higher compressive loads on lumbar joints and pose a threat to LBP compared with upright sitting. An approximately linear correlation is observed between spine angle and spinal load. All these results contribute to a deeper understanding of the differences of spinal loads among postures. It also provides more information for the therapists to suggest better sitting postures to people in daily life.

In the thesis, this proposed procedure has been validated by the study of six subjects. It can be applied to more subjects for a population study and other body postures or movements in the future.

In literature, there has been seldom quantitative analysis of the relationship between spinal loads and seat design due to the limitations in experimental procedures. The systematic studies in Chapter 4 about the influences of seat design parameters on compressive forces on spinal joints help fill this gap. Before studying seat design parameters, the necessity of implementing IAP in musculoskeletal model for the simulation with static posture is explored first. From the results, it is concluded that IAP is necessary as a stabilizing and compression-reducing mechanism in the musculoskeletal multi-body model for the study of static posture without the input of dynamic motion trajectories. Therefore, a sitting musculoskeletal multi-body model with normal IAP was developed in this chapter to evaluate the effects of seat design parameters. The seat design parameters studied include backrest inclination, seat pan inclination, seat pan depth, seat pan height and backrest height. The results of these studies provide guidelines for various parameters in seat design for both engineers and designers. For example, it is observed from the research that greater inclination of backrest can lead to less compressive forces with high friction coefficient, but more compressive forces with low friction coefficient. Through this approach, the influence of any seat design on the spinal loads of human body can be investigated. This sitting musculoskeletal multi-body model can be used as an evaluation solution for specific seat design in future.

Compared to the healthy people, the sitting condition of people with scoliosis is worse, because they may suffer from unbalanced sitting (Smith and Emans, 1992, Larsson et al., 2002). As a result, the study of sitting stability is very important for people with scoliosis (Smith and Emans, 1992). The studies in Chapter 5 contribute to a better understanding of sitting stability of people with scoliosis. From the experimental results, better sitting stability is achieved with smaller Cobb angle, upright and inclined backrest, and greater activation of lumbar muscles. Strategies have been proposed to improve the sitting stability of people with scoliosis, such as the reduction of Cobb angle by treatment or wearing brace, the application of backrest in seat system and frequent exercises to strengthen the related lumbar muscles. All these results can provide the doctors and therapists with more information in

suggestions on better sitting stability to people with scoliosis. The proposed procedure in this chapter can also be applied in the evaluation of sitting stability of specific patient with individual medical condition of scoliosis in the future.

6.2 Limitations and Future Works

One of the limitations of the current research is the lack of experimental validation. The main output results of the research are the compressive loads of spinal joints. The direct validation approach can be measuring the intradiscal pressure of the subject using transducer. This experimental approach would be most desirable for validation but very difficult to carry out due to its invasive effect to human body. Thus, the spine modeling is currently the only approach of the detailed investigation of the mechanical loading conditions of the whole spine. There are some studies about the load measurements of intervertebral disc in literature, and the results contribute to the database for the validation of computational models. Hence the only available method for validation at the moment is comparing the obtained results in this research to the results of existing experiments in literature. For example, the musculoskeletal spine model applied in this thesis has been validated by a limited number of experiments, including simplified conditions (McGill and Norman, 1987b, Wilke et al., 2001). Although the results of the preliminary validation are promising in consistent with those in the literature, it is necessary and desirable to have more extensive validations of the musculoskeletal model. However, due to the differences between the anthropometric data of the experimental subjects in the literature and those of the musculoskeletal models in this thesis, the direct validation approach based on the experiment results in literature is also limited. Lack of validation is in fact a common problem of the musculoskeletal multi-body models in the research area. Efforts from global researchers are required to solve this problem and enable a full validation of the musculoskeletal model.

Another limitation of the research is the neglect of the facet joints when considering spinal load distribution. In the human spine, not only the intervertebral disc, but also the facet joints connect the two adjacent vertebrae and undertake the spinal loads. However, the intervertebral joint considered in this research consists of both the intervertebral disc and the facet joints. In this way, the individual mechanical

loading condition of the facet joints is not covered in the current research. It is found in literature, the facet joints resist about 16% of the intervertebral compressive forces in the upright standing, and 0% in the upright sitting (Adams and Hutton, 1980). This percentage can change due to other reasons, such as spine extension, lordosis and degeneration of intervertebral disc (Levangie and Norkin, 2001). The mechanical load condition on the facet joints is also a very important factor in the understanding of spinal biomechanics.

In LifeMOD, the musculoskeletal models of two human subjects with similar anthropometric data are also similar, due to the application of GeBOD database during the modeling process. However, it is noted that every human body is unique. The geometries of body segments (such as vertebrae) can be different for two subjects with the same anthropometric data. In order to solve this problem, custom vertebrae geometry can be applied and imported into LifeMOD to develop the musculoskeletal model. The custom 3D spine model can be built by CT or MRI scans of human body using MIMICS, a software tool specialized in the segmentation of 3D medical images and the establishment of highly accurate models of body anatomy. Through this approach, a more accurate spine model can be obtained with detailed geometries of vertebrae (including facet joints) and sites of attachment of soft tissues. Furthermore, this model can provide a more accurate spine curvature for patients with spinal deformity, as shown in Figure 6.1 of a scoliosis spine model created based on the patient's CT scans by one research group (Watanabe et al., 2012).
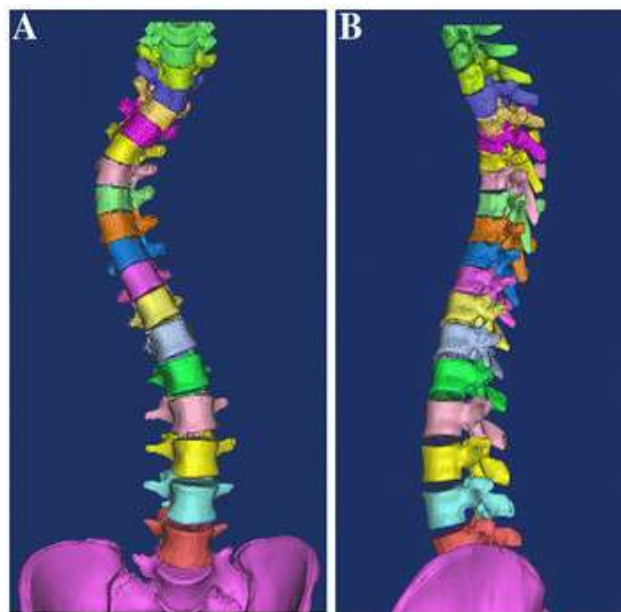
Figure 6.1 Custom 3D spine model created by MIMICS (Watanabe et al., 2012)

In the discretized spine model used in this thesis, the ribcage is modeled as one segment. In order to further refine the musculoskeletal model in LifeMOD, it is suggested to discretize the ribcage into individual rib pairs to connect with sternum and related vertebrae. A preliminary attempt has been carried out by exporting the ribcage from LifeMOD and discretizing it into 12 independent rib pairs using 3-Matic software (Hajizadeh, 2014), as shown in Figure 6.2. One possible future work might focus on importing this detailed ribcage into the musculoskeletal model in LifeMOD with corresponding vertebrae and sternum using appropriate rotational joints. This more detailed musculoskeletal model with the discretzied ribcage can be applied for the kinematic dynamic study of human body.
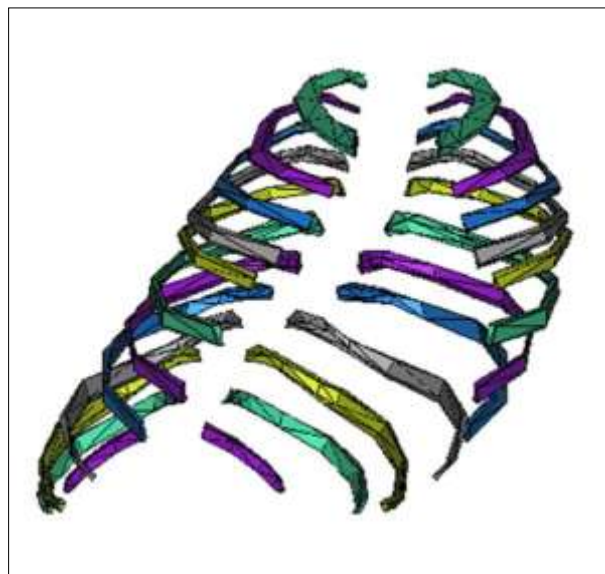
Figure 6.2 Discretized ribcage by 3-Matic (Hajizadeh, 2014)

Finally, one focus of the research is on the development of a novel procedure to study the spinal biomechanics through motion capture and musculoskeletal modeling. The results are promising showing that the proposed procedure can be applied to more future cases. In the current study, six healthy subjects (in Chapter 3) and one subject with scoliosis (in the preliminary study in Chapter 5) have been included. One possible future work is to conduct a population study about spinal biomechanics in various postures and movements involving more subjects (both healthy people and patients with scoliosis).

BIBLIOGRAPHY

ADAMS, M. & HUTTON, W. 1980. The effect of posture on the role of the apophysial joints in resisting intervertebral compressive forces. *J Bone Joint Surg Br,* 62**,** 358-362.

ADAMS, M., MCMILLAN, D., GREEN, T. & DOLAN, P. 1996. Sustained loading generates stress concentrations in lumbar intervertebral discs. *Spine,* 21**,** 434-438.

ÅKERBLOM, B. 1948. Standing and sitting posture.

ALTHOFF, I., BRINCKMANN, P., FROBIN, W., SANDOVER, J. & BURTON, K. 1992. An improved method of stature measurement for quantitative determination of spinal loading: application to sitting postures and whole body vibration. *Spine,* 17**,** 682-93.

ANDERSSON, B. & ORTENGREN, R. 1974a. Lumbar disc pressure and myoelectric back muscle activity during sitting. II. Studies on an office chair. *Scandinavian Journal of Rehabilitation Medicine,* 6**,** 115.

ANDERSSON, B. & ORTENGREN, R. 1974b. Myoelectric back muscle activity during sitting. *Scandinavian journal of rehabilitation medicine. Supplement,* 3**,** 73.

ANDERSSON, B., ORTENGREN, R., NACHEMSON, A. & ELFSTROM, G. 1974a. Lumbar disc pressure and myoelectric back muscle activity during sitting. I. Studies on an experimental chair. *Scand J Rehabil Med,* 6**,** 104-14.

ANDERSSON, B., ORTENGREN, R., NACHEMSON, A. & ELFSTROM, G. 1974b. Lumbar disc pressure and myoelectric back muscle activity during sitting. IV. Studies on a car driver's seat. *Scandinavian Journal of Rehabilitation Medicine,* 6**,** 128.

ANDERSSON, E., ODDSSON, L., GRUNDSTR M, H. & THORSTENSSON, A. 1995. The role of the psoas and iliacus muscles for stability and movement of the lumbar spine, pelvis and hip. *Scandinavian journal of medicine & science in sports,* 5**,** 10-16.

ANDERSSON, G. B. 1981. Epidemiologic aspects on low-back pain in industry. *Spine,* 6**,** 53-60.

BAKKER, E. W., VERHAGEN, A. P., VAN TRIJFFEL, E., LUCAS, C. & KOES, B. W. 2009. Spinal mechanical load as a risk factor for low back pain: a systematic review of prospective cohort studies. *Spine,* 34**,** E281-E293.

BALAN, A. O., SIGAL, L. & BLACK, M. J. Year. A quantitative evaluation of video-based 3D person tracking. *In:* Visual Surveillance and Performance Evaluation of Tracking and Surveillance, 2005. 2nd Joint IEEE International Workshop on, 2005. IEEE, 349-356.

BARTELINK, D. 1957. The role of abdominal pressure in relieving the pressure on the lumbar intervertebral discs. *Journal of Bone & Joint Surgery, British Volume,* 39**,** 718-725.

BELL, J. & STIGANT, M. 2007. Development of a fibre optic goniometer system to measure lumbar and hip movement to detect activities and their lumbar postures. *Journal of Medical Engineering & Technology,* 31**,** 361-366.

BELYTSCHKO, T., KULAK, R., SCHULTZ, A. & GALANTE, J. 1974. Finite element stress analysis of an intervertebral disc. *Journal of biomechanics,* 7**,** 277-285.

BENDIX, T. & BIERING-S RENSEN, F. 1982. Posture of the trunk when sitting on forward inclining seats. *Scandinavian Journal of Rehabilitation Medicine,* 15**,** 197-203.

BENNETT, H. E. 1928. *School posture and seating*.

BOGDUK, N., MACINTOSH, J. E. & PEARCY, M. J. 1992a. A universal model of the lumbar back muscles in the upright position. *Spine,* 17**,** 897-913.

BOGDUK, N., PEARCY, M. & HADFIELD, G. 1992b. Anatomy and biomechanics of psoas major. *Clinical Biomechanics,* 7**,** 109-119.

BOZIC, K. J., KEYAK, J. H., SKINNER, H. B., BUEFF, U. H. & BRADFORD, D. S. 1994. Three-dimensional finite element modeling of a cervical vertebra: an investigation of burst fracture mechanism. *Journal of Spinal Disorders & Techniques,* 7**,** 102-110.

BRIDWELL, K. 2010. *Intervertebral discs* [Online]. Available: http://www.spineuniverse.com/anatomy/intervertebral-discs [Accessed].

BRIDWELL, K. 2013. *Vertebral column* [Online]. Available: http://www.spineuniverse.com/anatomy/vertebral-column [Accessed].

BRIENZA, D., CHUNG, K., BRUBAKER, C., WANG, J., KANG, T. & LIN, C. 1996. A system for the analysis of seat support surfaces using surface shape control and simultaneous measurement of applied pressures. *Rehabilitation Engineering, IEEE Transactions on,* 4**,** 103-113.

BRUNSWIC, M. Year. Seat design in unsupported sitting. *In*, 1984. 294-298.

CHAFFIN, D. B. 1969. A computerized biomechanical model—development of and use in studying gross body actions. *Journal of biomechanics,* 2**,** 429-441.

CHAN, P. Y., WONG, H. K. & GOH, J. C. H. 2006. The repeatablity of spinal motion of normal and scoliotic adolescents during walking. *Gait & posture,* 24**,** 219-228.

CHOLEWICKI, J., JULURU, K. & MCGILL, S. M. 1999. Intra-abdominal pressure mechanism for stabilizing the lumbar spine. *Journal of biomechanics,* 32**,** 13-17.

CHRISTOPHY, M., SENAN, N. A. F., LOTZ, J. C. & O'REILLY, O. M. 2011. A musculoskeletal model for the lumbar spine. *Biomech Model Mechanobiol*.

CLAUS, A., HIDES, J., MOSELEY, G. L. & HODGES, P. 2008. Sitting versus standing: Does the intradiscal pressure cause disc degeneration or low back pain? *Journal of Electromyography and Kinesiology,* 18**,** 550-558.

COBB, W. S., BURNS, J. M., KERCHER, K. W., MATTHEWS, B. D., JAMES NORTON, H. & TODD HENIFORD, B. 2005. Normal intraabdominal pressure in healthy adults. *Journal of Surgical Research,* 129**,** 231-235.

DE JONGH, C. U., BASSON, A. H. & SCHEFFER, C. Year. Dynamic simulation of cervical spine following single-level cervical disc replacement. *In:* Engineering in Medicine and Biology Society, 2007. EMBS 2007. 29th Annual International Conference of the IEEE, 2007. IEEE, 4289-4292.

DEURETZBACHER, G. & REHDER, U. 1995. A CAE (computer aided engineering) approach to dynamic whole body modeling--the forces iin the lumbar spine in asymmetrical lifting]. *Biomedizinische Technik. Biomedical engineering,* 40**,** 93.

DEZEE, M., HANSEN, L., WONG, C., RASMUSSEN, J. & SIMONSEN, E. B. 2007. A generic detailed rigid-body lumbar spine model. *Journal of biomechanics,* 40**,** 1219-1227.

DŁUGOSZ, M. M., PANEK, D., MACIEJASZ, P., CHWAŁA, W. & ALDA, W. 2012. An improved kinematic model of the spine for three-dimensional motion analysis in the Vicon system. *Studies in health technology and informatics,* 176**,** 227.

DOLAN, P., ADAMS, M. & HUTTON, W. 1988. Commonly adopted postures and their effect on the lumbar spine. *Spine,* 13**,** 197-201.

EIDELSON, S. G. 2012. *Spinal ligaments and tendons* [Online]. Available: http://www.spineuniverse.com/anatomy/spinal-ligaments-tendons [Accessed].

EYCLESHYMER, A. C., SCHOEMAKER, D. M., POTTER, P., SMITH, C. & JONES, T. 1911. *A cross-section anatomy*, D. Appleton.

FLOYD, W. & ROBERTS, D. 1958. Anatomical and physiological principles in chair and table design. *Ergonomics,* 2**,** 1-16.

FRYMOYER, J. W., POPE, M. H., COSTANZA, M. C., ROSEN, J. C., GOGGIN, J. E. & WILDER, D. G. 1980. Epidemiologic studies of low-back pain. *Spine,* 5**,** 419-423.

FUJITA, Y., DUNCAN, N. A. & LOTZ, J. C. 2005. Radial tensile properties of the lumbar annulus fibrosus are site and degeneration dependent. *Journal of orthopaedic research,* 15**,** 814-819.

GARFIN, S. R. 2012. *Spinal structure and body mechanics* [Online]. Available: http://www.spineuniverse.com/anatomy/spinal-structure-body-mechanics [Accessed].

GIBSON, I. & LIU, G. 2013. Developing a 3D multi-body model of the scoliotic spine with lateral bending motion for comparison of ribcage flexibility. *International Journal of Advanced Design and Manufacturing Technology,* 6**,** 25-32.

GOEL, V. K., PARK, H. & KONG, W. 1994. Investigation of vibration characteristics of the ligamentous lumbar spine using the finite element approach. *Journal of biomechanical engineering,* 116**,** 377.

GOH, J., THAMBYAH, A. & BOSE, K. 1998. Effects of varying backpack loads on peak forces in the lumbosacral spine during walking. *Clinical Biomechanics,* 13**,** S26-S31.

GRAUER, J. N., PANJABI, M. M., CHOLEWICKI, J., NIBU, K. & DVORAK, J. 1997. Whiplash produces an S-shaped curvature of the neck with hyperextension at lower levels. *Spine,* 22**,** 2489.

GREAVES, C. Y., GADALA, M. S. & OXLAND, T. R. 2008. A three-dimensional finite element model of the cervical spine with spinal cord: an investigation of three injury mechanisms. *Annals of biomedical engineering,* 36**,** 396-405.

GREINER, K. A. 2002. Adolescent idiopathic scoliosis: radiologic decision-making. *American family physician,* 65**,** 1817.

GRUJICIC, M., PANDURANGAN, B., XIE, X., GRAMOPADHYE, A., WAGNER, D. & OZEN, M. 2010. Musculoskeletal computational analysis of the influence of car-seat design/adjustments on long-distance driving fatigue. *International Journal of Industrial Ergonomics,* 40**,** 345-355.

HAJIZADEH, K. 2013. *Developing a 3D multi-body simulation tool to study dynamic behaviour of human scoliosis* PhD, National University of Singapore.

HAJIZADEH, K. 2014. *Developing a 3D multi-body simulation tool to study dynamic behaviour of human scoliosis.* PhD, National University of Singapore.

HAJIZADEH, K., GIBSON, I., LIU, G. & HUANG, M. Year. Development of a virtual musculo-skeletal, multi-body scoliotic spine model. *In:* Proceedings of the International Conference on Rehabilitation Engineering and Assistive Technology, i-CREATe, 2012a.

HAJIZADEH, K., GIBSON, I., LIU, G. & HUANG, M. Year. Development of a virtual musculo-skeletal, multi-body scoliotic spine model. *In:* 6th International Convention on Rehabilitation Engineering and Assistive Technology, ICREATE, 2012b.

HARMS, M. 1990. Effect of wheelchair design on posture and comfort of users. *Physiotherapy,* 76**,** 266-271.

HARRISON, D. D., HARRISON, S. O., CROFT, A. C., HARRISON, D. E. & TROYANOVICH, S. J. 1999. Sitting biomechanics part I: review of the literature. *Journal of manipulative and physiological therapeutics,* 22**,** 594-609.

HATZE, H. 1981. Estimation of myodynamic parameter values from observations on isometrically contracting muscle groups. *European Journal of Applied Physiology and Occupational Physiology,* 46**,** 325-338.

HEDMAN, T. P. & FERNIE, G. R. 1997. Mechanical response of the lumbar spine to seated postural loads. *Spine,* 22**,** 734-743.

HILL, A. 1938. The heat of shortening and the dynamic constants of muscle. *Proceedings of the Royal Society of London. Series B, Biological Sciences,* 126**,** 136-195.

HODGES, P. W., CRESSWELL, A. G., DAGGFELDT, K. & THORSTENSSON, A. 2001. In vivo measurement of the effect of intra-abdominal pressure on the human spine. *Journal of biomechanics,* 34**,** 347-353.

HOOGENDOORN, W. E., VAN POPPEL, M. N., BONGERS, P. M., KOES, B. W. & BOUTER, L. M. 1999. Physical load during work and leisure time as risk factors for back pain. *Scandinavian journal of work, environment & health***,** 387-403.

HOOTON, E. A., COMPANY, H.-W. & ANTHROPOLOGY, H. U. D. O. 1970. *A survey in seating*, Greenwood Press.

HUANG, M., GIBSON, I., LEE, T. & HAJIZADEH, K. Year. Effect of sitting posture on spine joint angles and forces. *In:* 6th International Convention on Rehabilitation Engineering and Assistive Technology, ICREATE, 2012.

HUYNH, K., GIBSON, I., JAGDISH, B. & LU, W. 2013. Development and validation of a discretised multi-body spine model in LifeMOD for biodynamic behaviour simulation. *Computer methods in biomechanics and biomedical engineering***,** 1-10.

HUYNH, K. T. 2010. *Development and biodynamic simulation of a detailed musculo-skeletal spine model.* Ph.D, National University of Singapore.

KEEGAN, J. J. 1953. Alterations of the lumbar curve related to posture and seating. *The Journal of Bone and Joint Surgery,* 35**,** 589.

KELSEY, J. L. 1975. An epidemiological study of the relationship between occupations and acute herniated lumbar intervertebral discs. *International Journal of Epidemiology,* 4**,** 197-205.

KELSEY, J. L. & WHITE III, A. A. 1980. Epidemiology and impact of low-back pain. *Spine,* 5**,** 133-142.

KHOO, B., GOH, J. & BOSE, K. 1995. A biomechanical model to determine lumbosacral loads during single stance phase in normal gait. *Medical engineering & physics,* 17**,** 27-35.

KHOO, B., GOH, J., LEE, J. & BOSE, K. 1994. A comparison of lumbosacral loads during static and dynamic activities. *Australasian physical & engineering sciences in medicine/supported by the Australasian College of Physical Scientists in Medicine and the Australasian Association of Physical Sciences in Medicine,* 17**,** 55.

KIM, S. M., YANG, I. C. & LEE, M. P. Year. Cervical spine injury analysis regarding frontal and side impacts of wheelchair occupant in vehicle by LifeMOD. *In:* World Congress on Medical Physics and Biomedical Engineering 2006, 2007. Springer, 2521-2524.

KIRKALDY, W. H., BERNARD, T. & KIRKALDY-WILLIS, W. 1999. *Managing low back pain*, Churchill.

KNUTSSON, B., LINDH, K. & TELHAG, H. 1966. Sitting--an electromyographic and mechanical study. *Acta Orthopaedica Scandinavica,* 37**,** 415.

KOTTKE, F. 1961. Evaluation and treatment of low back pain due to mechanical causes. *Archives of physical medicine and rehabilitation,* 42**,** 426.

KROEMER, K. H. E. 1971. Seating in plant and office. *American Industrial Hygiene Association Journal,* 32**,** 633-652.

KUMARESAN, S., YOGANANDAN, N. & PINTAR, F. A. 1999. Finite element analysis of the cervical spine: a material property sensitivity study. *Clinical Biomechanics,* 14**,** 41-53.

KURTZ, S. M. & EDIDIN, A. 2006. *Spine technology handbook*, Access Online via Elsevier.

KWANG, T. S., GIBSON, I. & JAGDISH, B. N. Year. Detailed spine modeling with LifeMOD™. *In:* Proceedings of the 3rd International Convention on Rehabilitation Engineering & Assistive Technology, 2009. ACM, 25.

LARSSON, E.-L., AARO, S., NORMELLI, H. & ÖBERG, B. 2002. Weight distribution in the sitting position in patients with paralytic scoliosis: pre-and postoperative evaluation. *European Spine Journal,* 11**,** 94-99.

LAY, W. & FISHER, L. 1940. Riding comfort and cushions. *SAE Journal,* 47**,** 482-496.

LEIVSETH, G. & DRERUP, B. 1997. Spinal shrinkage during work in a sitting posture compared to work in a standing posture. *Clinical Biomechanics,* 12**,** 409-418.

LENGSFELD, M., FRANK, A., VAN DEURSEN, D. & GRISS, P. 2000. Lumbar spine curvature during office chair sitting. *Medical engineering & physics,* 22**,** 665-669.

LEVANGIE, P. K. & NORKIN, C. C. 2001. *Joint structure and function: a comprehensive analysis*, FA Davis Philadelphia, PA.

LIFEMODELER. *LifeMOD manual* [Online]. Available: http://www.lifemodeler.com/LM_Manual/index.shtml [Accessed].

LUOMA, K., RIIHIM KI, H., LUUKKONEN, R., RAININKO, R., VIIKARI-JUNTURA, E. & LAMMINEN, A. 2000. Low back pain in relation to lumbar disc degeneration. *Spine,* 25**,** 487-492.

MACINTOSH, J. E. & BOGDUK, N. 1987. 1987 Volvo Award in Basic Science: The Morphology of the Lumbar Erector Spinae. *Spine,* 12**,** 658-668.

MACINTOSH, J. E. & BOGDUK, N. 1991. The attachments of the lumbar erector spinae. *Spine,* 16**,** 783-792.

MACINTOSH, J. E., BOGDUK, N. & PEARCY, M. J. 1993. The effects of flexion on the geometry and actions of the lumbar erector spinae. *Spine,* 18**,** 884.

MACINTOSH, J. E., VALENCIA, F., BOGDUK, N. & MUNRO, R. R. 1986. The morphology of the human lumbar multifidus. *Clinical Biomechanics,* 1**,** 196-204.

MAGORA, A. 1972. Investigation of the relation between low back pain and occupation. 3. Physical requirements: sitting, standing and weight lifting. *IMS, Industrial medicine and surgery,* 41**,** 5-9.

MAJESKE, C. & BUCHANAN, C. 1984. Quantitative description of two sitting postures. *Physical Therapy,* 64**,** 1531.

MAKHSOUS, M., LIN, F., HENDRIX, R. W., HEPLER, M. & ZHANG, L. Q. 2003. Sitting with adjustable ischial and back supports: biomechanical changes. *Spine,* 28**,** 1113.

MANNHEIM, J. K. 2012. *Scoliosis* [Online]. Available: http://www.nlm.nih.gov/medlineplus/ency/imagepages/1114.htm [Accessed].

MARRAS, W. S., LAVENDER, S. A., LEURGANS, S. E., FATHALLAH, F. A., FERGUSON, S. A., GARY ALLREAD, W. & RAJULU, S. L. 1995. Biomechanical risk factors for occupationally related low back disorders. *Ergonomics,* 38**,** 377-410.

MAUREL, N., LAVASTE, F. & SKALLI, W. 1997. A three-dimensional parameterized finite element model of the lower cervical spine, study of the influence of the posterior articular facets. *Journal of biomechanics,* 30**,** 921-931.

MCGILL, S. & NORMAN, R. 1986. 1986 Volvo award in biomechanics: Partitioning of the L4-L5 dynamic moment into disc, ligamentous, and muscular components during lifting. *Spine,* 11**,** 666-678.

MCGILL, S. & NORMAN, R. W. 1987a. Reassessment of the role of intra-abdominal pressure in spinal compression. *Ergonomics,* 30**,** 1565-1588.

MCGILL, S. M. & NORMAN, R. W. 1987b. Effects of an anatomically detailed erector spinae model on L4L5 disc compression and shear. *Journal of biomechanics,* 20**,** 591-600.

MCKENZIE, R. A. & MAY, S. 1981. *The lumbar spine*, Spinal.

MCMAHON, T. A. 1984. *Muscles, reflexes, and locomotion*, Princeton University Press.

MORANT, G. 1947. Dimensional requirements for seats in RAF aircraft. *Flying Personnel Research Committee, Rep,* 682.

MYHR, U., WENDT, L., NORRLIN, S. & RADELL, U. 1995. Five year follow up of unctional sitting position in children with cerebral palsy. *Developmental Medicine & Child Neurology,* 37**,** 587-596.

NACHEMSON, A. 1965. The effect of forward leaning on lumbar intradiscal pressure. *Acta Orthopaedica,* 35**,** 314-328.

NACHEMSON, A. 1966. The load on lumbar disks in different positions of the body. *Clinical orthopaedics and related research,* 45**,** 107-122.

NACHEMSON, A. 1975. Towards a better understanding of low-back pain: a review of the mechanics of the lumbar disc. *Rheumatology and rehabilitation,* 14**,** 129.

NACHEMSON, A. & ELFSTROM, G. 1970. Intravital dynamic pressure measurements in lumbar discs. *Scand J Rehabil Med,* 2**,** 1-40.

NACHEMSON, A. & MORRIS, J. M. 1964. In vivo measurements of intradiscal pressure discometry, a method for the determination of pressure in the lower lumbar discs. *The Journal of Bone and Joint Surgery (American),* 46**,** 1077-1092.

NACHEMSON, A. L. 1981. Disc pressure measurements. *Spine,* 6**,** 93.

OKUSHIMA, H. 1970. Study on hydrodynamic pressure of lumbar intervertebral disc. *Nihon geka hokan. Archiv fur japanische Chirurgie,* 39**,** 45.

PANJABI, M. & WHITE, A. R. 1990. Clinical biomechanics of the spine. *Clinical biomechanics of the spine*.

PANKOKE, S., BUCK, B. & WOELFEL, H. 1998. Dynamic FE model of sitting man adjustable to body height, body mass and posture used for calculating internal forces in the lumbar vertebral disks. *Journal of Sound and Vibration,* 215**,** 827-839.

PENNING, L. 2000. Psoas muscle and lumbar spine stability: a concept uniting existing controversies. *European Spine Journal,* 9**,** 577-585.

PINTAR, F. A., YOGANANDAN, N., MYERS, T., ELHAGEDIAB, A. & SANCES JR, A. 1992. Biomechanical properties of human lumbar spine ligaments. *Journal of biomechanics,* 25**,** 1351-1356.

PLOYON, A., LAVASTE, F., MAUREL, N., SKALLI, W., ROLAND-GOSSELIN, A., DUBOUSSET, J. & ZELLER, R. 1997. In-vivo experimental research into the pre-and post-operative behavior of the scoliotic spine. *Human movement science,* 16**,** 299-308.

RASMUSSEN, J., T RHOLM, S. & DE ZEE, M. 2009. Computational analysis of the influence of seat pan inclination and friction on muscle activity and spinal joint forces. *International Journal of Industrial Ergonomics,* 39**,** 52-57.

ROBERSON, R. E. & SCHWERTASSEK, R. 1988. *Dynamics of multibody systems*, Springer-Verlag Berlin.

ROHLMANN, A., BURRA, N. K., ZANDER, T. & BERGMANN, G. 2007. Comparison of the effects of bilateral posterior dynamic and rigid fixation devices on the loads in the lumbar spine: a finite element analysis. *European Spine Journal,* 16**,** 1223-1231.

ROHLMANN, A., CLAES, L., BERGMANN, G., GRAICHEN, F., NEEF, P. & WILKE, H. J. 2001. Comparison of intradiscal pressures and spinal fixator loads for different body positions and exercises. *Ergonomics,* 44**,** 781-794.

SATO, K., KIKUCHI, S. & YONEZAWA, T. 1999. In vivo intradiscal pressure measurement in healthy individuals and in patients with ongoing back problems. *Spine,* 24**,** 2468.

SCHEDE, F. 1935. Grundlagen der körperlichen Erziehung.

SCHMIDT, H., HEUER, F., CLAES, L. & WILKE, H.-J. 2008. The relation between the instantaneous center of rotation and facet joint forces-A finite element analysis. *Clinical Biomechanics (Bristol, Avon),* 23**,** 270.

SCHOBERTH, H. 1962. *Sitzhaltung, sitzschaden, sitzmobel,* Berlin, Springer.

SCHULTHESS, W. 1905. Die pathologie und therapie der ruckgratsverkrummungen. *Chirurgie HBO, editor,* 1**,** 1905-1907.

SCHULTZ, A., ANDERSSON, G., ORTENGREN, R., HADERSPECK, K. & NACHEMSON, A. 1982. Loads on the lumbar spine. Validation of a biomechanical analysis by measurements of intradiscal pressures and myoelectric signals. *The Journal of bone and joint surgery. American volume,* 64**,** 713.

SCHULTZ, A. B. & ASHTON-MILLER, J. A. 1991. Biomechanics of the human spine. *Basic orthopaedic biomechanics***,** 337-374.

SCHUMACHER, G. & WOLFF, E. 1966. Dry weight and physiological cross section of human skeletal muscles. II. Physiological cross section]. *Anatomischer anzeiger,* 119**,** 259.

SEIDEL, H., BL THNER, R. & HINZ, B. 2001. Application of finite-element models to predict forces acting on the lumbar spine during whole-body vibration. *Clinical Biomechanics,* 16**,** S57-S63.

SHIRAZI-ADL, A., AHMED, A. & SHRIVASTAVA, S. 1986. A finite element study of a lumbar motion segment subjected to pure sagittal plane moments. *Journal of biomechanics,* 19**,** 331-350.

SMITH, R. & EMANS, J. 1992. Sitting balance in spinal deformity. *Spine,* 17**,** 1103-1109.

STAFFEL, F. 1884. Zur hygiene des sitzens. *Zbl F Allg Gesundheitspflege,* 3**,** 403-421.

STOKES, I. A. & GARDNER-MORSE, M. 1995. Lumbar spine maximum efforts and muscle recruitment patterns predicted by a model with multijoint muscles and joints with stiffness. *Journal of biomechanics,* 28**,** 173-186.

STOKES, I. A. & GARDNER-MORSE, M. 1999. Quantitative anatomy of the lumbar musculature. *Journal of biomechanics,* 32**,** 311-316.

SWEARINGEN, J. J. 1962. An analysis of sitting areas and pressures of man. CIVIL AERONAUTICS MEDICAL RESEARCH LAB OKLAHOMA CITY OK.

TEO, E. & NG, H. 2001. Evaluation of the role of ligaments, facets and disc nucleus in lower cervical spine under compression and sagittal moments using finite element method. *Medical engineering & physics,* 23**,** 155-164.

TEWARI, V. & PRASAD, N. 2000. Optimum seat pan and back-rest parameters for a comfortable tractor seat. *Ergonomics,* 43**,** 167-186.

TULCHIN, K. L., HARRIS, G. F., LIU, X.-C. & THOMETZ, J. Year. Non-radiographic analysis of the pediatric spine in adolescent idiopathic scoliosis. *In:* [Engineering in Medicine and Biology, 1999. 21st Annual Conf. and the 1999 Annual Fall Meeting of the Biomedical Engineering Soc.] BMES/EMBS Conference, 1999. Proceedings of the First Joint, 1999. IEEE, 508 vol. 1.

UWMEDICINE. *Scoliosis* [Online]. Available: http://www.rad.washington.edu/academics/academic-sections/msk/teaching-materials/online-musculoskeletal-radiology-book/scoliosis [Accessed].

V LLFORS, B. 1984. Acute, subacute and chronic low back pain: clinical symptoms, absenteeism and working environment. *Scandinavian journal of rehabilitation medicine. Supplement,* 11**,** 1-98.

VAN DIE N, J. H. 1997. Are recruitment patterns of the trunk musculature compatible with a synergy based on the maximization of endurance? *Journal of biomechanics,* 30**,** 1095-1100.

VERGARA, M. & PAGE, Á. 2002. Relationship between comfort and back posture and mobility in sitting-posture. *Applied Ergonomics,* 33**,** 1-8.

W HODGES, P., MARTIN ERIKSSON, A., SHIRLEY, D. & C GANDEVIA, S. 2005. Intra-abdominal pressure increases stiffness of the lumbar spine. *Journal of biomechanics,* 38**,** 1873-1880.

WATANABE, K., NAKAMURA, T., IWANAMI, A., HOSOGANE, N., TSUJI, T., ISHII, K., NAKAMURA, M., TOYAMA, Y., CHIBA, K. & MATSUMOTO,

M. 2012. Vertebral derotation in adolescent idiopathic scoliosis causes hypokyphosis of the thoracic spine. *BMC Musculoskeletal Disorders,* 13**,** 99.

WILKE, H. J., NEEF, P., CAIMI, M., HOOGLAND, T. & CLAES, L. 1999. New in vivo measurements of pressures in the intervertebral disc in daily life. *Spine,* 24**,** 755.

WILKE, H. J., NEEF, P., HINZ, B., SEIDEL, H. & CLAES, L. 2001. Intradiscal pressure together with anthropometric data-a data set for the validation of models. *Clinical Biomechanics,* 16**,** S111-S126.

WKC. 2006. *How to evvaluate permanent disability* [Online]. Available: http://dwd.wisconsin.gov/dwd/publications/wc/wkc-7761-p.htm [Accessed].

YOGANANDAN, N., KUMARESAN, S. & PINTAR, F. A. 2001. Biomechanics of the cervical spine Part 2. Cervical spine soft tissue responses and biomechanical modeling. *Clinical Biomechanics,* 16**,** 1-27.

YOGANANDAN, N., KUMARESAN, S., VOO, L. & PINTAR, F. A. 1996. Finite element applications in human cervical spine modeling. *Spine,* 21**,** 1824.

ZANDER, T., ROHLMANN, A., KL CKNER, C. & BERGMANN, G. 2002. Comparison of the mechanical behavior of the lumbar spine following mono- and bisegmental stabilization. *Clinical Biomechanics,* 17**,** 439-445.

ZHANG, Q. H., TEO, E. C. & NG, H. W. 2005. Development and validation of a CO-C7 FE complex for biomechanical study. *Journal of biomechanical engineering,* 127**,** 729-735.